Appendix PA

Attachment MASS

This page intentionally left blank

Table of Contents

List of Figures

List of Tables

ACRONYMS AND ABBREVIATIONS

An	actinide
ASTP	Actinide Source Term Program
BSEP	Brine Sampling and Evaluation Program
CCDF	complementary cumulative distribution function
CH	contact-handled
CCA	Compliance Certification Application
CPR	cellulosic, plastic, and rubber
CRA	Compliance Recertification Application
DCCA	Draft Compliance Certification Application
DOE	U.S. Department of Energy
DRZ	disturbed rock zone
DSEIS	Draft Supplement, Environmental Impact Statement
EPA	U.S. Environmental Protection Agency
FEIS	Final Environmental Impact Statement
FEPs	features, events, and processes
FMT	Fracture-Matrix Transport
FSEIS	Final Supplemental Environmental Impact Statement
LANL	Los Alamos National Laboratory
LEFM	linear elastic fracture mechanics
LLNL	Lawrence Livermore National Laboratory
MB	marker bed
PA	performance assessment
PAVT	Performance Assessment Verification Test
QA	quality assurance
RH	remote-handled
RoR	Rest of Repository
SMC	Salado Mass Concrete
SNL	Sandia National Laboratories
SSBI	Small-Scale Brine Inflow
SWCF	Sandia National Laboratories WIPP Central Files
TDEM	Time Domain ElectroMagnetic
TRU	transuranic
WIPP	Waste Isolation Pilot Plant
WQSP	Water Quality Sampling Program

This page intentionally left blank

MASS-1.0 INTRODUCTION

This attachment presents supplementary information to Appendix PA regarding the assumptions, simplifications, or approximations used in the models of the first recertification performance assessment (PA) of the Waste Isolation Pilot Plant (WIPP). Within this attachment, relevant issues in the formulation or development of the various types of models (for example, conceptual, mathematical, numerical, or computer code) used for the topic are discussed, and references to relevant historical information are included where appropriate.

Section MASS-2.0 contains a summary of changes in the PA since the Compliance Certification Application (CCA). Section MASS-3.0 includes a discussion of general modeling assumptions applicable to the disposal system as a whole, including a table of assumptions made in PA models, with cross-references. The remainder of this attachment discusses assumptions specific to the first recertification PA conceptual models. Historical development of the WIPP conceptual models that led to the PA used in the CCA is documented in CCA Appendix MASS-2.0.

MASS-2.0 SUMMARY OF CHANGES IN PERFORMANCE ASSESSMENT

Since the CCA, several concepts about the processes important to the performance of the WIPP have changed. Additionally, ongoing confirmatory experiments, monitoring results, and operational practices have generated information relevant to the conceptual models for the WIPP PA and provide additional support to the conceptual basis of the PA.

Changes that have occurred since the 1996 PA and new information that may be important to PA are as follows:

1. Features, events and processes (FEPs) assessment
    A. Inclusion of organic ligands in solubility calculations

2. Monitoring
    A. Changes resulting from Culebra water level investigations
    B. Drilling rate parameter change
    C. Changes in Borehole plugging configuration probabilities

3. Experimental Activities
    A. Magnesium-oxide investigations
    B. Changes resulting from actinide investigations

4. PA Models and Systems
    A. Administrative hardware and software updates
    B. Conceptual model changes
        i. Panels closures
        ii. Simplification of shafts
        iii. Grid refinements
        iv. North and South Rest of Repository (RoR)
    C. Spallings

    D. Recalculation of Culebra T-fields
    E. Performance Assessment Verification Test (PAVT) Baseline

5. Operational Considerations
    A. WIPP horizon moved up to Clay Seam G
    B. Waste inventory update
    C. Evaluation of waste structural impacts, emplacement, and homogeneity

A summary of each change is presented in this section. References to appropriate sections of this attachment are provided for those changes that impact modeling assumptions. Additional references are provided to other areas of the Compliance Recertification Application (CRA) discussing change implementation.

MASS-2.1 Features, Events, and Processes Assessment

Based on the PA methodology for WIPP (see Section 6.2), FEPs are important elements to help develop the conceptual models and modeling assumptions represented in PAs. The process used to develop and screen FEPs is outlined in Section 6.2. The results of the CCA FEPs screening was documented in CCA Appendix SCR. For the CRA, a reassessment of the baseline PA FEPs was conducted to determine if changes in WIPP activities and conditions changed the original FEPs descriptions, basis, or screening decisions. This assessment also determined if additional FEPs should be included in the CRA baseline. The reassessment results are documented in SNL (2003a) and have been used to develop Appendix PA, Attachment SCR. Changes to the FEPs' baseline include combining similar FEPs and deleting redundant or inclusive FEPs, separating general FEPs into more descriptive FEPs, and FEP screening decision changes.

MASS-2.2 Monitoring

Monitoring activities have continued since the certification of WIPP. These activities are used to validate assumptions and PA parameters, and also to detect substantial and detrimental deviation from expected repository performance. Monitoring, as discussed here, applies to the assurance requirement of 40 CFR §191.14(b) and the monitoring criteria at 40 CFR §194.42. Appendix MON details the monitoring program that meets these requirements. The monitoring program has led to three changes:

- Culebra water levels at some wells have exceeded the ranges used in the CCA steady-state T-field calibrations,
- The drilling rate for deep boreholes has increased since 1996, and
- The probabilities for borehole plug configurations have changed slightly since 1996.

The impacts and implementation of the new Culebra data are discussed in Section 2.2.1.4.1.2. and Appendix PA, Attachment TFIELD (see also MASS-2.4.2).

In the 2004 PA, two parameters have changed; the drilling rate and the probabilities for borehole plugging. The drilling rate for boreholes is discussed in Sections 6.0.2.3, 6.2.5.2; and Appendix DATA (Section DATA-2.0 and Attachment A). The probability for borehole plugging configurations is discussed in Section 6.4.7.2. No changes are necessary to modeling assumptions to account for these parameter changes.

MASS-2.3 Experimental Activities

The EPA requires the recertification documentation to include an update of "additional analyses and results of laboratory experiments conducted by the Department or its contractors as part of the WIPP program" (40 CFR 194.15(a)(3)). The following discusses analyses and experiments conducted to support compliance determinations. Only the analyses with conclusions relevant to this recertification are discussed here; all ongoing and supportive experiments are presented in biannual reports previously submitted to Environmental Protection Agency (EPA) (SNL 2001a, 2001b; SNL 2002a, 2002b; and SNL 2003b).

MASS-2.3.1 Magnesium-Oxide Investigations

Experiments have been preformed to support implementation of magnesium oxide (MgO) as an engineered barrier. These experiments investigate hydration and carbonization of MgO to confirm its ability to sequester carbon dioxide (CO_2), buffer brine pH, and subsequently reduce actinide solubilities in the repository. The conclusions drawn from these activities are described in Appendix BARRIERS. Specifically, the incorporation of MgO in PA has not changed from the 1996 PA.

MASS-2.3.2 Actinide Investigations

An Actinide Source Term Program (ASTP) has continued to investigate actinide (An) speciation and solubilities since the certification of WIPP. These investigations include work relating to organic ligands and colloid effects on solubilities, and the appropriateness of the use of the oxidation state analogy. These activities are described in SNL (2001a, 2001b; SNL 2002a, 2002b; and SNL 2003b). The conclusions drawn from these activities and the changes to the 2004 PA are described in Appendix PA, Attachment SOTERM. Specifically, organic ligands are considered in the 2004 PA through the solubility calculations.

MASS-2.4 Performance Assessment Models and Systems

Changes have been made to the systems that are used to perform PAs. The PA hardware, operating systems, and parameter database were updated since the 1996 PA. These changes were necessary to replace obsolete hardware and operating systems and to increase PA capabilities. These changes were implemented and approved under applicable quality assurance (QA) requirements.

Additionally, conceptual model changes were necessary to implement new or different representations of physical systems in PA. Changes to conceptual models led to revised or replacement codes, which implement the conceptual models in PA. The following discusses these changes.

MASS-2.4.1 Administrative Hardware and Software Updates

The computer systems and operating systems have been upgraded since the 1996 PA because of increasing obsolescence of the operating system and hardware. New hardware is being used along with a newer operating system for the 2004 PA. All changes to these systems are performed under the appropriate QA program, and include testing, validation, and verification to ensure that there is no impact on PA implementation. A synopsis of the changes and references to the QA documentation are found in Long (2003).

MASS-2.4.2 Conceptual Model Changes

The certification decision by the EPA (1998a) included several conditions that the U.S. Department of Energy (DOE) was required to meet. In the first of these conditions, the EPA required the DOE to implement a specific design for the panel closure system (referred to as "Option D") and using Salado Mass Concrete (SMC). The DOE had included in the CCA four Options (A-D) for the panel closure design. The Option D design consisted of two components, a large concrete monolith and an explosion wall constructed of concrete blocks. The 1996 PA generically represented the closures in BRAGFLO and did not model a specific closure. The representation of the Option D closure has been incorporated into the BRAGFLO grid. The Option D closure modeling assumptions are discussed in Section MASS-19.0 and MASS-4.2. Panel closure implementation in PA is discussed in Appendix PA, Section PA-4.2.8.

To account for this design in PA, the conceptual model for Repository Fluid Flow, Disturbed Rock Zone (DRZ), and the Disposal System Geometry were revised and peer reviewed. Chapter 9 and Appendix PEER contain information on the conceptual model peer review. These conceptual models are implemented in BRAGFLO. See Section MASS-2.5.2 and MASS-4.2 for information on modeling assumptions and implementation of these conceptual models. Implementation of these conceptual model changes led to the following changes in BRAGFLO.

1. Implementation of Option D panel closures,
2. Simplification of the shaft seal model,
3. Refinement of grid outside the excavated area to improve computational accuracy and efficiency,
4. Increased Segmentation in the North RoR and South RoR.

MASS-2.4.3 Spallings Model

An EPA guidance letter on recertification requested the DOE implement a new spallings conceptual model (EPA 2002). The original conceptual model for spallings was peer reviewed during the first certification, but was deemed inadequate by the peer review panel. The DOE later derived a method to represent spallings that was deemed conservative by the peer reviewers and was used by DOE in the 1996 PA. Since the CCA, however, a more appropriate and representative spallings model has been developed, peer reviewed, and implemented in the 2004 PA. Results of the peer review are found in Chapter 9 and Appendix PEER. Modeling assumptions concerning the Spallings model are detailed in Section MASS-16.1. Implementation of the spallings model is described in Appendix PA, Section PA-4.6.

No other conceptual models were revised for this recertification application.

MASS-2.4.4 Recalculation of Culebra T-fields

Water level rises in the Culebra have continued over recent years and the observed heads have exceeded the ranges of uncertainty established for the steady-state heads in many of the 32 wells used in the calibration of the transmissivity fields described in the CCA (SNL 2002b). Therefore, the DOE has recalculated T-Fields for the CRA using new Culebra data and geologic information (see Appendix PA, Attachment TFIELD; and Section 2.0). The DOE has implemented a program to identify other potential causes for the water-level rises (SNL 2003c).

MASS-2.4.5 Performance Assessment Verification Test Baseline

The EPA's PAVT parameters were incorporated into the 2004 PA parameter baseline (EPA 1998b, V-B-14). These parameters and a cross-reference of discussions concerning their incorporation into the 2004 PA are shown in Table 6-1.

MASS-2.5 Operational Considerations

Operational considerations are impacts to PA from changes to WIPP operations that the DOE has requested and the EPA has approved, or changes that have been mandated by the EPA.

MASS-2.5.1 Waste Isolation Pilot Plant Horizon Moved up to Clay Seam G

Operational changes to the repository design since the CCA include mining the repository horizon in the southern half of the waste panels at a different location than the northern half. Specifically, panels 3, 4, 5, 6, and 9 will be excavated at an elevation approximately 2.4 m above the level of panels 1, 2, 7, 8, and 10, and the operations and experimental areas. This change in horizon will bring the roof of the raised rooms to the level of the Clay Seam G. The change is expected to improve roof conditions and enhance operations and mine safety. The DOE submitted a planned change request to the EPA that described the change and presented an argument that the change would have minimal impact on long-term repository performance (DOE 2000). The EPA responded to the change request in a letter (EPA 2000) in which they agreed with DOE that the effects to long-term performance would be minimal. Further investigations led DOE to determine that no changes to the 2004 PA models were necessary to account for this change. Section MASS-20.0 discusses the justification for this determination.

MASS-2.5.2 Waste Inventory Update

The waste inventory used in the CCA was based on information contained in the TWBIR (CCA Appendix BIR). No waste had been emplaced in the repository at that time. Since 1996, waste has been emplaced in the repository and better estimates have been made of the existing and projected waste streams at the generator sites. The new waste information has been updated in the 2004 PA to include the emplaced, currently stored, and projected waste streams. This information was collected in the TWBID, Rev 2, with specific WIPP information detailed in

Appendix DATA, Attachment F. Inclusion of waste information in the 2004 PA is discussed in Appendix TRU WASTE.

MASS-2.5.3 Evaluation of Waste Structural Impacts, Emplacement, and Homogeneity

During the development of the CCA PA, the DOE choose to assume random placement of transuranic (TRU) waste in the WIPP, and developed conceptual and numerical models accordingly. The EPA reviewed these models and their results, and determined that DOE had modeled accurately random placement of waste in the disposal system. Since the time of the CCA, additional information about the waste and its emplacement has emerged and requires waste-related assumptions to be reevaluated. This evaluation is discussed in Section MASS-21.0.

MASS-3.0 GENERAL ASSUMPTIONS IN PERFORMANCE ASSESSMENT MODELS

Several assumptions are applied generally to the disposal system through the conceptual and mathematical models implemented in the major computer codes used in this PA. Several major assumptions are discussed here. A table of general assumptions is also presented in Section MASS-3.4.

MASS-3.1 Darcy's Law Applied to Fluid Flow Calculated by BRAGFLO, MODFLOW-2000, and SECOTP2D

A mathematical relationship expressing the flux of fluid as a function of hydraulic head gradients applied, commonly known as Darcy's Law, is applied to geologic media for all fluid-flow calculations. For details about the specific formulation of Darcy's Law used, refer to Appendix PA, Section PA-4.2 for the disposal system and Section PA-4.8 for the Culebra. Darcy's Law is not applied for flow up a borehole that is being drilled (see Section MASS-16.2; and Section 6.4.7.1.1 for more discussion of this topic).

Darcy's Law generally applies for flow models if certain conditions are satisfied: (1) the flow occurs in a porous medium with interconnected porosity, (2) flow velocities are low enough that viscous forces dominate inertial forces, and (3) a threshold hydraulic gradient is exceeded. In CCA Appendix MASS, these conditions were shown to be valid for the WIPP PA.

Darcy's Law assumes laminar flow, that is, there is no motion of the fluid at the fluid/solid interface. For liquids, it is reasonable to assume laminar flow under most conditions. For gases at low pressure, however, gas molecules near the solid interface may not have intimate contact with the solid and may have finite velocity, not necessarily zero. This effect, which results in additional flux of gas above that predicted by application of Darcy's Law, is known as the slip phenomenon, or Klinkenberg effect (Bear 1972, 128). A correction to Darcy's Law for the Klinkenberg effect is incorporated into the BRAGFLO model (see Appendix PA, Section PA-4.2).

Darcy flow for one and two phases implies that values for certain parameters must be specified. Some principal parameters relate to the properties of the fluid, others to the rock. Fluid properties in the Darcy flow model used for the WIPP are its density, viscosity, and compressibility. Rock properties in Darcy flow models are porosity, permeability, and compressibility (pore, bulk, or rock). In BRAGFLO, other parameters are required to describe the interactions or interference between the two phases present in the model, gas and brine, because they can occupy the same pore space. In the WIPP application of Darcy flow models, compressibility of both the liquid and rock are related to porosity through a dependence on pressure. Fluid density, viscosity, and compressibility are functions of fluid composition, pressure, and temperature. In BRAGFLO, fluid viscosity is a function of pressure, but its density and compressibility are held constant. Fluid composition for the purposes of modeling flow and transport is assumed to be constant.

MASS-3.2 Hydrogen Gas as Surrogate for Waste-Generated Gas Physical Properties in BRAGFLO and DRSPALL

Hydrogen gas is produced by the corrosion of steel in the repository by water or brine. As in the CCA, the gas phase in the BRAGFLO model is assigned the properties of hydrogen because hydrogen will, under most conditions reasonable for the WIPP, be the dominant component of the gas phase. The model for spallings, DRSPALL, also assigns physical properties of hydrogen to the gas phase. In the CCA, the effect of assuming flow of pure H_2 instead of a mixture of gases (including H_2, CO_2, H_2S, and CH_4), was shown to be minor relative to the permeability variations in the surrounding formations.

Other gases may be produced by processes occurring in the repository. If microbial degradation occurs, a significant amount of carbon dioxide (CO_2) and methane (CH_4) will be generated by microbial degradation of cellulosics, and, perhaps, plastics and rubbers in the waste. The CO_2 produced, however, will react with the magnesium-oxide (MgO) engineered barrier and cementitious materials to form brucite ($Mg(OH_2)$), hydromagnesite ($Mg_5(CO_3)_4(OH)_2 \cdot 4H_2O$), and calcite ($CaCO_3$) thus resulting in very low CO_2 fugacity in the repository. Although other gases exist in the disposal system, for BRAGFLO calculations it is assumed these gases are insignificant and are not included in the model.

With the average stoichiometry gas generation model, the total number of moles of gas generated will be the same whether the gas is considered to be pure H_2 or a mixture of several gases, because the generation of other gases is accounted for by specifying the stoichiometric factor y. Therefore, considering the moles of gas generated alone, the pressure buildup in the repository will be approximately the same, because the expected gases behave similarly to an ideal gas, even up to lithostatic pressures.

The effect of assuming pure H_2 instead of a mixture of gases (including H_2, CO_2, H_2S and CH_4) on flow behavior, and its resulting impact on the WIPP repository pressure is presented as follows:

Radial flow of a 100 percent saturated rock with nonideal gas is described by Darcy's Law (Amyx et al. 1960):

$$q_b = 1.988\_10^{-5}\left[\frac{T_b z_b}{P_b}\frac{kh\left(P_e^2 - P_w^2\right)}{\mu_{avg} z_{avg}\ln\left(\frac{r_e}{r_w}\right)}\right], \tag{2}$$

which can be rewritten:

$$P_e^2 - P_w^2 = \frac{q_b}{1.988\_10^{-5}}\left[\frac{P_b}{T_b z_b}\frac{\mu_{avg} z_{avg}\ln\left(\frac{r_e}{r_w}\right)}{kh}\right], \tag{3}$$

where:

q = gas flow rate, cubic feet per day at base (reference) conditions
T = temperature, K
P = pressure, pounds per square inch atmosphere
k = permeability, millidarcys
h = height, feet
μ = viscosity, centipoises
z = gas compressibility factor (a function of gas pressure and temperature)
r = radius, consistent units
e = external boundary (repository)
w = internal boundary (wellbore)
b = base or reference conditions for gas (temperature, pressure, compressibility factor)
avg = average properties between external and internal boundaries because u and z are functions of pressure which change with time.

This expression is very useful for looking at the relationships of gas properties (specifically μ and z [which is a function of the gas temperature and pressure]) and rock properties (namely k) on defining q and P.

In order to evaluate the effect of gas composition on q and P, a computer program developed by the National Institute of Standards and Technology (NIST) entitled SUPERTRAPP was used (NIST 1992). This computer program allows calculations of gas properties for 116 pure fluids and mixtures of up to 20 components for temperatures to 1,000 K and pressures to 300 megapascals. The computer program currently can evaluate hydrogen, CO_2, and water but does not have the capacity to evaluate brine (Friend and Huber 1994). Because such small quantities of H_2S are anticipated at the WIPP, its impact will be neglected.

Figure MASS-1 shows the relationship between gas viscosity H_2-CO_2 mixtures for various mole fractions of H_2 at pressures of 7 megapascals and 15 megapascals as determined from SUPERTRAPP. The viscosity at 50 percent mole fraction H_2 is 2.3 times greater than for 100 percent mole fraction H_2. As shown in Equation (2), viscosity has an inverse relationship to flow rate and, as shown in Equation (3), a direct relationship to the square of the repository pressure.

Hence viscosity differences that would result if gas properties other than those of hydrogen were incorporated would result in a decrease in flow rate and potentially higher pressures.

As shown in Figure MASS-2, the gas compressibility at 50 percent mole fraction H_2 is about 0.9 times that at 100 percent mole fraction H_2. Like viscosity, the gas compressibility factor is inversely related to flow rate and directly related to the square of the repository pressure. Hence changing composition from 100 percent to 50 percent H_2 would result in a slight increase in flow rate and a decrease in pressure. Therefore, the impact of variation in gas compressibility caused by composition is considered minor and so is neglected.

The viscosity and compressibility calculations described above for H_2-CO_2 mixtures were repeated for H_2-CH_4 mixtures for various mole fractions of H_2 at pressures of 7 MPa and 15 MPa (Kanney 2003). The variability of viscosity with the composition for the H_2-CH_4 mixtures is smaller than that observed for the H_2-CO_2 mixtures. For example, the gas viscosity of H_2-CH_4 at 50 percent mole fraction is only 1.6 times greater than that for 100 percent mole fraction H_2 at 15 MPa. The H_2-CH_4 mixtures are only slightly less compressible than the H_2-CO_2 mixtures. For example, the gas compressibility of H_2-CH_4 at 50 percent mole fraction is about 0.94 times that for 100 percent mole fraction H_2 at 15 MPa.

The absolute permeability of the surrounding formation plays a significant part with respect to both flow rate and pressure determinations. Because marker bed permeabilities range over four orders of magnitude (see Appendix PAR, Tables PAR-30 to PAR-32), these primary flow pathways will have a greater influence on pressure and flow rate determinations compared to either uncertainty in viscosity or gas compressibility effects.

It should also be noted that the BRAGFLO code includes a pressure-induced fracture model that will limit pressure increases in the repository (Schreiber 1997). For example, at high repository pressures, the factor of 2.3 pressure increase calculated here using the simplified Darcy's Law model is unlikely to be seen in the BRAGFLO results, since fracturing will lead to increased permeability, effectively limiting pressure increases.

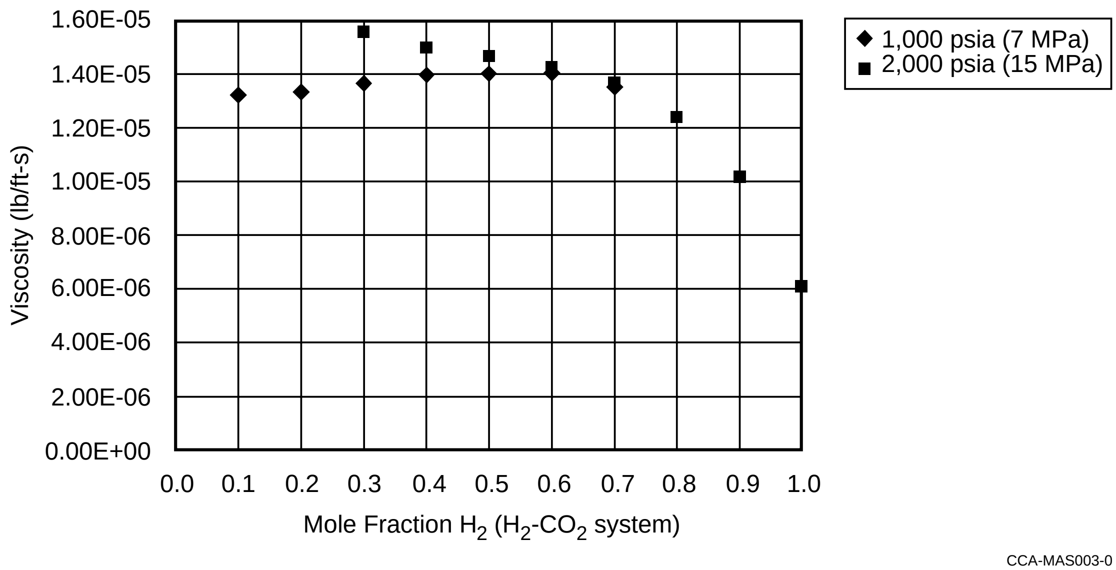

Figure MASS-1. Gas Viscosity as a Function of Mole Fraction H_2 at 7 Megapascals and 15 Megapascals Pressure

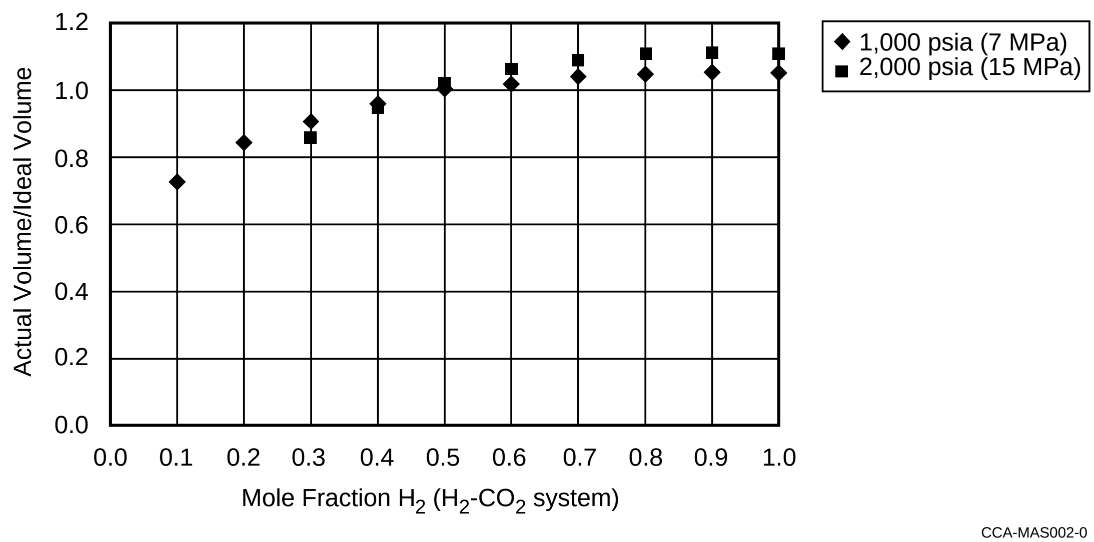

Figure MASS-2. Gas Compressibility as a Function of Mole Fraction H_2

MASS-3.3 Salado Brine as Surrogate for Liquid Phase Physical Properties in BRAGFLO

BRAGFLO models physical properties for all liquids as Salado brine properties. However, liquid in the modeled region may consist of (1) brine originally in the Salado, (2) liquid introduced in the excavation during construction, maintenance, and ventilation during the operational phase, (3) a very small amount of liquid introduced as a component of the waste, (4) liquid from overlying units, and (5) liquid from the Castile brine reservoir. However, for

BRAGFLO modeling it is assumed that the properties of all of these liquids are similar enough to Salado brine properties that the effect of variation in properties that may occur from liquids mixing is negligible. The variations in chemical properties of brine are accounted for as discussed in Section 6.4.3.4, and 6.4.3.5; and Appendix PA, Attachment SOTERM.

MASS-3.4 Table of General Modeling Assumptions

This section presents Table MASS-1, which lists modeling assumptions used in the PA. Table MASS-1 is a guide to general modeling assumptions used and provides some guidance for integrating the assumptions made with (a) the chapters or appendices in which they are discussed and (b) the code(s) that implement these assumptions.

The FEPs discussed in Appendix PA, Attachment SCR that are relevant to the assumptions are also indicated. The final column in the table indicates whether the DOE considers the assumption described to be reasonable or conservative. As discussed in Section 6.5, the DOE has not attempted to bias the overall results of the performance assessment toward a conservative outcome. However, where data or models are infeasible to obtain, or where effects on performance are not expected to be significant enough to justify development of a more complicated model, the DOE has chosen to use conservative assumptions. The designator R (reasonable) in the final column indicates that the DOE considers the assumption to be reasonable based on WIPP-specific data or information, data and information considered analogous to the WIPP disposal system, expert judgment, or other reasoning. The designator C (conservative) indicates the DOE considers the assumption made may overestimate a process or effect that may contribute to releases to the accessible environment. The regulatory designator (Reg) indicates that the assumption is based on regulations in 40 CFR Part 191, criteria in 40 CFR Part 194, or other regulatory guidance.

MASS-4.0 MODEL GEOMETRIES

This section presents supplementary information on the disposal system geometry.

MASS-4.1 Disposal System Geometry as Modeled in BRAGFLO

Overall, the conceptual model of the geometry of the disposal system is that the spatial effects of process interactions can be represented in two dimensions. The geometry used to represent the processes of long-term fluid flow in the Salado, flow between a borehole and overlying units, and flow within the repository (where processes coupled to fluid flow occur, such as creep closure and gas generation), is a vertical cross-section through the repository on a north-south axis. The dimension of this geometry in the direction perpendicular to the plane of the cross-section varies so that spatial effects of certain processes can be better represented, as discussed below.

Table MASS-1. General Modeling Assumptions

CRA Section and Appendix		Code	Modeling Assumption	Related FEP in Attachment SCR	Assumption Considered*
MASS-3.0 Some General Assumptions in Performance Assessment Models					
MASS-3.1 Darcy's Law Applied for Fluid Flow calculated by BRAGFLO, MODFLOW-2000, and SECOTP2D					
	1	BRAGFLO MODFLOW-2000	Flow is governed by mass conservation and Darcy's Law in porous media. Flow is laminar and fluids are Newtonian.	Saturated groundwater flow (N23) Unsaturated groundwater flow (N24) Brine inflow (W40)	R
	2	BRAGFLO	Two-phase flow in the porous media is by simultaneous immiscible displacement.	Fluid flow caused by gas production (W42)	R
	3	BRAGFLO	The Brooks-Corey or Van Genuchten/Parker equations represent interaction between brine and gas.	Fluid flow caused by gas production (W42)	R
	4	BRAGFLO	The Klinkenberg effect is included for flow of gases at low pressures.	Fluid flow caused by gas production (W42)	R
	5	BRAGFLO	Threshold displacement pressure for flow of gas into brine is constant.	Fluid flow caused by gas production (W42)	R
	6	BRAGFLO MODFLOW-2000 SECOTP2D	Fluid composition and compressibility are constant.	Saturated groundwater flow (N23) Fluid flow caused by gas production (W42)	R
MASS-3.2 Hydrogen Gas as Surrogate for Waste-Generated Gas Physical Properties in BRAGFLO					
	7	BRAGFLO DRSPALL	The gas phase is assigned the density and viscosity properties of hydrogen.	Fluid flow caused by gas production (W42)	R
MASS-3.3 Salado Brine as Surrogate for Liquid Phase Physical Properties in BRAGFLO					
	8	BRAGFLO	All liquid physical properties are assigned the properties of Salado brine.	Saturated groundwater flow (N23)	R
6.4.2 Model Geometries MASS-4.0 Model Geometries					
6.4.2.1 Disposal System Geometry MASS.4.1 Disposal System Geometry as Modeled in BRAGFLO					
		BRAGFLO	The disposal system is represented by a two-dimensional, north-south, vertical cross section.	Stratigraphy (N1) Physiography (N39)	R
		BRAGFLO	Flow in the disposal system is radially convergent or divergent centered on the repository, shaft, and borehole for disturbed performance.	Saturated groundwater flow (N23) Unsaturated groundwater flow (N24)	R
		BRAGFLO	Variable dip in the Salado is approximated by a 1 degree dip to the south.	Stratigraphy (N1)	R

Table MASS-1. General Modeling Assumptions — Continued

CRA Section and Appendix		Code	Modeling Assumption	Related FEP in Attachment SCR	Assumption Considered*
		BRAGFLO	Stratigraphical layers are parallel.	Stratigraphy (N1)	R
		BRAGFLO	The stratigraphy consists of units above the Dewey Lake, the Dewey Lake, the Forty niner, the Magenta, the Tamarisk, the Culebra, the Los Medaños, and the Salado (comprising impure halite, MB 138, anhydrites a and b [lumped together], and MB139). The dimensions of these units are constant. A Castile brine reservoir is included in all scenarios.	Stratigraphy (N1)	R
6.4.2.2 Culebra Geometry MASS-4.3 Historical Context of Culebra Geometries as Modeled in MODFLOW-2000 and SECOTP2D					
		MODFLOW-2000 SECOTP2D	The Culebra is represented by a two-dimensional, horizontal geometry for groundwater flow and radionuclide transport simulation.	Stratigraphy (N1)	R
		MODFLOW 2000 PEST	Transmissivity varies spatially. There is no vertical flow to or from the Culebra.	Groundwater recharge (N54) Groundwater discharge (N53)	R
		SECOTP2D	The regional flow field provides boundary conditions for local transport calculations.	Advection (W90)	R
6.4.3 The Repository MASS.5 BRAGFLO Geometry of the Repository					
		BRAGFLO	The repository comprises five regions separated by panel closures: the waste panel, a north RoR, a south RoR and the access drifts (separated by panel closures), the operations region, and the experimental region. Also, a single shaft region is modeled, and a borehole region is included for a borehole that intersects the separate waste panel. The dimensions of these regions are constant (see Figure 6-14).	Disposal geometry (W1)	R-C
		BRAGFLO	Long-term flow up plugged and abandoned boreholes is modeled as if all intrusions occur into a downdip (southern) panel.	Disposal geometry (W1)	C
		BRAGFLO	For each repository region the model geometry preserves design volume.	Disposal geometry (W1)	R
		BRAGFLO	Pillars individual drifts and rooms are not modeled for long-term performance, and containers provide	Disposal geometry (W1)	C

Table MASS-1. General Modeling Assumptions — Continued

CRA Section and Appendix	Code	Modeling Assumption	Related FEP in Attachment SCR	Assumption Considered*
		no barrier to fluid flow.		
	BRAGFLO	Long-term flow is radial to and from the borehole that intersects the waste disposal panel during disturbed performance.	Waste-induced borehole flow (H32)	R
	BRAGFLO	DRZ provides a pathway to Marker Beds		R
	BRAGFLO	Grid and material properties are consistent with the Option D design		R
6.4.3.1 Creep Closure MASS-6.0 Creep Closure Appendix PORSURF				
	SANTOS	Creep closure is modeled using a two-dimensional model of a single room. Room interactions are insignificant.	Salt creep (W20) Changes in the stress field Excavation-induced changes in stress (W19)	R
	SANTOS	Creep closure causes a decrease in room volume, which decreases waste porosity. The amount of creep closure is a function of time, gas pressure, and waste matrix strength.	Salt creep (W20) Changes in the stress field (W21) Consolidation of waste (W32) Pressurization (W26)	R
	BRAGFLO	Porosity of operations and experimental areas is fixed at a value representative of consolidated material.	Salt creep (W20)	R
6.4.3.2 Repository Fluid Flow MASS-7.0 Repository Fluid Flow				
	BRAGFLO	General assumptions 1 to 8.		See above
	BRAGFLO	The waste disposal region is assigned a constant permeability representative of average consolidated waste without backfill.	Saturated groundwater flow (N23) Unsaturated groundwater flow (N24)	R
MASS-7.1 Flow Interactions with the Creep Closure Model				
	BRAGFLO	The experimental and operations regions are assigned a constant permeability representative of unconsolidated material and a constant porosity representative of consolidated material.	Saturated groundwater flow (N23) Unsaturated groundwater flow (N24) Salt creep (N20)	R
MASS-7.2 Flow Interactions with the Gas Generation Model				
	BRAGFLO	For gas generation calculations, the effects of wicking are accounted for by assuming that brine in the	Wicking (W41)	R

Table MASS-1. General Modeling Assumptions — Continued

CRA Section and Appendix		Code	Modeling Assumption	Related FEP in Attachment SCR	Assumption Considered*
			repository contacts waste to an extent greater than that calculated by the Darcy flow model used.		
6.4.3.3 Gas Generation MASS-8.0 Gas Generation Appendix TRU WASTE					
		BRAGFLO	Gas generation occurs by anoxic corrosion of steel containers, and Fe and Fe-base alloys in the waste, giving H_2, and microbial consumption of cellulosics and, perhaps, plastics and rubbers, giving mainly CO_2 and CH_4. Radiolysis, oxic reactions, and other gas generation mechanisms are insignificant. Gas generation is calculated using the average - stoichiometry model, and is dependent on brine availability.	Container material inventory (W5) Waste inventory (W2) Degradation Consumption of (W44) Gases from metal corrosion (W49)	R
		BRAGFLO	The anoxic corrosion rate is dependent on liquid saturation. Anoxic corrosion of steel continues until all the steel is consumed. Steel corrosion will not be passivated by microbially-generated gases CO_2 or H_2S. Brine is consumed by the corrosion reaction.	Brine inflow (W40) Gases from metal corrosion (W49) Consumption of organic material (W44)	R
		BRAGFLO	Laboratory-scale experimental measurements of gas generation rates at expected room temperatures are used to account for the effects of biofilms and chemical reactions.	Effects of biofilms on microbial gas generation (W48) Effects of temperature on microbial gas generation (W45) Chemical effects of corrosion (W51)	R
		BRAGFLO	The rate of microbial gas production is dependent on the amount of liquid present. It is assumed that microbial activity neither produces nor consumes water. Significant microbial activity occurs in half the simulations. In half of the simulations with microbial activity, microbes consume all of the cellulosics but none of the plastics and rubbers. In the other half of the simulations with microbial activity, microbes consume all of the cellulosics and all of the plastics and rubbers. Microbial production will	Brine inflow (W40) Consumption of CPR (W44) Waste inventory (W2)	R

Table MASS-1. General Modeling Assumptions — Continued

CRA Section and Appendix		Code	Modeling Assumption	Related FEP in Attachment SCR	Assumption Considered*
			continue until all biodegradable CPR materials are consumed if brine is present. The MgO backfill will react with all of the CO_2 and remove it from the gaseous phase.		
		BRAGFLO	Gas dissolution in brine is of negligible consequence.	Fluid flow caused by gas production (W42)	R
		BRAGFLO	The gaseous phase is assigned the properties of hydrogen (general assumption 8).	Fluid flow caused by gas production (W42)	See above
6.4.3.4 Chemical Conditions in the Repository SOTERM-2.0 Conceptual Framework of Chemical Conditions					
		NUTS PANEL	Chemical conditions in the repository will be constant. Chemical equilibrium is assumed for all reactions that occur between brine in the repository, waste, and abundant minerals, with the exceptions of gas generation and redox reactions.	Speciation (W56) Redox kinetics (W66)	R
		NUTS PANEL	Brine and waste in the repository will contain a uniform mixture of dissolved and solid-state species. All actinides have instant access to all repository brine.	Heterogeneity of waste forms (W3) Speciation (W56)	C
		NUTS PANEL	No microenvironments that influence the overall chemical environment will persist.	Speciation (W56)	R
		NUTS PANEL	For the undisturbed performance and E2 scenarios, brine in the waste panels has the composition of Salado brine. For E1 and E1E2 scenarios, all brine in the waste panel intersected by the borehole has the composition of Castile brine.	Speciation (W56)	R
		NUTS PANEL	Chemical conditions in the waste panels will be reducing. However, a condition of redox disequilibrium will exist between the possible oxidation states of the actinide elements.	Redox kinetics (W56) Speciation (W56) Effects of metal corrosion (W64)	R
		NUTS PANEL	The pH and f_{CO2} in the waste panels will be controlled by the equilibrium between brucite and hydromagnesite ($Mg_5(CO_3)_4(OH)_2 \cdot 4H_2O$) (A result of this assumption is low f_{CO2} and mildly basic conditions).	Speciation (W56) Backfill chemical composition (W10)	R
6.4.3.5 Dissolved Actinide Source Term					

Table MASS-1. General Modeling Assumptions — Continued

CRA Section and Appendix		Code	Modeling Assumption	Related FEP in Attachment SCR	Assumption Considered*
SOTERM-3.3 The FMT Computer Code					
		NUTS PANEL	Radionuclide dissolution to solubility limits is instantaneous.	Dissolution of waste (W58)	C
		NUTS PANEL	Six actinides (Th, U, Np, Pu, Am, and Cm) are considered in PANEL for calculations of radionuclide transport of brine (up a borehole). Four actinides (Th, U, Pu, and Am) are considered in NUTS for calculations of radionuclide transport in brine (porous materials) (Leigh 2003). Choice of radionuclides is discussed in Appendix TRU WASTE, Table TRU WASTE-9.	Waste inventory (W2)	R
		NUTS PANEL	The reducing conditions in the repository will eliminate significant concentrations of Np(VI), Pu(V), Pu(VI), and Am(V)species. Am and Cm will exist predominantly in the +III oxidation state, Th in the +IV oxidation state. It is assumed that the solubilities and K_ds of U, Np, and Pu will be dominated by one of the remaining oxidation states: U(IV) or U(VI), Np(IV or Np(V), and Pu(III) or Pu(IV).	Speciation (W56) Redox kinetics (W66)	R
		NUTS PANEL	For a given oxidation state, the different actinides exhibit similar chemical behavior and thus have similar solubilities.	Speciation (W56)	R
		NUTS PANEL	For undisturbed performance and for all aspects of disturbed performance except for cuttings and cavings releases, radionuclide-bearing compounds are distributed evenly throughout the disposal panel.	Waste inventory (W2) Heterogeneity of waste forms (W3)	R
		NUTS PANEL	Mobilization of actinides in the gas phase is negligible.	Dissolution of waste (W58)	R
		NUTS PANEL	Actinide concentrations in the repository will be inventory limited when the mass of an actinide becomes depleted such that the predicted solubilities cannot be achieved.	Dissolution of waste (W58)	R
6.4.3.6 Source Term for Colloidal Actinides					
		NUTS PANEL	Four types of colloids constitute the source term for colloidal actinides; microbes, humic substances, intrinsic	Colloid formation and stability (W79) Humic and fulvic acids	R

Table MASS-1. General Modeling Assumptions — Continued

CRA Section and Appendix		Code	Modeling Assumption	Related FEP in Attachment SCR	Assumption Considered*
			colloids, and mineral fragments.	(W70)	
		NUTS PANEL	The only intrinsic colloids that will form are those of the plutonium Pu(IV) polymer.	Colloid formation and stability (W79)	R
		NUTS PANEL	Concentrations of intrinsic colloids and mineral-fragment colloids are modeled as constants that were based on experimental observations. Humic and microbial colloidal actinide concentrations are modeled as proportional to dissolved actinide concentrations.	Colloid formation and stability (W79)	R
		NUTS PANEL	The maximum concentration of each actinide associated with each colloid type is constant.	Actinide sorption (W61)	R
6.4.4 Shafts and Shaft Seals MASS-12.0 Shafts and Shaft Seals					
		BRAGFLO	General Assumptions 1 to 8.		See above
		BRAGFLO	The four shafts connecting the repository to the surface are represented by a single shaft with a cross-section and volume equal to the total volume of the four real shafts and separated from the waste by less than the distance of the nearest real shaft.	Disposal geometry (W1)	R
		BRAGFLO	The seal system is represented by an upper and lower shaft region representing a composite of the actual materials in those regions.	Seal geometry (W6) Seal physical properties (W7)	R
		BRAGFLO	The shaft is surrounded by a DRZ which heals with time. The DRZ is represented through the composite permeabilities of the shaft system itself, rather than as a discrete zone. The effective permeability of shaft materials are adjusted at 200 years after closure to reflect consolidation and possible degradation. Permeabilities are constant for the shaft seal materials through the Rustler formation.	Salt creep (W20) Consolidation of seals (W36) DRZ (W18) Microbial growth on concrete (W76) Chemical degradation of seals (W74) Mechanical degradation of seals (W37)	R
		BRAGFLO	Concrete shaft components of the lower shaft are modeled as if they degrade after emplacement.	Mechanical degradation of seals	C
		NUTS	Radionuclides are not retarded by the	Actinide sorption (W61)	C

Table MASS-1. General Modeling Assumptions — Continued

CRA Section and Appendix		Code	Modeling Assumption	Related FEP in Attachment SCR	Assumption Considered*
			seals.	Speciation (W56)	
6.4.5 The Salado MASS-13.0 Salado					
		BRAGFLO	General Assumptions 1 to 8.		See above
6.4.5.1 Impure Halite MASS-13.1 High Threshold Pressure for Halite-Rich Salado Rock Units					
		BRAGFLO	Rock and hydrologic properties are constant.	Stratigraphy (N1)	R
6.4.5.2 Salado Interbeds MASS-13.3 The Fracture Model					
		BRAGFLO	Interbeds have a fracture-initiation pressure above which local fracturing and changes in porosity and permeability occur in response to changes in pore pressure. A power function relates the permeability increase to the porosity increase. A pressure is specified above which porosity and permeability do not change.	Disruption caused by gas effects (W25)	R
		BRAGFLO	Interbeds have identical physical properties; they differ only in position, thickness, and some fracture parameters.	Saturated groundwater flow (N23)	R
6.4.5.3 Disturbed Rock Zone MASS-13.4 Flow in the Disturbed Rock Zone					
		BRAGFLO	The permeability of the DRZ is sampled with the low value similar to intact halite and a high value representing a fractured material. The DRZ porosity is equal to the porosity of impure halite to plus 0.29 percent.	Disturbed rock zone (W18) Roof falls (W22) Gas explosions (W27) Seismic activity (N12) Underground boreholes (W39)	C-R
6.4.5.4 Actinide Transport in the Salado MASS-13.5 Actinide Transport in the Salado					
		NUTS	Dissolved actinides and colloidal actinides are transported by advection in the Salado. Diffusion and dispersion are assumed negligible.	Advection (W90) Diffusion (W91) Matrix diffusion (W92)	R
		NUTS	Sorption of actinides in the anhydrite interbeds, colloid retardation, colloid transport at higher than average velocities, co-precipitation of minerals containing actinides, channeled flow, and viscous fingering are not	Actinide sorption (W61) Colloid transport (W78) Colloid filtration (W80) Colloid sorption (W81) Fluid flow caused by gas production (W42)	R

Table MASS-1. General Modeling Assumptions — Continued

CRA Section and Appendix		Code	Modeling Assumption	Related FEP in Attachment SCR	Assumption Considered*
			modeled.	Fracture flow (N25)	
		NUTS	Radionuclides having the same elemental form are grouped as discussed in Appendix TRU WASTE.	Radioactive decay and ingrowth (W12)	R
		NUTS	Sorption of actinides in the borehole is not modeled.	Actinide sorption (W61)	C
6.4.6 Units Above the Salado MASS-14.0 Geologic Units above the Salado					
		SECOTP2D	Above the Salado, lateral actinide transport to the accessible environment can occur only through the Culebra.	Saturated groundwater flow (N23) Unsaturated groundwater flow (N24) Solute transport (W77)	R
6.4.6.1 Los Medańos					
		MODFLOW-2000 BRAGFLO	The Los Medańos member of the Rustler Formation, Tamarisk, and Forty-niner are assumed to be impermeable.	Saturated groundwater flow (N23)	C
6.4.6.2 The Culebra MASS-15.0 Culebra Attachment TFIELD					
		MODFLOW-2000 SECOTP2D	General Assumptions 1, 6, and 8 (see first page of this table).		See above
		MODFLOW-2000 SECOTP2D	For fluid flow the Culebra is modeled as a uniform (single-porosity) porous medium. For radionuclide transport a double-porosity model is used (advection in high permeability features and diffusion and sorption in low-permeability features).	Saturated groundwater flow (N23) Fracture flow (N25) Advection (W90) Diffusion (W91)	R
		MODFLOW-2000	The Culebra flow field is determined from the observed hydraulic conditions and estimates of the effects of climate change and potash mining outside the controlled area, and does not change with time unless mining is predicted to occur in the disposal system in the future.	Saturated groundwater flow (N23) Climate change (N61) Precipitation (for example, rainfall) (N59) Temperature (N60) Changes in groundwater flow caused by mining (H37)	R
		BRAGFLO	The Culebra is assigned a single permeability to calculate brine flow into the unit from an intrusion borehole.	Natural borehole fluid flow (H31) Waste-induced borehole flow (H32)	R

Table MASS-1. General Modeling Assumptions — Continued

CRA Section and Appendix		Code	Modeling Assumption	Related FEP in Attachment SCR	Assumption Considered*
		MODFLOW-2000	Gas flow in the Culebra is not modeled. Gas from the repository does not affect fluid flow in the Culebra.	Saturated groundwater flow (N23) Fluid flow caused by gas production (W42)	R
		BRAGFLO MODFLOW-2000 SECOTP2D	Different thickness of the Culebra are assumed for BRAGFLO, MODFLOW-2000, and SECOTP2D calculations, although the transmissivities are consistent.	Effects of preferential pathways (N27)	R
		PEST	Uncertainty in the spatial variability of the Culebra transmissivity is accounted for by statistically generating many T-fields.	Saturated groundwater flow (N23) Fracture flow (N25) Shallow dissolution (N16)	R
		MODFLOW-2000 BRAGFLO	Potentiometric heads are set on the edges of the regional grid to represent flow in a portion of a much larger hydrologic system.	Groundwater recharge (N54) Groundwater discharge (N53) Changes in groundwater recharge and discharge (N56) Infiltration (N55)	R
6.4.6.2.1 Transport of Dissolved Actinides in the Culebra MASS-15.2 Dissolved Actinide Transport and Retardation in the Culebra					
		SECOTP2D	Dissolved actinides are transported by advection in high-permeability features and diffusion in low permeability features.	Solute transport (W77) Advection (W90) Diffusion (W91) Matrix diffusion (W92)	R
		SECOTP2D	Sorption occurs on dolomite in the matrix. Sorption on clays present in the Culebra is not modeled.	Actinide sorption (W61) Changes in sorptive surfaces (W63)	C
		SECOTP2D	Sorption is represented using a linear isotherm model.	Actinide sorption (W61) Kinetics of sorption (W62)	R
		SECOTP2D	The possible effects on sorption of the injection of brines from the Castile and Salado into the Culebra are accounted for in the distribution of actinide K_ds.	Actinide sorption (W61) Groundwater geochemistry (N36, N37) Natural borehole fluid flow (H31)	R
		SECOTP2D	Hydraulically-significant fractures are assumed to be present everywhere in the Culebra.	Advection (W90)	C
6.4.6.2.2 Transport of Colloidal Actinides in the Culebra MASS-15.3 Colloidal Actinide Transport and Retardation in the Culebra					

Table MASS-1. General Modeling Assumptions — Continued

CRA Section and Appendix		Code	Modeling Assumption	Related FEP in Attachment SCR	Assumption Considered*
		SECOTP2D	Humic actinides are chemically retarded identically to dissolved actinides and are treated as dissolved actinides.	Advection (W90) Diffusion (W91) Colloid transport (W78) Microbial transport (W87)	R
		SECOTP2D	The concentration of intrinsic colloids is sufficiently low to justify elimination from PA transport calculations.		R
		SECOTP2D	Microbial colloids and mineral fragments are too large to undergo matrix diffusion. Filtration of these colloids occurs in high permeability features (which is modeled using a decay approach). Attenuation is so effective that associated actinides are assumed to be retained within the disposal system and are not transported in SECOTP2D.	Microbial transport (W87) Colloid sorption (W81)	R
6.4.6.2.3 Subsidence Due to Potash Mining MASS-15.4 Subsidence Caused by Potash Mining in the Culebra					
		MODFLOW-2000	The effect of potash mining is to increase the hydraulic conductivity in the Culebra by a factor from 1 to 1,000.	Potash mining (H13) Changes in groundwater flow caused by mining (H37)	Reg.
6.4.6.3 The Tamarisk					
		MODFLOW-2000 BRAGFLO	The Tamarisk is assumed to be impermeable.	Saturated groundwater flow (N23)	R
6.4.6.4 The Magenta					
		BRAGFLO	General Assumptions 1 to 8 (see first page of this table).		See above
		BRAGFLO	The Magenta permeability is set to the lowest value measured near to the center of the WIPP site. This increases the flow into the Culebra.	Saturated groundwater flow (N23)	R
		NUTS	No radionuclides entering the Magenta will reach the accessible environment. However, the volumes of brine and actinides entering and stored in the Magenta are modeled.	Solute transport (W77)	R
6.4.6.5 The Forty-niner					
		BRAGFLO	The Forty-niner is assumed to be impermeable.	Saturated groundwater flow (N23)	R
6.4.6.6 Dewey Lake					

Table MASS-1. General Modeling Assumptions — Continued

CRA Section and Appendix		Code	Modeling Assumption	Related FEP in Attachment SCR	Assumption Considered*
		BRAGFLO	General Assumptions 1 to 8 (see first page of this table).		See above
		NUTS	The sorptive capacity of the Dewey Lake is sufficiently large to prevent any release over 10,000 years.	Saturated groundwater flow (N23) Actinide sorption (W61)	R
6.4.6.7 Supra-Dewey Lake Units					
		BRAGFLO	General Assumptions 1 to 8 (see first page of this table).		See above
		BRAGFLO	The units above the Dewey Lake are a single hydrostratigraphic unit.	Stratigraphy (N1)	R
		BRAGFLO	The units are thin and predominantly unsaturated.	Unsaturated groundwater flow (N24) Saturated groundwater flow (N23)	R
6.4.7 The Intrusion Borehole MASS-16.0 Intrusion Borehole					
6.4.7.1 Releases During Drilling					
		CUTTINGS_S BRAGFLO DRSPALL	Any actinides that enter the borehole are assumed to reach the surface.	—	C
MASS-16.1 Cuttings, Cavings, and Spall Releases during Drilling					
		BRAGFLO PANEL CUTTINGS_S DRSPALL	Future drilling practices will be the same as they are at present.	Oil and gas exploration (H1) Potash exploration (H2) Oil and gas exploitation (H4) Other resources (H8) Enhanced oil and gas recovery (H9)	Reg.
		CUTTINGS_S DRSPALL	Releases of particulate waste material are modeled (cuttings, cavings, and spallings). Releases are corrected for radioactive decay until the time of intrusion.	Drilling fluid flow (H21) Suspension of particles (W82) Cuttings (W84) Cavings (W85) Spallings (W86)	R
		CUTTINGS_S	Degraded waste properties are based on properties of marine clays, considered a worst case	Cavings (W85)	C
		DRSPALL	A hemispherical geometry with one-dimensional spherical symmetry defines the flow field and cavity in the waste	Spallings (W86)	**C**
		DRSPALL	Tensile strength, based on completely degraded waste surrogates, is felt to	Spallings (W86)	**C**

Table MASS-1. General Modeling Assumptions — Continued

CRA Section and Appendix		Code	Modeling Assumption	Related FEP in Attachment SCR	Assumption Considered*
			represent extreme, low-end tensile strengths because it does not account for several strengthening mechanisms		
		DRSPALL	Shape factor is 0.1, corresponding to particles that are easier to fluidize and entrain in the flow	Spallings (W86)	**C**
6.4.7.1.1 Direct Brine Release During Drilling MASS-16.2 Direct Brine Releases during Drilling					
		BRAGFLO PANEL	Brine containing actinides may flow to the surface during drilling. Direct brine release will have negligible effect on the long-term pressure and saturation in the waste panel.	Blowouts (W23)	R
		BRAGFLO	A two-dimensional grid (one degree dip) on the scale of the waste disposal region is used for direct brine release calculations.	Blowouts (H23)	R
		BRAGFLO CCDFGF	Calculation of direct brine release from several different locations provides reference results for the variation in release associated with location.	Blowouts (H23)	R
6.4.7.2 Long-Term Releases Following Drilling MASS-16.3 Long-Term Properties of the Abandoned Intrusion Borehole					
		BRAGFLO CCDFGF	Plugging and abandonment of future boreholes are assumed to be consistent with practices in the Delaware Basin.	Natural borehole fluid flow (H31) Waste-induced borehole flow (H32)	Reg.
6.4.7.2.1 Continuous Concrete Plug through the Salado and Castile					
		BRAGFLO CCDFGF	A continuous concrete plug is assumed to exist throughout the Salado and Castile. Long-term releases through a continuous plug are analogous to releases through a sealed shaft.	Natural borehole fluid flow (H31) Waste-induced borehole flow (H32)	Reg-R
6.4.7.2.2 The Two-Plug Configuration					
		BRAGFLO	A lower plug is located between the Castile brine reservoir and underlying formations. A second plug is located immediately above the Salado. The brine reservoir and waste panel are in direct communication though an open cased hole.	Natural borehole fluid flow (H31) Waste-induced borehole flow (H32)	Reg.-R
		BRAGFLO	The casing and upper concrete plug	Natural borehole fluid	R

Table MASS-1. General Modeling Assumptions — Continued

CRA Section and Appendix		Code	Modeling Assumption	Related FEP in Attachment SCR	Assumption Considered*
			are assumed to fail after 200 years, and the borehole is assumed to be filled with silty-sand like material. At 1,200 years after abandonment the permeability of the borehole below the waste panel is decreased by one order of magnitude as a result of salt creep.	flow (H31) Waste-induced borehole flow (H32)	
6.4.7.2.3 The Three-Plug Configuration					
		BRAGFLO	In addition to the two plug configuration, a third plug is placed within the Castile above the brine reservoir. The third plug is assumed not to fail over the regulatory time period.	Natural borehole fluid flow (H31) Waste-induced borehole flow (H32)	Reg.-R
6.4.8 Castile Brine Reservoir MASS-18.0 Castile Brine Reservoir					
		BRAGFLO	The Castile region is assigned a low permeability, which inhibits fluid flow. Brine occurrences in the Castile are bounded systems. Brine reservoirs under the waste panels are assumed to have limited extent and interconnectivity, with effective radii on the order of several hundred meters.	Brine reservoirs (N2)	R
6.4.9 Climate Change MASS-17.0 Climate Change					
		SECOTP2D	Climate-related factors are treated through recharge. A parameter called the Climate Index is used to scale the Culebra flux field.	Climate change (N61) Temperature (N60) Precipitation (for example, rainfall) (N59)	R
6.4.10 Initial and Boundary Conditions for Disposal System Modeling					
6.4.10.1 Disposal System Flow and Transport Modeling (BRAGFLO and NUTS)					
		BRAGFLO	There are no gradients for flow in the far-field of the Salado, and pressures are above hydrostatic, but below lithostatic. Excavation and waste emplacement result in partial drainage of the DRZ.	Saturated groundwater flow (N23) Brine inflow (W40)	R
		BRAGFLO	An initial water-table surface is set in the Dewey Lake at an elevation of 3,215 ft (980 m) above mean sea level. The initial pressures in the Salado are extrapolated from a sampled pressure in MB139 at the	Saturated groundwater flow (N23)	R

Table MASS-1. General Modeling Assumptions — Continued

CRA Section and Appendix		Code	Modeling Assumption	Related FEP in Attachment SCR	Assumption Considered*
			shaft and are in hydrostatic equilibrium. The excavated region is assigned an initial pressure of one atmosphere. The liquid saturation of the waste-disposal region is consistent with the liquid saturation of emplaced waste. Other excavated regions are assigned zero liquid saturation, except the shaft which is fully saturated.		
		NUTS	Molecular transport boundary conditions are no diffusion or dispersion in the normal direction across far-field boundaries. Initial actinide concentrations are zero everywhere except in the waste.	Radionuclide decay and ingrowth (W12) Solute transport (W77)	R
6.4.10.2 Culebra Flow and Transport Modeling (MODFLOW-2000, SECOTP2D)					
		MODFLOW-2000	Constant head and no flow boundary conditions are set on the far-field boundaries of the flow model.	Saturated groundwater flow (N23)	R
		MODFLOW-2000	Initial actinide concentrations in the Culebra are zero.	Solute transport (W77)	R
6.4.10.3 Initial and Boundary Conditions for Other Computational Models					
		NUTS PANEL BRAGFLO (direct brine release) CUTTINGS_S	Initial and boundary conditions interpolated from previously executed BRAGFLO calculation.		R
6.4.12 Sequences of Future Events					
		CCDFGF	Each 10,000 year future (random sequence of future events) is generated by randomly and repeatedly sampling: the time between drilling events; the location of drilling events; the activity level of the waste penetrated by each drilling intrusion; the plug configuration of the borehole, and the penetration of a Castile brine reservoir, and by randomly sampling the occurrence of mining in the disposal system.	Oil and gas exploration (H1) Potash exploration (H2) Oil and gas exploitation (H4) Other resources (H8) Enhanced oil and gas recovery (H9) Natural borehole fluid flow (N31) Waste-induced borehole flow (H32)	Reg.-R
6.4.12.1 Active and Passive Institutional Controls in Performance Assessment Chapter 7.0					
		CCDFGF	Active institutional controls are effective for 100 years and completely eliminate possibility of		Reg.-R

Table MASS-1. General Modeling Assumptions — Continued

CRA Section and Appendix		Code	Modeling Assumption	Related FEP in Attachment SCR	Assumption Considered*
			incompatible activities. No credit is taken for passive institutional controls.		
6.4.12.2 Number and Time of Drilling Intrusions					
		CCDFGF	Drilling may occur after 100 years according to a Poisson process.	Loss of records (H57) Oil and gas exploration (H1) Potash exploration (H2) Oil and gas exploitation (H4) Other resources (H8)	Reg.-R
6.4.12.3 Location of Intrusion Boreholes					
		CCDFGF	The waste disposal region is discretized with 144 regions with the probability of each region being intersected equal. A borehole can penetrate only one region.	Disposal geometry (W1)	R
6.4.12.4 Activity of the Intersected Waste Appendix TRU WASTE					
		CCDFGF	693 waste streams identified for contact-handled (CH)-TRU and all 86 remote-handled (RH)-TRU waste streams were grouped (binned) together into one equivalent or average (WIPP-scale) RH-TRU waste stream.	Heterogeneity of waste form (W3)	R
6.4.12.5 Diameter of the Intrusion Borehole CCA Appendix DEL					
		CUTTINGS_S	The diameter of the intrusion borehole is constant at 12.25 in. (31.12 cm).		Reg.-R
6.4.12.6 Probability of Intersecting a Brine Reservoir					
		CCDFGF	One brine reservoir is assumed to exist below the waste panels. The probability that a deep borehole intersects a brine reservoir below the waste panels is sampled uniformly from 0.01 to 0.60.	Brine reservoirs (N2)	R
6.4.12.7 Plug Configuration in the Abandoned Intrusion Borehole					
		CCDFGF	The two-plug configuration has a probability of 0.698. The three-plug configuration has a probability of 0.289. The continuous concrete plug has a probability of 0.015.		Reg.-R
6.4.12.8 Probability of Mining Occurring in the Land Withdrawal Area					

Table MASS-1. General Modeling Assumptions — Continued

CRA Section and Appendix		Code	Modeling Assumption	Related FEP in Attachment SCR	Assumption Considered*
		CCDFGF	Mining in the disposal system occurs a maximum of once in 10,000 years (a 10^{-4} probability per year).		Reg.-R
6.4.13 Construction of a Single CCDF					
		CCDFGF	Deterministic calculations are executed with BRAGFLO, NUTS, MODFLOW-2000, SECOTP2D, CUTTINGS_S, and PANEL to generate reference conditions. These reference conditions are used to estimate the consequences associated with random sequences of future events. These are in turn used to develop CCDFs.		R
		CCDFGF	10,000 random sequences of future events are generated for each CCDF plotted.		R
6.4.13.1 Constructing Consequences of the Undisturbed Performance Scenario					
		CCDFGF	A BRAGFLO and NUTS calculation with undisturbed conditions is sufficient for estimating the consequences of the undisturbed performance scenario.		R
6.4.13.2 Scaling Methodology for Disturbed Performance Scenarios					
		CCDFGF	Consequences for random sequences of future events are constructed by scaling the consequences associated with deterministic calculations (reference conditions) to other times, generally by interpolation but sometimes by assuming either similarity or no consequence.		R
6.4.13.3 Estimating Long-Term Releases from the E1 Scenario					
		CCDFGF NUTS	Reference conditions are calculated or estimated for intrusions at 100, 350, 1,000, 3,000, 5,000, 7,000, and 9,000 years.	Waste-induced borehole flow (H32)	R
6.4.13.4 Estimating Long-Term Releases from the E2 Scenario					
		CCDFGF NUTS SECOTP2D	The methodology is similar to the methodology for the E1 scenario. For multiple E1 intrusions into the same panel, the additional source term to the Culebra for the second and subsequent intrusions is assumed to be negligible.	Waste-induced borehole flow (H32) Waste inventory (W2)	R

Table MASS-1. General Modeling Assumptions — Continued

CRA Section and Appendix		Code	Modeling Assumption	Related FEP in Attachment SCR	Assumption Considered*
6.4.13.5 Estimating Long-Term Releases from the E1E2 Scenario					
		CCDFGF PANEL	The concentration of actinides in liquid moving up the borehole assumes homogeneous mixing within the panel.	Waste-induced borehole flow (H32)	C
		PANEL	Any actinides that enter the borehole reach the Culebra.	Waste-induced borehole flow (H32)	C
		CCDFGF PANEL	Reference conditions are calculated or estimated for intrusion at 100, 300, 1,000, 2,000, 4,000, 6,000 and 9,000 years.	Oil and Gas Exploration (H1)	
6.4.13.6 Multiple Scenario Occurrences					
		CCDFGF PANEL	The panels are assumed not to be interconnected for long term brine flow.	Saturated groundwater flow (N23) Unsaturated groundwater flow (N24)	R
6.4.13.7 Estimating Releases During Drilling for All Scenarios					
		CCDFGF PANEL NUTS	Repository conditions will be dominated by Castile brine if any borehole connects to a brine reservoir.	Brine reservoirs (N2) Natural borehole fluid flow (H31)	R
		CUTTINGS_S PANEL CCDFGF	Depletion of actinides in parts of the repository that have been penetrated by boreholes is not accounted for in calculating the releases from subsequent intrusions at such locations.	Waste-induced borehole flow (N32) Waste inventory (W2)	C
6.4.13.8 Estimating Releases in the Culebra and the Impact of the Mining Scenario					
		CCDFGF MODFLOW-2000 SECOTP2D	Releases from intrusions at random times in the future are scaled from releases calculated at 100 years with a unit source of radionuclides in the Culebra.		R
		CCDFGF	Actinides in transit in the Culebra when mining occurs are transported in the flow field used for the undisturbed case. Actinides introduced subsequent to mining are transported in the flow field used for the disturbed case (that is, mined case).		R

* R = Reasonable
C = Conservative
Reg. - Based on regulatory guidance
See above - Refers to assumptions 1 through 8 listed at the beginning of this table.

Three other two-dimensional model geometries are used in performance assessment. For fluid flow and transport modeling in the Culebra, the geometry is a horizontal two-dimensional plane (see Sections 6.4.2 and 6.4.6.2). For modeling brine flow from the intruded panel to the borehole during drilling, the geometry is a two-dimensional, horizontal representation of a waste panel (see Section 6.4.7). For modeling brine flow that might occur between an E-type borehole and other boreholes penetrating the repository, the geometry used is a two-dimensional, horizontal representation of the entire repository (see Section 6.4.2). These geometries are mentioned here but not discussed in detail because they are components of other conceptual models requiring geometric assumptions.

The two-dimensional geometry developed for the Salado is based on the assumption that brine and gas flow will converge upon and diverge from the repository horizon. The impact of this conceptual model and its implementation in a two-dimensional grid has been compared to a model that does not make the assumption of convergent and divergent flow (see Attachment 4-1 for additional information). The conceptual model for the Salado includes the slight and variable dip of beds in the vicinity of the repository, which might affect fluid flow.

Above and below the repository, it is assumed that any flow between the borehole or shaft (see Section 6.4.3) and surrounding materials will converge or diverge. With respect to flow in units overlying the Salado, the only purpose of this conceptual model is to determine the quantity (flux) of fluid leaving or entering the borehole or shaft. Fluid movement through the units above the Salado is treated in a different conceptual model (see Section 6.4.6). Below the repository, the possible presence of a brine reservoir is considered to be important, so a hydrostratigraphic layer representing the Castile and a possible brine reservoir in it is included (see CCA Appendix MASS, Section MASS.4.2 for the disposal system geometry historical context prior to the CCA).

MASS-4.2 Change to Disposal System Geometry Since the CCA

Changes have been made to the disposal system geometry since the first WIPP certification. The disposal system geometry is specifically represented in BRAGFLO. This section describes the methodology used to create the two-dimensional BRAGFLO computational grid used for the 2004 PA calculations. The CRA-2004 grid is similar to that used for the CCA and PAVT, except for the differences that are described below.

The most important changes with respect to the CRA BRAGFLO grid are the implementation of the Option D panel closures and a simplified shaft seal model. Additional grid refinements have also been implemented to increase numerical accuracy and computational efficiency and to reduce numerical dispersion, but these refinements do not entail any changes to conceptual models. All conceptual model changes were approved by the Salado Flow Peer Review Panel in February 2003 (Caporuscio et al. 2003). For completeness, all changes from the CCA/PAVT grid are described here.

MASS-4.2.1 Baseline Grid Changes

The baseline grid used in the CCA and PAVT had (NX, NY) dimensions of (33, 31). The grid used for the CRA-2004 calculations has dimensions (68, 33). The specific changes that have been implemented in the CRA-2004 grid are listed below and then discussed in more detail in the following sections. Logical grids for the CCA/PAVT and CRA are shown in Figures MASS-3 and MASS-4.

Changes implemented in the CRA-2004 Grid:

1. A simplified shaft seal model is implemented,
2. Option D type panel closures are implemented,
3. Segmentation of the waste regions is increased,
4. A grid flaring method is redefined and simplified,
5. X spacing of the grid beyond the repository to the north and south is refined, and
6. Layers above and below MB 139 have been made relatively thin (~1 m thick), and Y-spacing in Salado has been changed.

MASS-4.2.2 Simplified Shaft Seal Model

A shaft seal model is included in the CRA-2004 grid, but it is implemented in a simpler fashion than was used for the CCA and PAVT. A detailed description of the parameters used to define the simplified model is discussed in AP-094 (James and Stein 2002) and the resulting

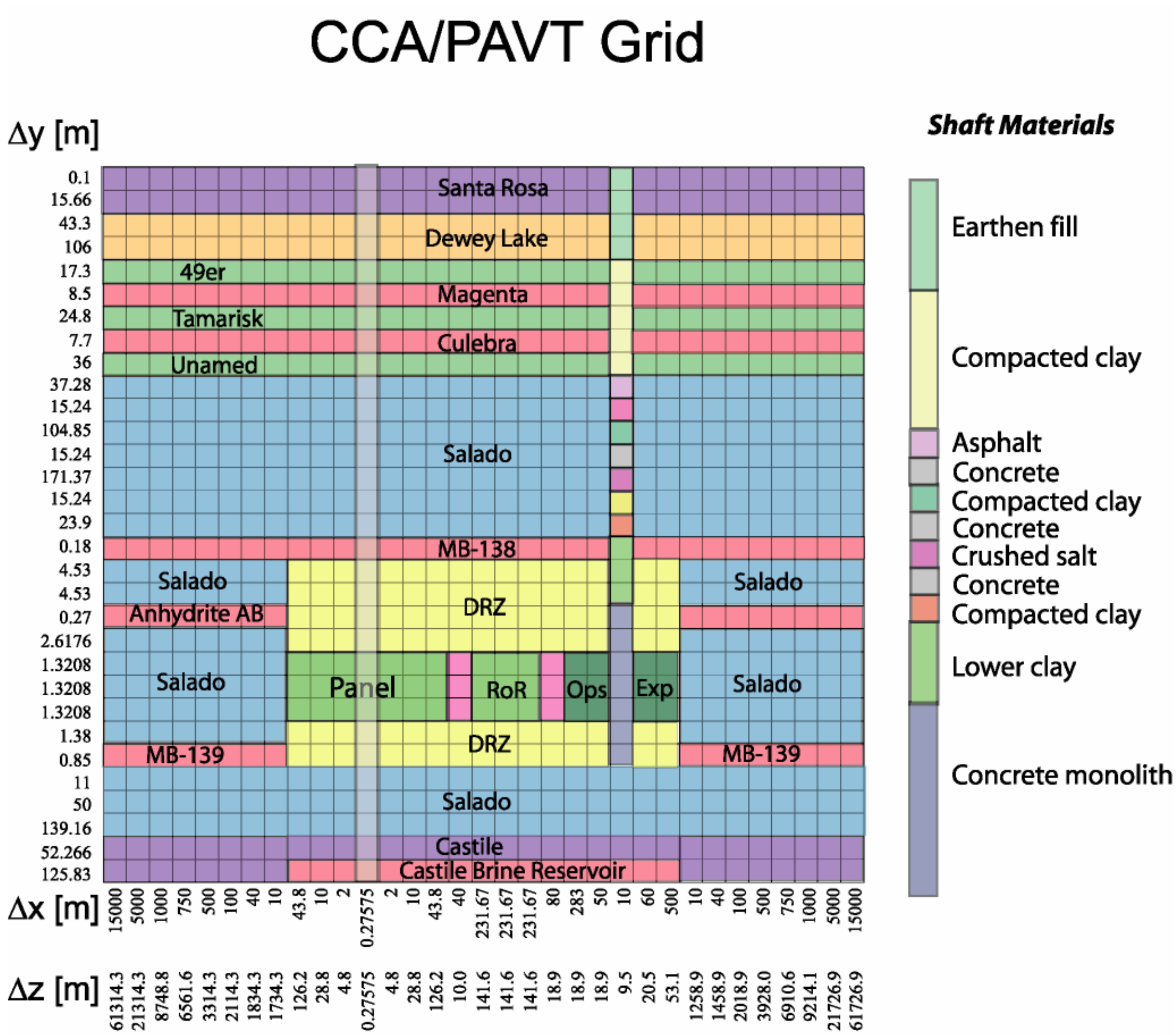

Figure MASS-3. Logical Grid Used for the 1996 WIPP PA BRAGFLO Calculations

analysis report (James and Stein 2003). The model that is used in the 2004 PA is described by Stein and Zelinski (2003a; 2003b), and was approved by the Salado Flow Peer Review panel (Caporuscio et al. 2003).

The new model does not alter the conceptual model of the shaft seal components as described in the CCA. Rather, it represents the behavior of seal components in the repository system model. Specifically, the original 11 separate material layers that defined the shaft model for the CCA were reduced to two layers each with properties equivalent to the composite effect of the original materials combined in series. Additionally, the six time intervals that were used to represent the evolution of the shaft seal materials over time were reduced to two intervals. The CRA and CCA shaft models are graphically compared in Figure MASS-5. The simplified shaft model was tested in the AP-106 calculations (Stein and Zelinski 2003a; 2003b), which supported the Salado Flow Peer Review. The results of this analysis demonstrated that brine flow through the simplified shaft model was comparable to brine flows seen through the

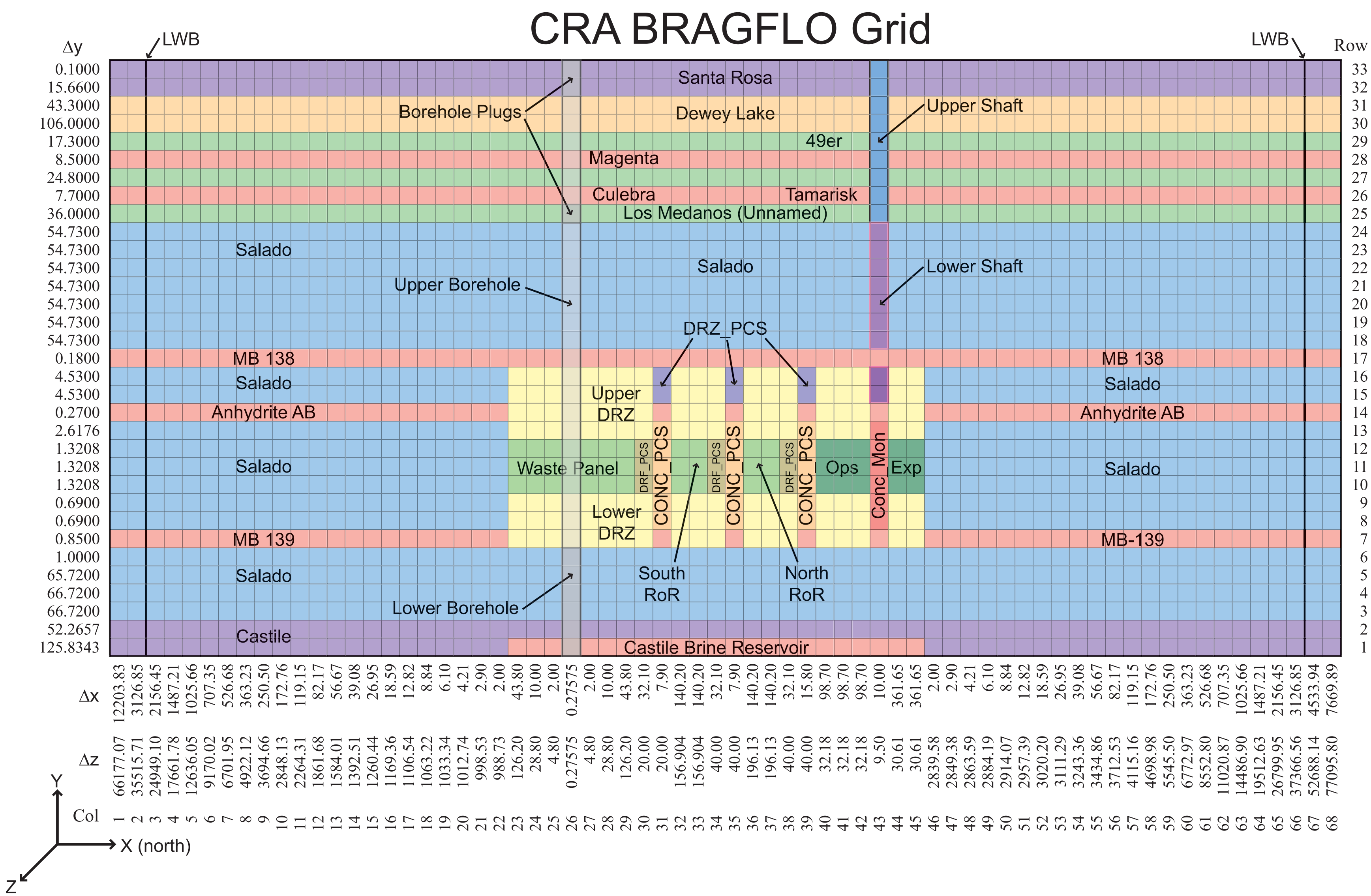

Figure MASS-4. Logical Grid Used for the 2004 PA BRAGFLO Calculations

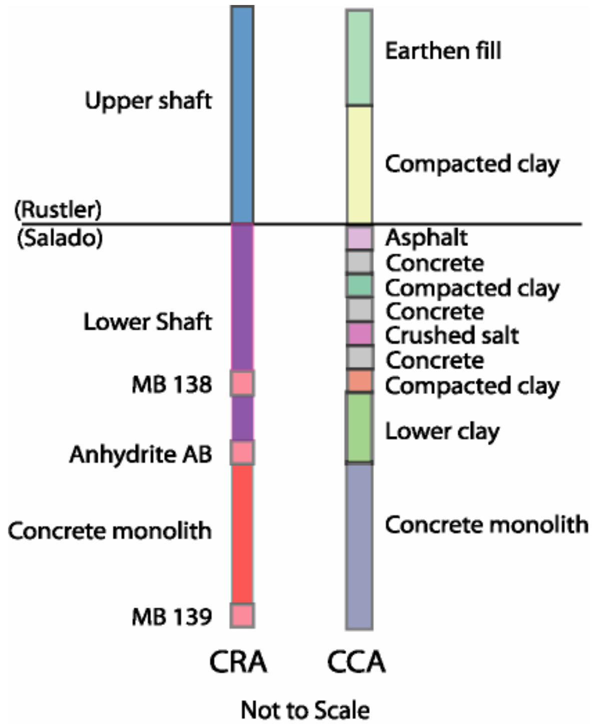

Figure MASS-5. Comparison of the Simplified Shaft (CRA-2004) and the Detailed Shaft (CCA) Models

detailed shaft model in the 1997 PAVT calculations. The conclusion remains that the shaft seals are very effective barriers to flow throughout the 10,000-year regulatory period.

MASS-4.2.3 Implementation of Option D Type Panel Closure

In the CCA, the DOE presented four options for panel closure designs (A through D). Upon reviewing the CCA, the EPA mandated the implementation of the Option D design. For CRA-2004, the true cross-sectional area of the Option D panel closures is represented in the flow model. In addition, to appropriately represent the effect of Option D geometry on repository fluid flow, the segmentation of the waste regions was increased in the grid. This change is described fully in MASS-4.2.4.

For CRA-2004, three sets of panel closures are included in the model domain. The southernmost set of closures represents a pair of closures separating a single waste panel from the other waste areas. The middle set of closures represents four panel closures that will be emplaced between the southern and northern extended panels. The northernmost set of panel closures represents two sets of four panel closures that will be emplaced between the waste regions and the shaft seals.

Each set of panel closures is represented in the CRA-2004 grid with four materials. Refer to Figure MASS-6.

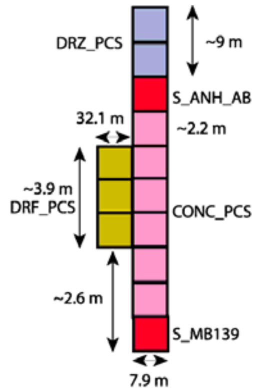

Figure MASS-6. Logical Grid Representation of the Option D Panel Closures for the CRA.

1. CONC_PCS: This material represents the concrete monolith, which has properties of SMC.

2. DRZ_PCS: This material represents the DRZ immediately above the concrete monolith that is expected to heal after the emplacement of the monolith.

3. DRF_PCS: This material represents the empty drift and explosion wall portion of the panel closure. This material has the same properties as WAS_AREA (including creep closure).

4. Marker bed materials: These materials are the same as those used to represent the anhydrite marker beds in other parts of the grid. Marker bed materials were used because they have permeability ranges very close to the material CONC_PCS and in the case when pressures near the panel closures exceed the fracture initiation pressure of the marker beds, fractures could extend around the concrete monolith out of the 2-D plane represented by the numerical grid. By using marker bed materials to represent the parts of the panel closures that intersect marker beds, both the permeability of the closure and the potential fracture behavior of marker bed material near the closures are represented.

Figure MASS-7 is a schematic diagram comparing the panel closure implementation in the CCA and CRA-2004 grids. Permeability ranges are indicated for all materials. Figure MASS-6 shows the 13 grid cells used to represent each set of Option D panel closures in the CRA-2004 BRAGFLO grid.

MASS-4.2.4 Increased Segmentation of Waste Regions in Grid

The CCA/PAVT grid divided the waste regions into two regions; a single panel in the southern end of the repository referred to as the Waste Panel, and a larger region containing the other nine panels referred to as the RoR. The Waste Panel is intersected by an intrusion borehole and is used to represent conditions in any panel that is intersected by a borehole. It is assumed that the Option D panel closures are effective at impeding flow between panels. Therefore, it was considered necessary to divide the RoR into northern and southern blocks

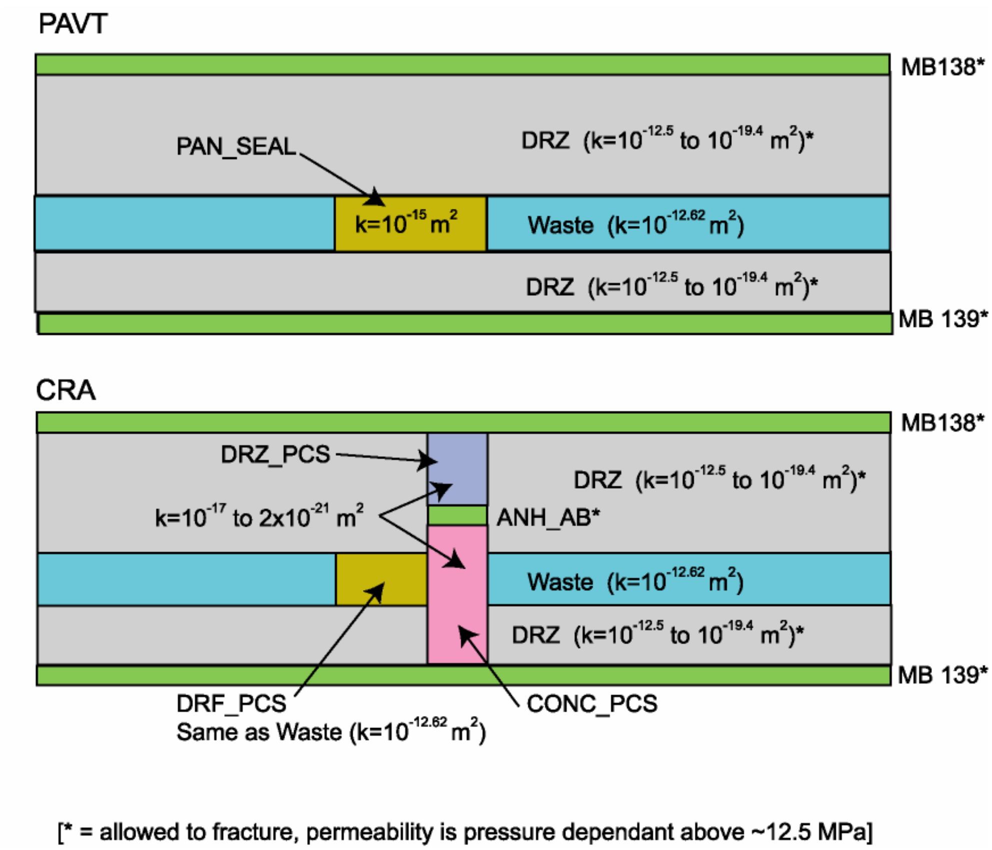

Figure MASS-7. Schematic Comparison of the Representation of Panel Closures in the PAVT and CRA-2004.

separated by a set of panel closures. The south RoR block represents conditions in a panel directly adjacent to an intruded panel. The north RoR block represents conditions in a nonadjacent panel far from the intruded panel (has at least two panel closures between it and the intruded panel). This representation assumes that the effects of drilling intrusions will be damped in nonintruded panels and the degree of damping will depend on the proximity of the drilling intrusion and the number of panel closures separating the intruded panel from other regions of the repository. The delta Z dimensions of the RoR blocks were chosen so that the volume of the southern and northern RoR blocks were equivalent to four and five panels, respectively.

It should be noted that the total volume of the waste-filled areas represented in the CCA/PAVT grid (approximately 4.36×10^5 m^3) was found to be approximately 0.5 percent less than the designed volume (approximately 4.38×10^5 m^3) (Stein 2002). For CRA-2004, the larger correct volume has been used.

MASS-4.2.5 Redefined and Simplified Grid Flaring Method

Grid flaring is a method to represent 3-D volumes in a 2-D grid. Flaring is used when flows can be represented as divergent and convergent from the center of flaring. The CCA/PAVT grid used flaring at two different scales: locally around the borehole and shaft, and regionally to the north and south of the excavated regions (around a point in the northern end of the RoR). For CRA-2004, the local flaring around the borehole is the same as in the CCA/PAVT grid. The local flaring around the shaft has been eliminated because it has been demonstrated not to be a release pathway. Likewise, the manner in which the regional flaring is calculated has been simplified.

The regional rectangular flaring occurs only for the grid blocks to the north and south of the excavated region. The CRA flaring is very similar to what was done for the CCA/PAVT grid; however the CRA flaring methodology is easier to implement. To define the flaring, it is assumed that looking from the top of the grid (x-z plane), the excavated regions of the grid can be approximated by a rectangle with length equal to the distance between the southern edge of the Waste Panel and the northern edge of the Experimental Area in the grid (x = 1830 m) and width, defined so that the area of the rectangle is equal to the total area of the excavated regions of the grid in the x-z plane (z = 80 m). In order to calculate the rectangular flaring for the grid cells outside the excavated regions, a centerline is defined to divides the flaring on the north and south. Because the waste panels are located in the southern part of the excavated area, the centerline is chosen to be the “center of waste” as the middle of the panel closure that separates the northern RoR from the southern RoR. The position of this center of the waste is described as the distances from the north and south edges of the gridded repository, DN and DS, respectively DN = 1378 m, DS = 452 m, DN + DS = 1830 m. Each flared grid block has length, Dx, and width, Dz. The block can be thought of as wrapped around the excavated area like half a rectangular onion, with the center at the center of waste (Figure MASS-8). Each Dz can be calculated from the preceding Dxs as follows.

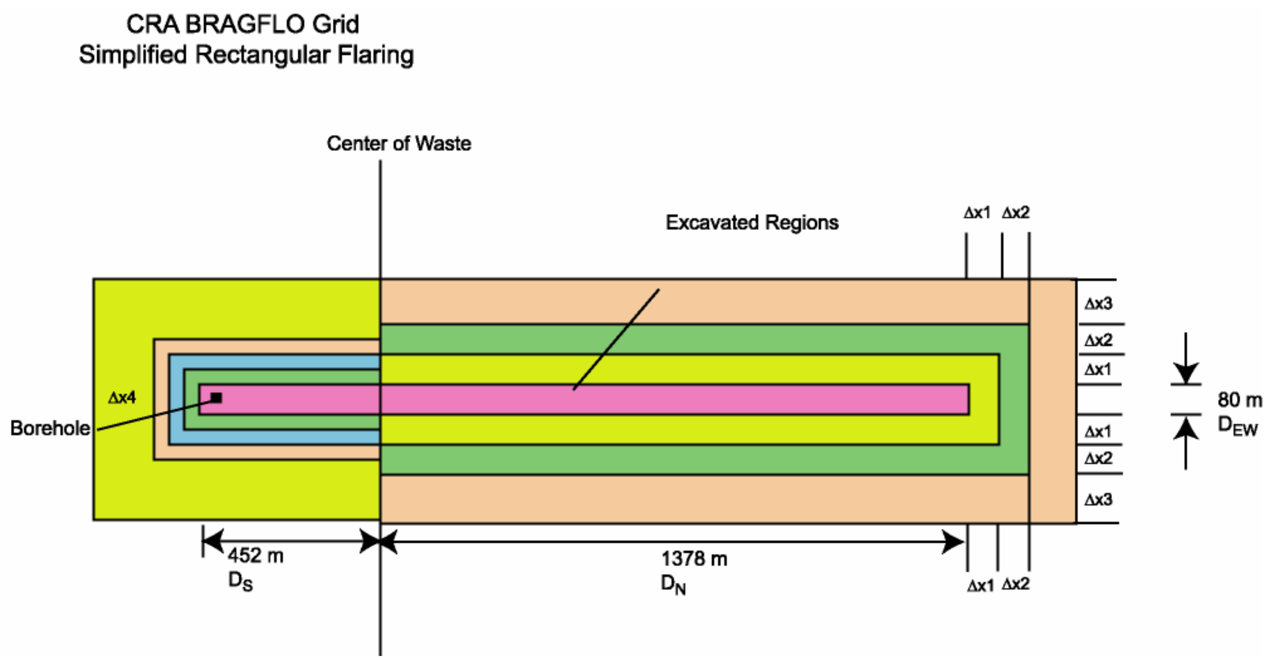

Figure MASS-8. CRA Flaring

For the northern end:

$$\Delta z_1 = 2D_N + D_{EW} + 2\Delta x_1$$

$$\Delta z_2 = 2D_N + D_{EW} + 4\Delta x_1 + 2\Delta x_2$$

$$\Delta z_3 = 2D_N + D_{EW} + 4\Delta x_1 + 4\Delta x_2 + 2\Delta x_3$$

Flaring for blocks wrapped around the southern end is the same with D_S substituted for D_N.

This method of rectangular flaring ensures that the grid accounts for all the volume surrounding the repository.

MASS-4.2.6 Refinement of the X-Spacing Outside the Repository

The grid blocks to the north and south of the excavated region will be refined in the x-direction from the baseline grid. The x-dimension of the grid cells immediately to the north and south of the repository start at 2 m and increases by a factor of 1.45. Exceptions to this are

$$\Delta z_n = 2D_N + D_{EW} + 4\sum_{i=1}^{n-1}\Delta x_i + 2\Delta x_n$$

made to ensure that the location of the Land Withdrawal Boundary (LWB) and the total extent of the grid matches that in the baseline grid. This refinement factor was chosen to reduce numerical dispersion caused by rapid increases in cell dimensions (Anderson and Woessner 1992; Wang and Anderson 1982).

MASS-4.2.7 Refinement of the Y-Spacing

In the y-direction, the grid spacing within layers representing the Salado has been changed from the CCA/PAVT. The CCA grid spacing in the Salado was dictated by the thickness of different shaft seal materials. Since the shaft is no longer represented in the model domain, the y spacing in the Salado is now uniform. In addition, two layers were added immediately above and below MB 139 to refine the grid spacing and reduce numerical dispersion. These changes result in a total of 33 y-divisions for the grid, and will increase the numerical accuracy of flow and transport calculations.

MASS-5.0 BRAGFLO GEOMETRY OF THE REPOSITORY

The repository geometry conceptual model is represented using the BRAGFLO code. As with the geometry of the disposal system discussed in Section 6.4.2.1 and earlier in this section, the principal process considered in setting up the repository geometry is fluid flow. Several features considered to be important in fluid flow are included in the conceptual model. The first is the overall dimension of the repository along the north-south trend of the cross section, as well as the major divisions within the repository (waste disposal region, operations region, and experimental region). The second is the volume of a single panel, because fluid flow to a borehole penetrating the repository can potentially access only the volume in a waste panel directly and other regions of the repository only by flow through or around a panel closure. The third is the physical dimensions of panel closures separating the single panel and the other major divisions of the repository.

Notably absent from the conceptual model for the long-term performance of the repository are pillars and individual drifts and rooms. These are excluded from the model for simplicity, and it is assumed that they have either negligible impact on fluid flow processes or, alternatively, that including them in the conceptual model would be beneficial to long-term performance because their presence could make flow paths more tortuous and decrease fluxes. This assumption includes lumping four and five of the 10 panels into the south RoR and north RoR regions respectively (see MASS-4.2.4).

The BRAGFLO model of the WIPP disposal system is a two-dimensional array of three-dimensional grid blocks. Each grid block has a finite length, width, height, volume, and surface area for its boundaries with neighboring grid blocks. The BRAGFLO two-dimensional grid is similar to any other two-dimensional grid used to treat flows, except that the grid-block dimension in the direction perpendicular (z-direction) to the plane of the grid varies from block to block as a function of the lateral direction (x-direction; see MASS-4.2.5). This allows the BRAGFLO grid to treat important geometric aspects of the WIPP disposal system, such as the very small intrusion borehole, the moderate-size shaft, and the larger controlled areas. The grid configurations used in the 1996 CCA PA and 1997 PAVT are shown in Figure MASS-3 while the 2004 PA grid is shown in Figure MASS-4.

MASS-5.1 Historical Context of the Repository Model

Several early models of repository fluid-flow behavior (models of radionuclide migration pathways, gas flow from the disposal area to the shaft, Salado brine flow through panel to borehole, effects of anhydrite layers on Salado brine flow through a panel, and flow from a brine reservoir through a disposal room) are summarized in a 1990 report (Rechard et al. 1990). In the preliminary performance assessment of 1992, all waste was lumped into a single region (WIPP Performance Assessment Department 1993). Because human intrusion boreholes were treated in detail for the 1996 performance assessment, it was necessary to model a single waste panel with a borehole surrounded by two-dimensional radial-flaring gridblocks. This approach is continued for the 2004 PA. The 1996 PA treated the remainder of the waste area as a single RoR. For the 2004 PA, the RoR is divided into two areas separated by a panel closure system. This change was made to more adequately simulate the effects of the Option D closure in impeding fluid flow between panels.

MASS-6.0 CREEP CLOSURE

The model used for creep closure of the repository is discussed in Appendix PA, Attachment PORSURF.4.11. Historical information is contained in CCA Appendix PORSURF.

MASS-7.0 REPOSITORY FLUID FLOW

This model represents the long-term flow behavior of liquid and gas in the repository and its interaction with other regions in which fluid flow may occur, such as the Salado, shafts, or intrusion borehole. This model is not used to represent the interaction of fluids in the repository with a borehole during drilling. Historical information on alternative conceptual models for brine inflow to the repository is contained in CCA Appendix MASS, Section MASS.7.

The third conceptual model for flow, the clay consolidation model, arises from observations made as part of the BSEP. On the basis of observations recorded during more than nine years of

The first principle in the conceptual model for fluid flow in the repository is that gas and brine can be both present and mobile (two-phase flow), governed by conservation of energy and mass and by Darcy's Law for their fluxes (see Appendix PA, Section PA-4.2). Consistent with typical concepts of two-phase flow, the phases can affect each other by impeding flow caused by partial saturation (relative permeability effects) and by affecting pressure caused by capillary forces (capillary pressure effects).

The flow of brine and gas in the repository is assumed to behave as two-phase, immiscible, Darcy flow (see Appendix PA, Section PA-4.2). BRAGFLO is used to simulate brine and gas flow in the repository and to incorporate the effects of disposal room closure and gas generation. Fluid flow in the repository is affected by the following factors:

- the geometrical association of pillars, rooms, and drifts; panel closure caused by creep; and possible borehole locations;
- the varied properties of the waste areas resulting from creep closure and heterogeneous contents;
- flow interactions with other parts of the disposal system; and
- reactions that generate gas.

The geometry of the panel around the intrusion borehole is consistent with the assumption that fluid flow there will occur directly toward or directly away from the borehole. The geometry represents a semi-circular volume north of the borehole and a semi-circular volume south of the borehole (representing the assumption of radial flow in a subregion of a two-dimensional representation of the repository.

Approximating convergent and divergent flow around the intrusion borehole creates a narrow neck in the otherwise fairly uniform width grid in the region representing the repository. In the undisturbed performance scenario and under certain conditions in other scenarios, flow in the repository may pass laterally through this neck. In reality, this neck does not exist. The presence in the model is expected to have a negligible or conservative impact on model predictions compared to predictions that would result from use of a more realistic model geometry. The time scale involved and the permeability contrast between the repository and surrounding rock are sufficient that lateral flow that may occur in the repository is restricted by the rate at which liquid gets into or out of the repository, rather than the rate at which it flows through the repository.

Gas generation is affected by the quantity of liquid in contact with metal. However, the distribution of fluid in the repository can be only approximated. For example, capillary action can create wicking that would increase the overall region in which gas generation occurs, but this cannot be modeled at the necessary resolution to fundamentally stimulate processes without undesirable effects on the duration of the model simulations. Therefore, as a bounding measure for gas generation purposes, brine in the repository is distributed to an extent greater than actually estimated by the Darcy flow models used and values of parameters chosen.

Option D panel closures and the surrounding rocks are represented by a group of materials, which include:

1. SMC,
2. a material representing the empty drift and explosion wall,
3. a material representing healed DRZ, and
4. Marker beds.

SMC and healed DRZ materials are assigned permeability values that are sampled independently from a distribution ranging from 2×10^{-21} to 1×10^{-17} m^2. This value range is considered reasonable because the shape of the Option D closure assumes a compressive state and concrete permeability range similar to the tighter end of the 1997 PAVT permeability. This range captures the uncertainty in the long-term performance of the Option D panel closure design.

Modeling of flow within the repository is based on homogenizing the room contents into relatively large computational volumes. The approach ignores heterogeneities in disposal room contents that may influence gas and brine behavior in the room by causing fluid flow among channels or preferential paths in the waste, bypassing entire regions. Isolated regions could exist for several reasons:

- they may be isolated by low-permeability regions of waste that serve as barriers,
- connectivity with the interbeds may occur only at particular locations within the repository, or
- the repository dip may promote preferential gas flow in the upper regions of the waste.

For the CCA, the adequacy of the repository homogeneity assumption was examined in screening analyses DR-1 (Webb 1995) and DR-6 (Vaughn et al. 1995a). The analyses used an additional parameter in BRAGFLO to specify the minimum active (mobile) brine flow saturation (pseudo-residual brine saturation). Above this saturation, the normal descriptions of two-phase flow apply (that is, either the Brooks and Corey or van Genuchten and Parker relative permeability models). Below this minimum, brine is immobile, although it is available for reaction and may still be consumed during gas-generation reactions. The assumption of a minimum saturation limit was justified based on the presumed heterogeneity of the waste and the slight dip in the repository. The minimum active brine saturation was treated as an uncertain parameter and sampled uniformly between values 0.1 and 0.8 during the analysis. This saturation limit was applied uniformly throughout the disposal room to bound the impact of heterogeneities on flow (Webb 1995; Vaughn et al. 1995a). Results of this analysis showed that releases to the accessible environment in the baseline case (homogenization) are consistently higher.

The experimental and operations regions were represented in performance assessment (for the CCA) by a fixed porosity of 18.0 percent and a permeability of 10^{-11} m^2. The combination of low porosity and high permeability conservatively overestimated fluid flow through these regions and limit the capacity of these regions to store fluids, thus potentially overestimating releases to the environment. This conclusion was based on a screening analysis (Vaughn et al. 1995b) that examined the importance of permeability varying with porosity in closure regions (waste disposal region, experimental region, and operations region). To perform this analysis, a model for estimating the change in permeability with porosity in the closure regions was implemented in BRAGFLO. A series of BRAGFLO simulations was performed to determine whether permeability varying with porosity in the closure regions could enhance contaminant migration to the accessible environment. Two basic scenarios were considered in the screening analysis, undisturbed performance and disturbed performance. To assess the sensitivity of system performance on dynamic permeability in the closure regions, CCDFs of normalized contaminated brine releases were constructed and compared with the corresponding baseline conditional CCDFs. The baseline model treated permeabilities in the closure regions as fixed values. Results of this analysis showed that the inclusion of dynamic closure of the waste disposal region, experimental region, and operations region in BRAGFLO resulted in computed releases to the accessible environment that are essentially equivalent to the baseline case.

A separate analysis (Park and Hansen 2003) examined the possible effects of heterogeneity in waste container and waste material strength on room closure. The analysis of room closure found that the room porosity may vary widely depending on the type of waste container and on the emplacement of waste in the repository. However, analysis of a separate PA (Hansen et al. 2003a) found that PA results are relatively insensitive to the uncertainty in room closure and room porosity. The conclusions of the separate PA are summarized in Section MASS-21.0.

MASS-7.1 Flow Interactions with the Creep Closure Model

The dynamic effect of halite creep and room consolidation on room porosity is modeled only in the waste disposal region. Other parts of the repository, such as the experimental region and the operations region, are modeled assuming fixed (invariant with time) properties. In these regions, the permeability is held at a fixed high value representative of unconsolidated material, while the porosity is maintained at relatively low values associated with highly consolidated material. It is assumed that this combination of low porosity and high permeability conservatively overestimates flow through these regions and minimizes the capacity of this material to store fluids, thus maximizing the release to the environment. To examine the acceptability of this assumption, a screening analysis (Vaughn et al. 1995c) evaluated the effect of including closure of the experimental region and operations region. In this analysis, consolidation of the experimental region and operations region was implemented in BRAGFLO by relating pressure and time to porosity using a porosity-surface method. The porosity surface for the experimental region and operations region differs from the one used for consolidation of the disposal room and is based on an empty excavation (see Appendix PA, Attachment PORSURF). Results of the screening analysis showed that disregarding dynamic closure of the experimental region is acceptable because it is conservative: lower releases occur when closure of the experimental region and operations region is computed compared to simulations with time-invariant high permeability and low porosity.

MASS-7.2 Flow Interactions with the Gas Generation Model

Gas generation affects repository pressure, which in turn is an important parameter in other processes such as two-phase flow, creep closure, and fracturing of the interbeds and DRZ. Gas generation processes considered in performance assessment calculations include anoxic corrosion and microbial degradation. Radiolysis is excluded from performance assessment calculations on the basis of laboratory experiments and a screening analysis (Vaughn et al. 1995d) that concluded that radiolysis does not significantly affect repository performance.

In modeling gas generation, the effective liquid in a computational cell is the computed liquid in that cell plus an adjustment to account for the uncertainty associated with wicking by the waste (see Appendix PA, Section PA-4.2). Capillary action (wicking) is the ability of a material to carry a fluid by capillary forces above the level it would normally seek in response to gravity. Because the current gas-generation model computes substantially different gas-generation rates depending on whether the waste is wet or merely surrounded by water vapor, the physical extent of wetting could be important. A screening analysis (Vaughn et al. 1995e) examined wicking and concluded that it should be included in performance assessment calculations. The baseline gas-generation model in BRAGFLO accounts for corrosion of iron and microbial degradation of cellulosics. The net reaction rate of these processes depends directly on brine saturation: an increase in brine saturation will increase the net reaction rate by weighting the inundated portion more heavily and the slower humid portion less heavily. To simulate the effect of wicking on the net reaction rate, an effective brine saturation, which includes a wicking saturation contribution, is used to calculate reaction rates rather than the actual brine saturation. To account for uncertainty in the wicking saturation contribution, this contribution was sampled from a uniform distribution that ranged from 0.0 to 1.0 for each BRAGFLO simulation in the analysis.

MASS-8.0 GAS GENERATION

This model represents the possible generation of gas in the repository by corrosion of steel and microbial degradation of cellulosic, plastic, and rubber (CPR) materials. Additional discussion of this topic may be found in Appendix PA, Section PA-4.2.5 and Attachment SCR (FEPs W44 through W48, W53, and N71) and Section 6.4.3.3.

Gas will be produced in the repository by a variety of chemical reactions, principally those between brine, metals, microbes, CPR materials and by liberation of dissolved gases to the gaseous phase. The processes assumed for long-term performance are anoxic corrosion of steel waste containers and Fe-base metals in the waste and possible microbial consumption of CPR materials in the waste (a significant quantity of plastic is also present as drum liners). Anoxic-corrosion reactions between brine and steel are expected to occur and produce H_2; they are included in the conceptual model. Microbial consumption of cellulosics, plastics and rubbers, might occur. If it does, it may produce various gases, primarily CH_4 and CO_2. However, by reaction with the MgO backfill that will be emplaced to control the chemistry of the repository, CO_2 produced by microbial activity will be rapidly removed from the gaseous phase (see Appendix PA, Attachment SOTERM, Section SOTERM-2.2.2; and Section 6.4.3.4). Other gases such as N_2 and H_2S produced by microbial activity are insignificant in quantity (see CCA Appendix MASS, Attachment 8-1). Thus the conceptual model for gas generation assumes that anoxic corrosion of steel will produce H_2; microbial consumption of CPR materials might occur and produce CH_4, CO_2, and other gases, but any CO_2 produced will be rapidly removed by reaction with MgO.

In the conceptual model, the rate of gas production in the repository by anoxic corrosion can be limited by several factors. Anoxic corrosion cannot occur unless brine (water) is present and in contact with steel. The corrosion rate is assumed to be dependent on brine saturation. Because anoxic corrosion consumes steel, the rate of gas production can be limited by the quantity of steel left in the repository. Because corrosion is a surface reaction, it proceeds at quantifiable rates per unit surface area of steel. In addition, anoxic corrosion consumes water. Because of these factors, the rate of gas generation in the repository can vary through time as conditions change. It is assumed that anoxic corrosion can occur in the repository as soon as the shafts are sealed.

Microbial consumption of CPR materials is limited by several factors, chiefly the long-term viability of microbes in the repository. Whether microbes consume plastics and rubbers is also important. The rate of microbial production is dependent on brine saturation. Because of uncertainty, however, it is assumed that there is no effect of microbial activity on brine (water) content in the repository.

A limited quantity of O_2 will be trapped in the panels after repository closure. However, this O_2 will be consumed quickly by both oxic corrosion and aerobic microbial activity, and reducing conditions will dominate in the repository over 10,000 years. The contribution of oxic corrosion and aerobic microbial activity to overall gas production is negligible. Thus, oxic reactions are not considered in the conceptual model for gas generation.

Addition of an MgO engineered barrier significantly reduces the impact of microbial production of CO_2 (see Appendix PA, Attachment SOTERM). As discussed in Section 6.4.3.4, the MgO backfill will react with carbon dioxide produced by microbial degradation and remove it from the gaseous phase.

Because the conceptual model comprises the general processes and interactions assumed to occur without direct reference to the mathematical equations used, no parameters are defined by this conceptual model. The mathematical model used to implement it, the average-stoichiometry model, is discussed in Section 6.4.3.3. The most important parameter in the average-stoichiometry model is the rate at which gas production occurs with brine and steel present, because this is the principal control on the total quantity of gas generated. The assumptions made about the principal reactions and their stoichiometries are also important, however, because they affect the quantity of gas created per unit quantity of steel and water reacted.

The feedback between the gas generation conceptual model and the repository fluid flow conceptual model is important to understand. Gas production cannot continue for long with the low initial quantity of liquid present in the waste, as specified by waste-acceptance criteria. For gas production to occur, brine must flow into the repository; for gas production to be sustained, brine consumed by gas production must be replenished. Gas production, however, tends to increase repository pressure and keep brine from flowing into it. Thus the rates at which various processes proceed are important in determining the conditions of the repository. There is important feedback as well between the gas-generation model and other conceptual models through pressure effects, such as those calculating creep closure (Section 6.4.3.1), interbed fracturing (Section 6.4.5.2), two-phase flow (Section 6.4.3.2), and the radionuclide release associated with spalling and direct brine release during an inadvertent drilling intrusion (Section 6.4.7).

Single-process laboratory studies of anoxic corrosion of steels and Al-based materials by R. E. Westerman and his colleagues at Pacific Northwest National Laboratory (PNNL) from November 1989 through September 1995 have shown that the factor with the greatest effect on the rate of H_2 generation by anoxic corrosion is the quantity of brine in WIPP disposal rooms (see also CCA Appendix MASS, Attachment 8-2). This is because anoxic corrosion occurs rapidly under inundated conditions, but not at all under humid conditions. The pressure difference between WIPP disposal rooms and the far field and the porosity of the room contents also affect the extent of brine inflow and outflow and, hence, the anoxic-corrosion rate. Because the average-stoichiometry model is incorporated in BRAGFLO, gas production is coupled with brine and gas inflow and outflow. Moreover, because BRAGFLO uses a porosity surface to simulate room closure (Butcher and Mendenhall 1993), it also couples gas production to room closure. Telander and Westerman (1993, 1997) and subsequent studies of anoxic corrosion at PNNL have shown that pH, pressure, and the composition of the gaseous phase also affect the H_2 production rate.

The greatest uncertainty in modeling gas generation in WIPP disposal rooms is whether microbial gas generation will occur and, if so, to what extent it will occur and what its effects will be. The following sources of microbial uncertainty have been described:

- whether microorganisms capable of carrying out the potentially significant respiratory pathways identified by Brush (1990) (denitrification sulfate (SO_4^{2-}) reduction, and methanogenesis) will be present when the repository is filled and sealed,
- whether these microbes will survive for a significant fraction of the 10,000-year period of performance of the repository,
- whether sufficient H_2O will be present in the waste or brine,
- whether sufficient electron acceptors (oxidants) will be present and available,
- whether enough nutrients, especially N and P, will be present and available,
- whether microbes will consume significant quantities of plastics and rubbers during the 10,000-year period of performance of the repository, and
- the stoichiometry of the overall reaction for each significant respiratory pathway, especially the number of moles of electron acceptors, nutrients, gases, and H_2O consumed or produced per mole of substrate consumed.

With regard to the first five of these uncertainties, it has been concluded that, although significant microbial gas production is possible, it is by no means certain. To incorporate this uncertainty in PA, it is assumed that there is a probability of 0.50 for significant microbial activity. In the event of significant microbial activity, microbes would consume 100 percent of the cellulosics in the repository. Furthermore, there is a probability of 0.50 that microbes would consume all of the plastics and rubbers after consuming all of the cellulosics. Thus, there is microbial consumption of all of the cellulosics, but no plastics or rubbers, in about 25 percent of the PA realizations (vectors); microbial consumption of all of the CPR materials in 25 percent of the vectors; and no microbial activity at all in the remaining 50 percent of the vectors (see CCA Appendix MASS, Attachment 8-3).

Single-process laboratory studies of microbial consumption of cellulosics by A.J. Francis and his colleagues at Brookhaven National Laboratory from May 1991 through September 2003 showed that if significant microbial activity occurs, the factor with the greatest effect on the microbial gas-generation rate is the quantity of brine in the repository (see Francis and Gillow 1994, 2000; Francis et al. 1997; Gillow and Francis 2001a, 2001b, 2002a, 2002b; CCA Appendix MASS, Attachment 8-2). This is because microbial gas production occurs rapidly under inundated conditions, but at much lower rates under humid conditions. These studies also found that inoculation with halophilic microbes from the WIPP site and nearby lakes, amendment with NO_3^- (an electron acceptor), amendment with nutrients, and addition of bentonite (a previously proposed backfill material) affect the rate or extent of microbial gas generation. Other factors that could affect the rate or extent of microbial gas generation, but which these studies did not quantify, are the pH; the dissolved or suspended concentrations of actinides or other heavy metals, which could inhibit or preclude microbial activity; and the concentrations of microbial byproducts, which could inhibit or preclude additional microbial activity. High pressure will not preclude or even inhibit microbial activity significantly, even when it increases to 150 atmospheres (lithostatic pressure at the depth of the repository).

Data summarized by Molecke (1979) imply that radiolysis of CPR materials will not be a significant, long-term gas-generation process in WIPP disposal rooms. (Radiolysis here refers to α radiolysis, the breaking of chemical bonds by α particles emitted during the radioactive decay of the actinide elements in TRU waste. Because molecular dissociation caused by other types of radiation will be insignificant in a TRU-waste repository such as the WIPP, this discussion considers only α radiolysis.) Based on calculations using the results of laboratory studies of brine radiolysis carried out for the WIPP by Reed et al. (1993) on estimates of the quantities of brine that could be present in the repository after filling and sealing, and on estimates of the solubilities of Pu, Am, Np, Th, and U summarized by Trauth et al. (1992), it was concluded that radiolysis of H_2O will not significantly affect the overall gas or H_2O content of the repository (see Appendix PA, Attachment SCR, FEP W52,).

Gas generation models are implemented in BRAGFLO with the assumption that the substrates (CPR materials and Fe-base metals) are homogeneously distributed throughout the waste. A separate PA (Hansen et al. 2003a) examined the possible effects of heterogeneity in substrate concentrations on PA results, and found that PA results are insensitive to the heterogeneity in substrate concentrations. The conclusions of the separate PA are summarized in Section MASS-21.0.

MASS-8.1 Historical Context of Gas Generation Modeling

See CCA Appendix MASS, Section MASS.8.1 for historical information that led to the CCA gas generation conceptual model.

MASS-9.0 CHEMICAL CONDITIONS

The models used for chemical conditions in the repository are discussed in Appendix BARRIERS and Appendix PA, Attachment SOTERM and Section 6.4.3.4.

MASS-10.0 DISSOLVED ACTINIDE SOURCE TERM

The models used for the dissolved actinide source term in the repository are discussed in Appendix PA, Attachments SOTERM and SCR and Section 6.4.3.5)

MASS-11.0 COLLOIDAL ACTINIDE SOURCE TERM

The models used for the colloidal actinide source term are discussed in Appendix PA, Attachment SOTERM (Section SOTERM.6) and Section 6.4.3.6.

MASS-12.0 SHAFTS AND SHAFT SEALS

The conceptual model for the shafts and shaft seals used in the performance assessment has been chosen to provide a reasonable and realistic basis for simulating long-term fluid flow through the shaft seal system and to allow evaluation of the effect that uncertainty about the long-term properties of the shaft seal system may have on cumulative radionuclide releases from the disposal system. The conceptual model and seal system design are also discussed in Section 6.4.4 and CCA Appendix SEAL (Section 2).

The conceptual model of the seals is based on results of detailed numerical models of the shaft seal system design. These models were developed to evaluate the performance of the shaft seal system under a range of conditions. Both fluid flow and structural response of the system have been evaluated. The principal uncertainties associated with the detailed models follow:

- reconsolidation of the crushed salt component,
- construction, permeability, and gas threshold pressure of the clay components, and
- damage, permeability, healing, and character of the Salado disturbed rock zones.

These uncertainties are also present in the performance assessment model and have been accounted for in the values specified for seal parameters. The consequences of uncertainty in seal component performance were a primary motivation in the development of the proposed seal system design. Although there is uncertainty in many of the materials and models, the shaft will be completely filled with high density, low permeability materials. The use of multiple materials and components for each sealing function results in a robust system. Time dependency of the performance of seal components is incorporated directly into the model through temporal variation in seal properties.

The processes that can affect the performance of the shaft seals—structural, hydraulic, and coupled structural and hydrological—are discussed in some detail in CCA Appendix SEAL, Sections 7 and 8. Evaluation of these issues required the use of existing structural and both single-and two-phase flow codes. In addition, development of conceptual and numerical models for crushed salt reconsolidation, the disturbed rock zone, and the shaft seal system was required. These models have been reviewed by independent, qualified experts, are well documented, and have been developed within an accepted quality assurance program. Codes used in the analyses include SPECTROM-32 (structural) (Callahan 1994), SWIFT II (single-phase flow) (Reeves et al. 1986), and TOUGH2 (multi-phase flow) (Pruess 1991). These codes were selected for their capability to simulate the processes thought to affect seal performance. They are also well-documented, accepted, and widely used within the scientific community. The codes were modified to implement the conceptual models specific to the seals, and these modifications were made within a program that establishes criteria for assuring software quality.

The BRAGFLO model of the shaft seal system requires consistency with parameters associated with the surrounding system. The BRAGFLO shaft seal model implemented for the 2004 PA calculations grouped several shaft seal materials into two composite materials having properties derived from the combination of grouped materials in series. For example, the permeability of the material used to represent the lower portion of the shaft seal that lies in the Salado formation is derived from the permeability and thickness of the asphalt, concrete crushed salt, and clay layers of the seal in this horizon. This permeability changes after 200 years to incorporate the combined effects of the consolidation of these materials. The effects of the halite DRZ surrounding the shafts is included in the derivation of the composite properties used in the BRAGFLO model. A detailed description of the shaft model used in the 2004 PA BRAGFLO calculations can be found in James and Stein (2002 and 2003).

MASS-12.1 Historical Development of the Shaft Seals

The four shafts into the repository will be sealed after completion of disposal activities at the WIPP. The shaft seal system design has evolved over time (Stormont 1988; Nowak et al. 1990; DOE 1995). The Initial Reference Seal System Design proposed a two-component design to achieve a sealing strategy with two phases: concrete and clay seals formed a short-term seal, and a crushed salt seal formed long-term protection. The use of native rock (that is, crushed salt) as a permanent sealing material is considered the most effective means to eliminate the shafts as a preferred pathway for migration of hazardous constituents. Because some interim period must pass for the crushed salt to reconsolidate to sufficiently high densities, short-term seals were proposed as a means to prevent fluid migration during the interim. Estimates of this interim period ranged from 100 to 200 years.

Seal design changes and refinements have been incorporated into the conceptual model of the seals used by the DOE (Bertram-Howery et al. 1990; WIPP Performance Assessment Department 1991; Sandia WIPP Project 1992). Performance assessments conducted prior to 1992 addressed general sealing issues but did not include specific seal components.

Results of the scoping calculations using the DCCA model demonstrated that low-permeability materials were required for the shaft seals (DOE 1995, Appendix D). However, the simplicity of the conceptual model limited the applicability of results to the detailed seal system design.

The shaft seal design for the WIPP is presented in CCA Appendix SEAL (Sections 4 and 5).

MASS-13.0 SALADO

The purpose of this model is to reasonably represent the effects of fluid flow in the Salado on long-term performance of the disposal system. The conceptual model is also discussed in Section 6.4.5.

Fluid flow in the Salado is considered in the conceptual model of long-term disposal system performance for several reasons. First, some liquid could move from the Salado to the repository because of the considerable gradients that can form for liquid flow inward to the repository. This possibility is important because such fluid can interact with creep closure, gas generation, actinide solubilities, and other processes occurring in the repository. Second, gas generated in the repository is thought to be capable of fracturing the Salado interbeds under certain conditions, creating increased permeability channels that could be pathways for lateral transport. The pathway of lateral transport in intact Salado is also modeled, but it is considered unlikely to result in any significant radionuclide transport to the accessible environment boundary.

The fundamental principle in the conceptual model for fluid flow in the Salado is that it is a porous medium within which gas and brine can be both present and mobile (two-phase flow), governed by conservation of energy and mass, and by Darcy's Law for their fluxes (see Appendix PA, Sections PA-4.2). Consistent with typical concepts of two-phase flow, each phase can affect the other by impeding flow because of partial saturation (relative permeability effects) and by affecting pressure by capillary forces (capillary pressure effects). It is assumed that no waste-generated gas is present initially. Future states are modeled as producing gas by corrosion and microbial activities. Should high pressure develop over the regulatory period, it is allowed to access marker beds in the Salado.

Some variability in composition exists between different horizons of the Salado. The largest differences occur between the anhydrite-rich layers called interbeds and those dominated by halite. Within horizons dominated by halite, composition varies from nearly pure halite to halite plus several percent other minerals, in some instances including clay (see Chapter 2.0, Section 2.1.3.4). The Salado is modeled as impure halite except for those interbeds that intersect the DRZ near the repository. This conceptual model and an alternative model that explicitly represented all stratigraphically distinct layers of the Salado near the repository (Christian-Frear and Webb 1996) produced similar results.

From other modeling and theoretical considerations, flow between the Salado and the repository is expected to occur primarily through interbeds that intersect the DRZ. Because of the large surface areas between the interbeds and surrounding halite, the interbeds serve as conduits for the flow of brine in two directions: from halite to interbeds to the repository, or, for brine flowing out of the repository, from the repository into interbeds and then into halite. Because the repository is modeled as a relatively porous and permeable region, brine is considered most likely (but not constrained) to leave the repository through MB139 below the repository because of the effect of gravity. If repository pressures become sufficiently high, gas is modeled to exit the repository via the marker beds in the proximity of the disposal room.

The effect of gravity may also be important in the Salado because of the slight and variable natural stratigraphic dip. For long-term performance modeling, the dip in the Salado within the domain is taken to be constant and 1 degree from the north to south.

Fluid flow in the Salado is conceptualized as occurring either convergently upon the repository, or divergently from it, as discussed in detail in Section 6.4.2.1. Because the repository is not conceptualized as homogeneous, implementing a geometry for the conceptual model of convergent or divergent flow in the Salado is somewhat complicated and is discussed in Section 6.4.2.1.

The conceptual model for Salado fluid flow has primary interactions with three other conceptual models. The interbed fracture conceptual model allows porosity and permeability of the interbeds to increase as a function of pressure. The repository fluid flow model is directly coupled to the Salado fluid flow model by the governing equations of flow in BRAGFLO (in the governing equations of the mathematical model, they cannot be distinguished), and it differs only in the region modeled and the parameters assigned to materials. The Salado model for actinide transport is directly coupled to the conceptual model for flow in the Salado through the process of advection.

MASS-13.1 High Threshold Pressure for Halite-Rich Salado Rock Units

A parameter used to describe the effects of two-phase flow is threshold pressure. The threshold pressure is important because it helps determine the ease with which gas can enter a liquid-saturated rock unit. For a brine-saturated rock, the threshold pressure is defined as "equal to the capillary pressure at which the relative permeability to the gas phase begins to rise from its zero value, corresponding to the incipient development of interconnected gas flow paths through the pore network" (Davies 1991, p. 9).

The threshold pressure, as well as other parameters used to describe two-phase characteristics, has not been measured for halite-rich rocks of the Salado. The Salado, however, is thought to be similar in pore structure to rocks for which threshold pressures have been measured (Davies 1991). Based on this observation, Davies (1991) postulated that the threshold pressure of the halite-rich rocks in the Salado could be estimated if an empirical correlation exists between rocks postulated to have similar pore structure.

Davies developed a correlation between threshold pressure and intrinsic permeability applicable to the Salado halites. (A similar correlation was developed for Salado anhydrites; subsequent testing confirmed that the correlation predicted threshold pressures accurately.) The correlation developed by Davies predicts threshold pressures in intact Salado halites on the order of 20 megapascals or greater (Davies 1991). This threshold pressure predicted by correlation is so high that for all practical and predictive purposes, no gas will flow into intact Salado halites (see Section 6.4.5.1).

Because threshold pressure helps control the flow of gas, and because the greatest volume of rock in the Salado is rich in halite, a high threshold pressure effectively limits the volume of gas that can be accommodated in the pore spaces of the host formation. Thus high threshold pressure is considered conservative as well as realistic, because if gas could flow into the pore spaces of Salado halite, repository pressures could be reduced dramatically.

MASS-13.2 Historical Context of the Salado Conceptual Model

See CRA Appendix MASS, Section MASS.13.2 for the historical information relating to the CCA Salado conceptual model. The Salado conceptual model is unchanged for CRA-2004.

MASS-13.3 The Fracture Model

The purpose of this model is to alter the porosity and permeability of the anhydrite interbeds and the DRZ if their pressure approaches lithostatic, simulating some of the hydraulic effects of fractures with the intent that unrealistically high pressures (in excess of lithostatic) do not occur in the repository or disposal system. The conceptual model is also discussed in Section 6.4.5.2.

In the 1992 preliminary performance assessment, repository pressures were shown to greatly exceed lithostatic pressure if a large quantity of gas was generated. Pressures within the waste repository and surrounding regions were predicted to be roughly 20 to 25 megapascals. It was expected that fracturing within the anhydrite marker beds would occur at pressures slightly below lithostatic pressure. An expert panel on fractures was convened to develop the conceptual bases for the fracturing within the anhydrite marker beds.

The porosity and permeability increases are conceptualized as occurring vertically throughout the affected interbed; in other words, throughout the porous medium as a whole rather than on discrete portions. This simplification facilitates numerical implementation and execution.

Two parametric behaviors must be quantified in the conceptual model. First, the change of porosity with pressure in the anhydrite marker beds must be specified. This is done with a relatively simple equation, described in Appendix PA, Section PA-4.2, that relates porosity change to pressure change using an assumption that the fracturing can be thought of as increasing the compressibility of interbeds. Parameters in the model are treated as fitting parameters and have little relation to physical behavior except that they affect the porosity change. The second parametric behavior is the change of permeability with pressure, which is incorporated by a functional dependence on the porosity change. It is assumed that a power function is appropriate for relating the magnitude of permeability increase to the magnitude of porosity increase. The parameter in this power function, an exponent, is also treated as a fitting parameter and can be set so that the behavior of permeability increase with porosity increase fits the desired behavior.

The fracture enhancement model assumes fracture propagation is uniform in the lateral direction to flow within the marker beds in the absence of dip. The 1-degree dip modeled in BRAGFLO may affect fracture propagation direction. That is, within the accuracy of the finite difference grid, a fracture will develop radially outward. This would not account for fracture fingering or a preferential fracturing direction; however, no existing evidence supports heterogeneous anhydrite properties that would contribute to preferential fracture propagation. This evidence is discussed in CCA Appendix MASS, Attachment 13-2).

The maximum enhanced fracture porosity controls the storativity within the fracture. The extent of the migration of the gas front into the marker bed is sensitive to this storativity. The additional storativity caused by porosity enhancement will mitigate gas migration within the marker bed. The enhancement of permeability by marker-bed fracturing will make the gas more mobile and will contribute to longer gas-migration distances. Thus the effects of porosity enhancement at least partially counteract the effects of permeability enhancement in affecting the gas-migration distances.

Because intact anhydrite is partially fractured, the pressure at which porosity or permeability changes are initiated is close to the initial pressure within the anhydrite. The fracture treatment within the marker beds will not contribute to early brine drainage from the marker bed, because the pressures at these times are below the fracture initiation pressure.

The input data to the interbed fracture model (see Appendix PA, Attachment PAR) were chosen deterministically to produce the appropriate pressure and porosity response as predicted by a linear elastic fracture mechanics (LEFM) model, as discussed in Mendenhall and Gerstle (1993).

MASS-13.4 Flow in the Disturbed Rock Zone

The conceptual model for the DRZ around the waste disposal, operations, and experimental regions has been chosen to provide a reasonably conservative estimate of fluid flow between the repository and the intact halite and anhydrite marker beds. The conceptual model is also discussed in Section 6.4.5.3 of this application.

The conceptual model implemented in the performance assessment uses values for the permeability and porosity of the DRZ that do not vary with time. A screening analysis examined an alternative conceptual model for the DRZ in which permeability and porosity changed dynamically in response to changes in pressure (Vaughn et al. 1995). This analysis implemented a fracturing model in BRAGFLO for the DRZ. This fracturing model is identical to the existing anhydrite interbed alteration model. In this model, formation permeability and porosity depend on brine pressure as described by Freeze et al. (1995, 2-16 to 2-19) and Appendix PA, Section PA-4.2.1. This model permits the representation of two important formation alteration effects. First, pressure build-up caused by gas generation and creep closure within the waste will slightly increase porosity within the DRZ and offer additional fluid storage with lower pressures. Second, the accompanying increase in formation permeability will enhance fluid flow away from the DRZ. Because an increase in porosity tends to reduce outflow into the far field, parameter values for this analysis were selected so that the DRZ alteration model greatly increases permeability while only modestly increasing porosity.

Two basic scenarios were considered in the screening analysis by Vaughn et al. (1995), undisturbed performance and disturbed performance. Both scenarios included a 1-degree formation dip downward to the south. Intrusion event E1 is considered in the disturbed scenario and consists of a borehole that penetrates the repository and pressurized brine in the underlying Castile. Two variations of intrusion event E1 were examined, E1 updip and E1 downdip. In the

E1 updip event, the intruded panel region was located on the updip (north) end of the waste disposal region, whereas in the E1 downdip event, the intruded panel region is located on the downdip (south) end of the disposal region. These two different geometries permitted evaluation of the possibility of increased brine flow into the panel region caused by higher brine saturations downdip from the borehole and the potential for subsequent impacts on contaminant migration. To incorporate the effects of uncertainty in each case (E1 updip, E1 downdip, and undisturbed), a Latin hypercube sample size of 20 was used, for a total of 60 simulations. To assess the sensitivity of system performance on formation alteration of the DRZ, conditional CCDFs of normalized contaminated brine releases were constructed and compared with the corresponding baseline model conditional CCDFs that were computed with constant DRZ permeability and porosity values. Based on comparisons between conditional CCDFs, computed releases to the accessible environment were determined to be essentially equivalent between the two treatments.

Preliminary performance assessments considered alternative conceptual models that allowed for some lateral extent of the DRZ into the halite surrounding the waste disposal region and for the development of a transition zone between anhydrites a and b and MB 138 (SNL 1993, Figures 4.1-2 and 5.1.2; Davies et al. 1993; Gorham et al. 1992). The transition zone was envisioned as a region that had experienced some hydraulic depressurization and perhaps some elastic stress relief because of the excavation, but probably no irreversible rock damage and no large permeability changes. Modeling results indicated that including the lateral extent of the DRZ had no significant effect on fluid flow. Communication vertically to MB 138 was thought to be a potentially important process, however, and the model adopted for the performance assessment assumes that the DRZ extends upward to MB 138 and permeability is sampled over the same range used in the 1997 PAVT.

MASS-13.5 Actinide Transport in the Salado

The purpose of this model is to represent the transport of actinides in the Salado. The model for actinide transport in the Salado is implemented in the code NUTS. This model is also discussed in Section 6.4.5.4 and Appendix PA, Section PA-4.3.

Actinide transport in the Salado is conceptualized as occurring only by advection through the porous medium described in the Salado hydrology conceptual model. Advection is the movement of material with the bulk flow of fluid. Other processes that might disperse actinides, such as diffusion, hydrodynamic dispersion, and channeling in discrete fractures, are not included in the conceptual model.

Advection is a direct function of fluid flow, which is discussed in the conceptual model for Salado fluid flow.

This application of NUTS treats the transport of radionuclides within all the regions for which BRAGFLO computes brine and gas flow. The brine must pass through some part of the repository at some period in its history to become contaminated. While there, it is assumed to acquire radioactive constituents, which it then transports by advection to other regions outside the repository. NUTS uses BRAGFLO's velocity field, pressures, porosities, saturations, and other model parameters (including geometrical grid, residual saturation, material map, brine compressibility, and time step) averaged over a given number of time steps (20 for this performance assessment calculation), which it takes as input for its transport calculations. Consequently, the results of NUTS are subject to all the uncertainties associated with BRAGFLO's conceptual model and parameterization, which will not be repeated here. Details of the source term are discussed in Appendix PA, Attachment SOTERM.

This application of NUTS disregards sorptive and other retarding effects throughout the entire flow region, even though retardation must occur at some level within the repository, the marker beds, and the anhydrite interbeds, and especially in zones with clay layers or clay as accessory minerals.

This application of NUTS neglects molecular dispersion, which leads to uncertainty. For materials of interest in the WIPP repository system, molecular diffusion coefficients are at a maximum on the order of 4×10^{-10} m^2 per second. Thus, the simplest scaling argument using a time scale of 10,000 years leads to a molecular diffusion (that is, mixing) length scale of approximately 33 ft (10 m), which is negligible compared to the lateral advection length scale of roughly 7,874 ft (2,400 m) (the lateral distance from the repository to the accessible environment).

This application of NUTS also neglects mechanical dispersion, which leads to additional uncertainty (see Section 6.4.5.4.2). Dispersion is quantified by dispersivities, which are empirical (tensor) factors that are proportional to flow velocity (to within geometrical factors related to flow direction). They account for both the downstream and cross-stream spreading of local extreme values in concentration of dissolved constituents. Physically, the spreading is caused by the fact that both the particle paths and velocity histories of once-neighboring particles can be vastly different because of material heterogeneities characterized by permeability variations. These variations arise from the irregular cross-sectional areas and tortuous nonhomogeneous, nonisotropic connectivity between pores. Because of its velocity dependence, the transverse component of mechanical dispersivity tends to transport dissolved constituents from regions of relatively rapid flow (where mechanical dispersion has a larger effect) to regions of slower flow (where mechanical dispersion has a smaller effect). In the downstream direction, dispersivity merely spreads constituents in the flow direction. Conceptually, ignoring lateral spreading assures that dissolved constituents will remain in the rapid part of the flow field, which assures their transport toward the boundary. Similarly, ignoring longitudinal dispersivity ignores the elongation of a feature in the flow direction, which ignores foreshortening (or lengthening) of arrival times. However, because the EPA release limits are time-integrated measures, the exact times of arrival are unimportant for constituents that arrive at the accessible environment within the assessment period (10,000 years).

Advection is therefore the only transport mechanism considered important, which underscores NUTS' reliance on BRAGFLO. Because the Darcy flows are given to NUTS as input, the maximum solubility limits for combined dissolved and colloidal components are the most important NUTS parameters. These components are described in Appendix PA, Attachment SOTERM.

MASS-14.0 GEOLOGIC UNITS ABOVE THE SALADO

The model for geologic units above the Salado was developed to provide a reasonable and realistic basis for simulations of fluid flow within the disposal system and detailed simulations of groundwater flow and radionuclide transport in the Culebra. The conceptual model for these units is also discussed in Section 6.4.6 of this application.

The conceptual model used in PA for the geologic units above the Salado is based on the overall concept of a groundwater basin, as introduced in Chapter 2.0 (Section 2.2.1.1) of this recertification application, and developed further in CCA Appendix MASS, Section MASS.14.2. The computer code SECOFL3D was used to evaluate the effect on regional-scale fluid flow by recharge and rock properties in the groundwater basin above the Salado (CCA Appendix MASS, Attachment 17-2). However, simpler models for this region are implemented in codes used in performance assessment. For example, in the BRAGFLO model, layer thicknesses, important material properties including porosity and permeability, and hydrologic properties such as pressure and initial fluid saturation are specified, but the model geometry and boundary conditions are not suited to groundwater basin modeling (nor is the BRAGFLO model used to make inferences about groundwater flow in the units above the Salado). In PA the Culebra is the only subsurface pathway modeled for radionuclide transport above the Salado, although the groundwater basin conceptual model includes other flow interactions. The Culebra model implemented in PA includes spatial variability in hydraulic conductivity and uncertainty and variability in physical and chemical transport processes. Thus, the geometries and properties of units in the different models applied to the units above the Salado by the DOE are chosen to be consistent with the purpose of the model.

The MODFLOW-2000 and SECOTP2D codes are used directly in PA to model fluid flow and transport in the Culebra. The assumptions made in these codes are discussed in Section 6.4.6.2 and Section MASS-15.0.

With respect to the units above the Salado, the BRAGFLO model is used only for determination of fluid fluxes between the shaft or intrusion borehole and hydrostratigraphic units. For this purpose, it does not need to resolve regional or local flow characteristics.

The basic stratigraphy and hydrology of the units above the Salado are described in Sections 2.1.3.5 through 2.1.3.10, and Section 2.2.1.4, respectively. Additional supporting information is contained in CCA Appendices GCR, HYDRO, and SUM. Details of the conceptual model for each unit are described in Sections 6.4.6.1 through 6.4.6.7.

MASS-14.1 Historical Context of the Units above the Salado Model

See CCA Appendix MASS, Section MASS.14.1 for historical information relating to the conceptual models for units above the Salado for the CCA. The conceptual models for the units above the Salado are unchanged for CRA-2004. However, CRA-2004 uses MODFLOW-2000 in place of SECOFL2D to model fluid flow in the Culebra.

MASS-14.2 Groundwater-Basin Conceptual Model

For a discussion on the groundwater-basin conceptual model, see CCA Appendix MASS, Section MASS.14.2.

MASS-15.0 CULEBRA

The conceptual model for groundwater flow in the Culebra (a) provides a reasonable and realistic basis for simulating radionuclide transport in the Culebra and (b) allows evaluation of the extent to which uncertainty about groundwater flow in the Culebra may contribute to uncertainty in the estimate of cumulative radionuclide releases from the disposal system. See Section 6.4.6.2 for additional references to other relevant discussions on this conceptual model.

The conceptual model used in performance assessment for groundwater flow in the Culebra treats the Culebra as a confined two-dimensional aquifer with constant thickness and spatially varying transmissivity (see CCA Appendix MASS, Attachment 15-7). Flow is modeled as single-phase (liquid) Darcy flow in a porous medium.

Basic stratigraphy and hydrology of the units above the Salado are described in Chapter 2.0, Sections 2.1 and 2.2. Additional supporting information is contained in CCA Appendices GCR, HYDRO, and SUM.

The conceptual model for flow in the Culebra is discussed in Section 6.4.6.2. Details of the calibration of the T-fields, based on available field data, are given in Appendix PA, Attachment TFIELD, Section TFIELD-4. Initial and boundary conditions used in the model are given in Section 6.4.10.2. A discussion of the adequacy of the two-dimensional assumption for PA calculations is included as Attachment 15-7 to CCA Appendix MASS.

The principal parameter used in the PA to characterize flow in the Culebra is an index parameter (the transmissivity index) used to select a single T-field for each Latin hypercube sample element from a set of calibrated fields, each of which is consistent with available data (see Appendix PAR).

MASS-15.1 Historical Context of the Culebra Model

Since the FEIS in 1980, the model used to describe flow and transport within the Culebra has changed significantly. In the FEIS, the Culebra and Magenta were combined and modeled as one layer referred to as the Rustler aquifers. In the modeling, the Rustler aquifers were assumed to be an isotropic porous medium with a uniform porosity of 0.10 (Lappin et al. 1989, Table K-2, K-18). A uniform T-field was assumed across the model domain except in Nash Draw. Regional flow was assumed to be toward the southwest discharging at Malaga Bend on the Pecos River. (There was no regulatory framework or boundary defined at this time.) Numerical modeling was not able to consider the possible effect of variations in brine density within the Rustler, so modeling used an equivalent freshwater head. Steady-state flow directions and rates were assumed. As for physical-transport characteristics, the Culebra was incorporated into the Rustler aquifers and assumed to be an isotropic, homogeneous porous medium.

Haug et al. (1987) calibrated a flow model to the H-3 pumping test (Beauheim 1987a) and the effects from the excavation of the shafts. Data from numerous new boreholes installed and tested since the 1980 study were included in this model. The boundaries of the model were not much larger than the extent of the WIPP site. Brine densities were also used as a calibration target. The brine densities were assigned at the boundaries and subsequently modified to match the observed fluid densities. Vertical leakage was included in an attempt to calibrate the brine densities. This attempt led to the recommendation that future modeling studies treat the Culebra as a leaky-confined aquifer. The T-field was estimated by kriging and modified by the addition of pilot points, which were located by trial and error. In this model, single- and double-porosity effects on the flow field were investigated. At the regional scale, the use of a double-porosity vs. single-porosity (matrix-only) conceptual model had little effect on the flow field.

A modeling study (LaVenue et al. 1990) conducted to support the DSEIS only slightly modified the conceptual model used by Haug et al. (1987). The differences in the conceptual model were the assumptions that brine density varied spatially but was held constant through time, and vertical leakage was not included. It was assumed that the brine concentrations could be considered to have changed little over the period of time modeled. The boundaries of the 1989 study were much larger than those of the 1987 study, extending approximately 18.6 mi (30 km) north and south and 12.4 mi (20 km) in east and west. The model grid was centered on the WIPP site. The boundaries were selected to include the region for which head data were available and to minimize the boundary effects during transient simulation of the H-3, WIPP-13, and H-11 pumping tests. Fixed heads were assigned around all four boundaries based upon the regional head values. Transmissivities were estimated by kriging and ranged over seven orders of magnitude in this study. Pilot points were added to modify the T-field during steady-state and transient calibration. Pilot-point locations were selected using an adjoint sensitivity analysis technique. The Culebra T-field were calibrated on the basis of 41 test locations. Transmissivity was recognized to vary by approximately three orders of magnitude within the WIPP site. Modern flow in Culebra was recognized as being predominantly north to south on the WIPP site, and strongly affected by a high-transmissivity zone in the southeastern portion of the WIPP site. Flow was calculated on the basis of a fully confined Culebra and boundary conditions applied at the WIPP site scale. As discussed in Lappin et al. (1989), local flow and transport behavior were affected by fracturing where the transmissivity is greater than approximately 10^{-6} m^2 per second. For physical transport, a double-porosity (matrix-diffusion) transport model for off-site transport from waste panels was assumed. Transport parameters were based on best estimates from nonsorbing tracer tests at three locations (Jones et al. 1992). It was assumed that the effective thickness was equal to the total thickness. Contaminant-transport calculations were one-dimensional.

The initial conditions for the Culebra flow field have been taken from the hydrographs of the WIPP boreholes. Prior to excavation of the salt handling shaft, the hydrographs showed little evidence of head change over the ten years preceding the shaft excavations. Head values were selected for each borehole with a hydrograph that preceded shaft excavation or that was located far from the shaft effects on the flow field. These data provided an estimate of the undisturbed head field and were subsequently used as initial conditions for the Culebra model's transient simulation.

In modeling the hydrologic characteristics of the Culebra, SNL (1992-1993) generated multiple T-field conditioned on hydraulic test data (point transmissivity data and transient head data) and then sampled those fields. This procedure addressed uncertainties in the location-specific values of the Culebra transmissivity. The geologic conceptual model was further revised to indicate that the degree of fracture flow was related to the degree of gypsum cement in the fractures. Contaminant-transport calculations were two-dimensional. The effective thickness of the Culebra was taken to be equal to the total thickness. A range of physical-transport parameters was used, as opposed to best estimates, to address the variability of physical-transport properties within the Culebra. The maximum fracture spacing was assumed to be equal to the total thickness of the Culebra (approximately 26 ft [8 m]). The fracture spacing used in modeling was a convenient modeling simplification based on the concept of through-going parallel fractures. Representing fracturing in terms of fracture spacing is a mechanism to ensure that the proper surface-to-volume ratios are used in estimating the role of matrix diffusion. Calculations considered the possibility of both single-porosity (fracture-flow-only) and double-porosity (matrix diffusion) behavior.

The main differences between the 1989 and 1992 models were the model boundary locations, boundary conditions, and the geostatistical approach used to develop and modify the T-field (LaVenue and RamaRao 1992). The 1992 model boundaries were rotated 38 degrees east to align with the axis of Nash Draw. This permitted the specification of a no-flow boundary condition along a portion of the western boundary, which was selected to coincide with the axis of Nash Draw. In addition, the northeastern corner of the model was treated as a no-flow boundary because of the low transmissivities in the area and the lack of any nearby regional heads to provide boundary head estimates. Transmissivities were simulated by conditional simulation. Pilot points were automatically located and assigned transmissivity values using an optimization routine during steady-state and transient-state calibration.

By 1994, the model of the Culebra's hydrologic characteristics was unchanged from that of December 1992. For the physical-transport characteristics, double-porosity transport was assumed, but the base case had large fracture spacing, effectively the same as the Culebra thickness. A single block size was assumed in each realization. Calculations still assumed an effective thickness equal to the total thickness.

For the 1996 CCA, the model of the Culebra's regional hydrologic characteristics had not changed from the 1994 model, although additional large-scale information from pumping at H-19 and small-scale information at Water Quality Sampling Program (WQSP) wells was incorporated into the calibration. Existing borehole-transmissivity interpretations were refined. The model of the physical-transport characteristics were changed on the basis of analysis of new data from H-19 and H-11 and reanalysis of previous tests of H-3, H-11, H-6. The Culebra was conceived of as a fractured porous medium with inherent local variability in the degree and scale of fracturing. Examination of core and shaft exposures revealed that there are multiple scales of porosity within the Culebra including fractures from microscale to large, vuggy zones, and inter-particle and inter-crystalline porosity. This variability leads to both lateral and vertical variations in permeability. Advection is believed to occur largely through fractures; however, in some areas it may also occur through vugs connected by small fractures and interparticle porosity. Diffusion occurs into all connected porosity. PA, rather than conceiving of transport in terms of fracture and matrix porosities, conceives the Culebra as being composed of advective and diffusive porosities. Matrix diffusion is still believed to be effective and significant. The effective transport thickness is thought to be less than the total stratigraphic thickness. The available data suggest that the permeability of the upper portion of the Culebra is relatively low. Therefore the DOE has concluded that the Culebra is adequately represented by a double-porosity continuum model on the scale of PA calculations, and it is not necessary to use a discrete-fracture model on this scale.

For the 2004 PA, the method of defining the initial (pre-calibration) distribution of T within the Culebra has been revised to explicitly include the geologically zoned distribution of T first developed for the basin-scale model. Three zones are identified: an eastern zone in which halite is present in the Rustler members immediately above and/or below the Culebra and the Culebra transmissivity is consistently low (log T [m^2/s] < -5.4), a western zone in which dissolution of the upper Salado has occurred and the Culebra T is consistently high (log T [m^2/s] > -5.4), and an intermediate transition zone that includes most of the WIPP site. Areas of high T are distributed stochastically within 27.8 percent of the intermediate transition zone to represent the current uncertainty in their locations. Within each of the three zones, T is inversely correlated to the thickness of overburden above the Culebra.

The flow code used for the CRA T-fields was MODFLOW-2000 (Harbaugh et al. 2000). The model domain for CRA-2004 is similar in size (22.4 km [13.9 mi] wide by 30.7 km [19.1 mi] long) to that used for the CCA (approximately 22 km [13.7 mi] wide by 30 km [18.6 mi] long), but is oriented with the long axis extending north to south. The model domain was discretized into uniform 100-m [328-ft] by 100-m [328-ft] grid blocks. Constant-head conditions were prescribed for the eastern boundary of the model, as well as for the eastern portions of the northern and southern boundaries. Flow lines (no-flow boundaries) were prescribed from northeast to southwest down the axis of the northern part of Nash Draw, and from northwest to southeast down the southern arm of Nash Draw. Model cells in the northwest and southwest portions of the model domain beyond the flow lines were treated as inactive by MODFLOW-2000.

Implementation of the pilot-point method for T-field calibration was also revised for the CRA-2004 T-fields. Instead of using an adjoint-sensitivity approach to optimize the locations of the same number of pilot points as there were well locations, 100 pilot points were located to provide a relatively uniform distribution of wells and pilot points within the intermediate transition zone and near the borders of the other two zones. The regularization technique described by Doherty (2003) was used to prevent the large number of pilot points from causing numerical instability. PEST v. 5.5 (Doherty 2002) was used instead of GRASP to optimize T at pilot-point locations during the model-calibration process. The calibration process involved matching to heads measured in late 2000 and to transient heads at 40 wells resulting from seven major pumping tests.

Additional information on the T-field modeling performed for the 2004 PA is given in Chapter 6 and Appendix PA, Attachment TFIELD. Transport modeling for CRA-2004 was performed in the same manner as for the CCA.

MASS-15.2 Dissolved Actinide Transport and Retardation in the Culebra

The purpose of this model is to represent the effects of advective transport, physical retardation, and chemical retardation on the movement of actinides in the Culebra. This conceptual model is also discussed in Section 6.4.6.2.1.

The properties of the Culebra have been characterized by direct observation in outcrop, boreholes, and shafts (Holt and Powers 1984, 1986, 1988, 1990), field hydraulic testing and analysis (Beauheim 1987b), field tracer testing and analysis (Attachment 15-6; Jones et al. 1992; Mercer and Orr 1979), and laboratory testing and analysis (Papenguth and Behl 1996a, 1996b). The conceptual model for dissolved actinide transport in the Culebra is based on these observations, tests, and analyses. Because testing and analysis of the Culebra suggest that its upper portion does not play a significant role in transport, transport is modeled only for the lower portion of the Culebra.

The conceptual model for actinide transport in the Culebra has three principal components: advective transport, physical retardation, and chemical retardation. Two types of porosity are present—porosity in which advective transport occurs, and porosity that is relatively inactive in advective transport. This type of behavior is typically referred to as double porosity

Advective transport refers to the transport of actinides in those pores of the Culebra where the principal fluid flow occurs. This flow primarily occurs in fractures, but may also occur in microfractures connecting vugs in vuggy regions or other portions of the porosity of the Culebra that contain large pore-throat apertures (that is, high permeability regions). This mechanism includes the effects of diffusion and dispersion in advective porosity as well as the movement of actinides with the bulk fluid flow. Advective transport is thought to be controlled by hydraulic gradient, hydraulic conductivity, formation thickness, and advective porosity.

Physical retardation refers to the process of diffusion from advective porosity into diffusive porosity, that is, those portions of the porosity of the Culebra that are relatively inactive in advective transport. Once in the diffusive porosity, the transport of actinides is controlled by diffusion and sorption. Diffusion can be an important process for effectively retarding solutes by transferring mass from the porosity where advection (flow) is the dominant process into other portions of the rock. The properties that control the diffusion of actinides into the diffusive porosity are the surface-area-to-volume ratio of the matrix blocks, the tortuosity of the diffusive porosity, and actinide free-water diffusion coefficients (see CCA Appendix MASS, Attachment 15-3).

Chemical retardation refers to the sorption of actinides on minerals present in the Culebra. Sorption is thought to occur on dolomite grains, but will also occur on clay or other minerals. In the conceptual model, chemical retardation occurs only in the diffusive porosity, and adds to the effects of the physical retardation. The governing properties for sorption are described in a parametric expression of the degree to which dissolved actinides tend to sorb or remain in solution (in the mathematical model, a K_d or a linear isotherm is used), which requires the concentration of actinides in solution and the abundance of minerals on which sorption can occur (see CCA Appendix MASS, Attachment 15-1).

Advective porosity is thought to be a small percentage of the total volume of the Culebra. This porosity is interconnected and contains high-permeability features such as fractures or vuggy pore structures. In this advective porosity, little actual rock material is considered to exist (in other words, it is the fracture apertures and pore volumes without surrounding rock). In contrast, diffusive porosity makes up the major portion of the Culebra pore volume. It comprises lower-permeability features and most of the rock material. The rate at which diffusion removes solutes from advective porosity is a function of the surface area-to-volume ratio of the matrix blocks. For a given geometry of advective porosity assumed in a model (for example, parallel-plate fractures), this surface area-to-volume ratio can be expressed as a characteristic length, which is known as the matrix block length (for example, the thickness of a matrix slab between two parallel-plate fractures).

In summary, the conceptual model for dissolved actinide transport in the Culebra includes two types of porosity: advective porosity associated with high-permeability features of the Culebra, and diffusive porosity associated with lower-permeability features. These two types of porosity are distributed throughout the Culebra and are intertwined on a small scale; hence, mapping their regional extent or boundaries between them is not feasible. Advection, diffusion, and dispersion of dissolved actinides occur within the advective porosity. Diffusion (physical retardation) and sorption (chemical retardation) occur within the diffusive porosity. Advective porosity makes up a small portion of the overall pore volume of the Culebra; diffusion is an important process for transferring actinides into other portions of the rock in which there is a larger surface area for sorption. Because the upper portion of the Culebra has been observed to be relatively inactive in solute transport in tests, it is assumed to be unimportant and is not included in the conceptual model. Attachment 15-6 of CCA Appendix MASS contains additional information on the transport properties of the Culebra.

Several parameters are referred to or implied in the conceptual model as discussed in Section 6.4.6.2. For transport in advective porosity, the principal parameter is the porosity of the network, but because of links to the Culebra fluid flow model, the hydraulic gradient and hydraulic conductivity largely control the specific discharge calculated by MODFLOW-2000. Within diffusive porosity, the porosity, tortuosity, and diffusion coefficients for various actinides are important because of their effect on the rate of diffusion. A parameter called matrix block length, a measure of the surface area between the advective and diffusive porosities, is also important. The density of sorbing minerals and their sorption properties, expressed by K_d, are important in chemical retardation.

It is commonly assumed that there should be a relationship between the conductivity of advective porosity and its porosity and distribution, that is, that the fracture permeability, porosity, and aperture or spacing should be correlated. Data collected and analyzed at the WIPP do not support this assumption. There are no meaningful trends among these parameters for the data that have been collected. Therefore, values of these parameters are not correlated in the PA (see CCA Appendix MASS, Attachment 15-6, page 14 and Attachment 15-10).

Transport of actinides in the Culebra is coupled to several other conceptual models. An important coupling is to models for features that can introduce actinides to the Culebra, for example, the exploratory borehole, shafts and shaft seals, and dissolved actinide source term. The most important coupling is to the model for flow in the Culebra. Because transport in the

Culebra is one of the last processes to occur along this pathway prior to release, it does not feed back to other conceptual models in any significant manner. This conceptual model falls at the downstream end of the overall disposal system model, and thus has little or no impact on models that come before it.

MASS-15.2.1 Current Studies of Sorption in the Culebra

Several factors affect the sorption of Pu, Am, U, Th, and Np, the elements for which K_d values are required in PA for Culebra transport calculations (Ramsey 1996) including:

- the properties of the sorbents (solids) that will sorb actinides from solution,
- the composition of solutions that currently exist in the Culebra or could enter the Culebra after human intrusion into WIPP disposal rooms,
- the oxidation state of the sorbate (actinide elements) in the Culebra,
- dissolved actinide concentration,
- equilibration time, and
- direction of reaction (sorption versus desorption).

The two most important sorbents in the Culebra are dolomite, a carbonate mineral that constitutes most of the Culebra, and corrensite, an ordered mixture of chlorite and saponite associated with fracture surfaces and dispersed in the matrix (intact rock between the fractures) of the Culebra. Dolomite is important because it is by far the most abundant mineral in the Culebra. Corrensite is important because, although a minor constituent, it sorbs actinide elements more strongly than dolomite. The work of Sewards (1991) and Sewards et al. (1991, 1992) indicates that corrensite is associated with fracture surfaces and dispersed in the matrix at concentrations high enough to increase the retardation of Pu, Am, U, Th, and Np relative to that observed in laboratory studies with dolomite-rich rock. (Np was not transported in the 1996, the 2004 PA, or the 1997 PAVT, but K_ds were also determined for this element for completeness.) However, the DOE does not include K_ds for clay minerals in the ranges and probability distributions for the matrix K_ds used in PA calculations because laboratory data for clay-rich rock under expected Culebra conditions are insufficient at this time. Furthermore, the DOE does not take any credit for sorption by clay minerals associated with fracture surfaces. Omitting K_ds for clays is conservative.

The experimental basis for the ranges and probabilities of matrix distribution coefficients is documented in CCA MASS Attachment 15-1.

MASS-15.2.2 Historical Studies of Sorption in the Culebra

See CCA Appendix MASS, Section MASS.15.2.2 for historical information relating to the CCA Culebra conceptual model.

MASS-15.3 Colloidal Actinide Transport and Retardation in the Culebra

The purpose of this model is to represent the effects of colloidal actinide transport in the Culebra. This model is also discussed in Section 6.4.6.2.2 and Attachments 15-2, 15-8, and 15-9.

A particle is referred to as being in the colloidal state when the particle size lies roughly in the range between 1 nanometer and 1 micron. These particles are generally much larger than simple ions, and as a result, the transport behavior of colloids in groundwater systems can be quite different from that of dissolved species. In a groundwater system, colloids are essentially a third phase consisting of a mobile solid that can associate with or contain actinides and potentially increase transport rates slightly relative to the average groundwater velocity.

In the WIPP disposal system, for instance, colloids are often too large to pass through the small pore throats of diffusive porosity. Such colloids will be restricted to the advective portion of the flow system. Colloids may also be less reactive than dissolved actinides with the host rock. Therefore, even though a colloid is small enough to penetrate the diffusive porosity, the retardation coefficient associated with the colloid will in some cases be smaller than the retardation coefficient of the actinide associated with the colloid.

Colloid-facilitated actinide transport has not been included in the 1996 PA, the 2004 PA calculations, or the 1997 PAVT because of a lack of adequate information to model this phenomenon and demonstrate its impact on compliance (see, for example, SNL, 1992-1993, Vol. 1, 4-12, line 29). Transport of actinides by colloidal particles has been recognized only relatively recently as a phenomenon of potential importance to the performance of nuclear waste repositories (Jacquier 1991; Avogadro and de Marsily 1984). In fact, the study of colloid-facilitated contaminant transport is a relatively new topic to the geosciences in general. Nyhan et al. (1985) was one of the first investigations to demonstrate the potential importance of colloid-facilitated radionuclide transport. Since then, a number of researchers have investigated colloids as a potential transport mechanism (for example, McCarthy and Zachara 1989; Corapcioglu and Jiang 1993; Grindrod 1993; Ibaraki and Sudicky 1995). Grindrod (1993) and Ibaraki and Sudicky (1995) addressed the topic of colloid-facilitated transport through fractured porous media. Consequently, their work is most applicable to the colloid-transport problem in the Culebra.

Among the most sophisticated and rigorous numerical models developed are those by van der Lee et al. (1993, 1994) and Bennett et al. (1993). Many of the colloid-transport numerical models described in the literature focus on simulating solute transport through fractured media with double-porosity flow characteristics, and they have been generalized to include unique features of colloid transport (for example, Hwang et al. 1989; Grindrod and Worth 1990; Light et al. 1990; Smith and Delgueldre 1993; Harmand and Sardin 1994). Some numerical models, such as the population-balance model by Travis and Nuttall (1985), assume equilibrium colloid concentrations. That is, the loss of colloidal particles by attachment to the medium wall is compensated by the generation of new colloidal particles by various mechanisms such as condensation and entrainment. The modeling approach developed by Travis and Nuttall (1985) is similar to the double-porosity transport model.

MASS-15.3.1 Experimental Results

As discussed in Section 6.4.6.2.2, the four types of colloids and colloidal sized particles modeled to be introduced to the Culebra are microbes, mineral fragments, humic substances, and actinide intrinsic colloids. To investigate the impact of these four colloid types on radionuclide transport in the Culebra, an experimental program was developed and implemented at SNL with significant contributions from Lawrence Livermore National Laboratory (LLNL), Battelle National Laboratory, Los Alamos National Laboratory (LANL), and Florida State University. The intent of this experimental program was to develop parameter ranges and distributions for the conceptual models discussed above. With the exception of the Pu (IV) polymer, the experimental results indicated that colloid-facilitated actinide transport is not a viable mechanism for actinide transport in the Culebra. Furthermore, the potential amount of Pu (IV) polymer that could be introduced to the Culebra was found to be insignificant with respect to the EPA normalized release limit. Consequently, colloid-facilitated actinide transport was not simulated in the PA.

The experimental results and implications for PA modeling are summarized as follows:

- Mineral fragments and microbes are attenuated so effectively it was deemed unnecessary to include them in the transport calculations (see CCA Appendix MASS, Attachments 15-8 and 15-9).

- The total potential amount of Pu (IV) polymer introduced to the Culebra was found to be insignificant with respect to the EPA normalized release limit (Attachment 15-8). Therefore, the contribution of Pu (IV) polymer to the integrated discharge was disregarded in the PA.

- Under neutral to slightly basic brine conditions, the presence of humic substances in the brine did not influence the sorption behavior of dissolved actinides. Results indicate that at these geochemical conditions, humic substances were not effective complexants in the presence of dolomite (Attachment 15-8). Therefore, actinides associated with humic substances are assumed to disassociate upon entering the Culebra.

MASS-15.3.2 Indigenous Colloidal Transport

In an intrusion scenario at the WIPP, as dissolved actinide elements are introduced to the Culebra, it is possible that those dissolved actinides could sorb onto a separate population of indigenous mineral fragments, microbes, and humic substances. The physical and chemical behavior of these newly formed actinide-bearing colloidal particles will be nearly identical to the behavior of colloids introduced from the repository. Microbes and mineral fragments will be rapidly filtered out of the advective flow domain; hence, disregarding the interaction between dissolved actinides and these types of colloids is considered to be a conservative approach. Experimental results indicate that humic substances do not interact with dissolved actinides under the expected Culebra geochemical conditions. Consequently, the quantity of newly formed actinide-bearing humics will be insignificant.

MASS-15.3.3 Alternative Approaches Considered

As discussed above, results of experimental studies show that colloidal actinides are strongly attenuated or present in negligible concentrations, making it unnecessary to include them in PA simulations. The following section describes the three alternative transport conceptual models considered prior to the completion of these experimental results.

After the introduction of colloidal actinides and dissolved actinides into the Culebra, realistically a new equilibrium condition will be established, with the stipulation that the total concentration of actinide must be preserved. As in the repository, quantifying an equilibrium assemblage is not practicable.

Three approaches were considered to quantify colloid-facilitated actinide transport at the WIPP. First, the transport of one or more types of actinide-bearing colloidal particles in the Culebra could be assumed to be instantaneous. In other words, as actinides associated with that type of colloidal particle migrate to the Culebra from the repository, or are generated within the Culebra, the mass of actinides associated with those colloidal particles becomes part of the integrated release of actinides at the accessible environment boundary. This approach can be useful if the concentrations of actinides associated with one or more types of colloidal particles are very low. Treating colloid-facilitated actinide transport as instantaneous, however, is a significant shortcoming, because of the potentially large expected retardation effects of colloidal particles.

Second, SECOTP2D and supporting codes could be used to simulate the effects of one or more of the colloid retardation phenomena (Ramsey 1996). The double-porosity advection and diffusion equation solved by SECOTP2D can simulate colloid sorption in the matrix and to the fracture walls. The code can also model colloid filtration using the decay term of the governing equation. For colloids considered too large to diffuse into the matrix, matrix diffusion can be disabled by setting the matrix tortuosity to zero. This approach was used for some calculations completed in 1994. Specifically, microbes, because of their relatively large size, were excluded from matrix diffusion and limited to advective flow in fractures. Humic substances were allowed to diffuse into intercrystalline pores, but at a reduced rate relative to dissolved actinide species.

This approach requires a number of simplifying assumptions under the presumption they are conservative with respect to the integrated release of radionuclides. The first assumption is that the dissolved concentration will be greatest at the source point and therefore, the concentration of radionuclides associated with colloids will be greatest at the source as well. Second, a radionuclide associated with a colloid is assumed to remain fixed to that colloid throughout the simulation. Given these assumptions, the colloidal actinide concentration is no longer a function of the dissolved actinide concentration, and it is not necessary to solve the dissolved species transport problem and the colloid transport problem simultaneously. As a result, the standard advection-diffusion transport equation can be used to predict colloid transport and compute integrated colloid releases. Given the initial concentration of radionuclides sorbed to each specific type of colloid, the integrated colloid release can be converted to an integrated radionuclide release by postprocessing the colloid transport results. Radionuclide decay can also be accounted for in postprocessing.

The third assumption is that colloid-facilitated actinide transport could be quantified by a rigorous numerical modeling code developed for the WIPP. Such a rigorous transport model would address all physical and chemical processes that could affect the movement and fate of the four colloidal particle types, including colloid generation; interactions with solutes, the dispersant, and rock; advection; dispersion; diffusion; filtration; gravitational settling; attachment and detachment; adsorption and desorption; coagulation; flocculation; and peptization. Ideally, permeability reduction caused by pore clogging by colloids, which would affect solute transport as well, would also be considered. Currently available models do not include all of these processes (see CCA Appendix MASS, Attachments 15-2, 15-8, and 15-9).

The most practical approach to evaluating the transport of colloidal actinides is the second option presented above, using the SECOTP2D code. Where possible, the DOE considered reducing the number of phenomena treated in the transport code and address them in the source term. For example, the effect of ionic strength on colloid stability would have been included in the colloid source term. Retardation of colloidal particles was to be quantified using a retardation factor, and filtration was to be quantified through the decay term.

MASS-15.4 Subsidence Caused by Potash Mining in the Culebra

This model incorporates the effects of potash mining in the McNutt on disposal system performance (see Appendix PA, Attachment SCR, FEPs H13, H37, and H38). 40 CFR Part 194 provides a conceptual model and parts of a mathematical model for these effects. The DOE has implemented the EPA conceptual model to be consistent with EPA criteria and guidance. It is described in Section 6.4.6.2.3 of this recertification application. Additional information on the implementation of the mining subsidence model is available in Appendix PA, Attachment TFIELD, Section TFIELD-9.0; CCA Appendix MASS, Attachments 15-4 and 15-7; and Wallace (1996).

The principal parameter in this model is the range assigned to a factor by which hydraulic conductivity in the Culebra is increased (CCA Appendix MASS, Attachment 15-4). As allowed in supplementary information to 40 CFR Part 194, it is the only parameter changed to account for the effects of mining.

Mining in the McNutt has been considered in the performance of the WIPP since the original siting activities. Siting criteria for both the site abandoned in 1975 and the current site included setbacks from active mines. (See, for example, Section MASS-2.0.) The 1980 FEIS for the WIPP (DOE 1980) considered the possibility of an indirect dose arising from the effects of solution mining for potash or halite; it concluded that direct access of waste by solution mining for potash was not likely because of the methods that would be used to control the flow of solvent through the formation. See Appendix PA, Attachment SCR (FEPs H58 and H59).

Mining has been included in scenario development for the WIPP since the earliest work on this topic (for example, Hunter 1989; Marietta et al. 1989; Guzowski 1990; Tierney 1991; and WIPP Performance Assessment Division 1991). These early scenario developments considered both solution and room-and-pillar mining. The focus was generally on effects of mining outside the disposal system. The two primary effects of mining considered were changes in the hydraulic conductivity of the Culebra or other units and changes in recharge as a result of surface subsidence. These mining effects were not formally incorporated into quantitative assessment of repository performance in preliminary PAs.

The inclusion of mining in PA satisfies the criteria of 40 CFR Part 194 to consider the effects of this activity on the disposal system.

MASS-16.0 INTRUSION BOREHOLE

The inclusion of intrusion boreholes in PA adds to the number of release pathways for radionuclides from the disposal system. Direct releases to the surface may occur during drilling as particulate material from cuttings, cavings, and spall are carried to the surface. Also, dissolved actinides may be carried to the surface in brine during drilling. Once abandoned, the borehole presents a possible long-term pathway for fluid flow, such as might occur between a hypothetical Castile brine reservoir, the repository, and overlying units. This topic is also addressed in Chapter 6.0, (Section 6.4.7) and Appendix PA Attachment SCR (FEPs H1 and H21).

MASS-16.1 Cuttings, Cavings, and Spall Releases during Drilling

These models estimate the quantity of actinides released as solids directly to the surface during drilling through the repository by three mechanisms: the drillbit boring through the waste (cuttings), the drilling fluid eroding the walls of the borehole (cavings), and high repository gas pressure causing solid material failure and entrainment into the drilling fluid in the wellbore (spallings). See Section 6.4.7.1 and references to other appendices cited in that section for additional information. Stochastic uncertainty with respect to parameters relevant to these release mechanisms is addressed in Section 6.4.12. The conceptual model for cuttings, cavings, and spallings is discussed in three parts because of the differing process by which the three types of material are produced.

Cuttings are materials removed to the surface through drilling mud by the direct mechanical action of the drill bit. The volume of waste removed to the surface is a function of the repository height and the drill bit area. The cuttings model has as a principal parameter the diameter of the drill bit (see Appendix DATA, Attachment A).

Cavings are materials introduced into the drilling mud by the erosive action of circulating drilling fluid on the waste in the walls of the borehole annulus. Erosion is driven solely by the shearing action of the drilling fluid (or mud) as it moves up the borehole annulus. Shearing may be caused by either laminar or turbulent flow. Repository-pressure effects on cavings, which are negligible, are covered by the spall process. The principal parameters in the cavings model are the properties of the drilling mud, drilling rates, the drill string angular velocity, and the shear resistance of the waste. See Appendix PA, Attachment PAR (Tables PAR-13 and PAR-18) for details on the sampled parameters used in the cavings model, the drill string angular velocity, and the effective shear resistance to erosion.

Spallings are solids introduced into the wellbore by the fluid pressure difference between the repository and the bottom of the wellbore. If the repository pressure is sufficiently high (~ >12 MPa) relative to the well bottom hole pressure (~8 MPa), the stress state in the repository may cause repository solids to fail in the vicinity of the wellbore. In turn, these solids may become entrained in the gas flowing toward the well, ultimately to be carried up to the land surface, constituting a release. The principal parameters in the spallings model are the gas pressure in the repository when it is penetrated and properties of the waste such as permeability, tensile strength, and particle diameter. Because the release associated with spalling is sensitive to gas pressure in the repository, it is strongly coupled to the BRAGFLO-calculated conditions in the repository at the time of penetration.

MASS-16.1.1 Historical Context of Cuttings, Cavings and Spallings Models

Cuttings and cavings releases are straightforward. The analytical equations governing erosion (cavings) based on laminar and turbulent flow (Appendix PA, Section PA-4.5) have been implemented in the code CUTTINGS_S. Using selected input based on assumed physical properties of the waste and other drilling parameters, this code calculates the final caved diameter of the borehole that intersects the waste.

The various approaches used for spallings up to the CCA PA are documented in CCA Appendix MASS.16.1.1. Since the CCA PA, the spallings model has been extensively revised and has changed fundamentally from an end-state erosional model to a mechanically based coupled material failure and transport model (WIPP PA 2003a). This model is implemented in a new code, DRSPALL. The following discussion traces the historical steps from the CCA erosional model to DRSPALL.

According to the WIPP Conceptual Models Peer Review Report (CCA Section 9.3.1.2.7), the three primary objections to the erosional spallings model were; (1) channel flow scenario needed additional validation, (2) waste erosion resistance process and parameters had not been adequately evaluated, and (3) assumptions concerning waste degradation and strength. Though the strength value used, 1 lb/in^2, was consistent with the strength of soils, salt and clay mixtures, and similar mixtures with MgO (see CCA Appendix PEER, Section 2.6 for Berglund 1996), the peer review panel was not convinced of the applicability of this value in the model (Wilson et al. 1996b). Hansen et al. (1997) decided to revise the approach to estimating spall release and embarked on a two-part effort that sought to (1) derive mechanical strength estimates from laboratory measurements on surrogate WIPP wastes, and (2) develop a new mechanically-based model for spall that attempts to encompass the entire system response from bit penetration to near steady state rather than just the end state, as done in the erosional model. The results of the model development efforts were implemented in the code GASOUT (Hansen et al. 1997, Appendix C).

MASS-16.1.2 Waste Mechanistic Properties

The spalling event can occur only in cases that combine high pressure with highly degraded waste. A systematic approach was implemented to characterize the waste after compaction, corrosion, and microbial consumption through the used of waste surrogate materials. The primary emphasis of the waste surrogate testing was devoted to quantifying tensile strength, although many other characteristics, such as particle size, permeability, and heterogeneity, will greatly influence potential spall release. Utilizing a projected inventory of waste materials placed in the repository and assuming extensive degradation, recipes (mixtures) for surrogate products were determined. Surrogate recipes derived from corrosion of 50 percent and 100 percent of the

Fe-based inventory were fabricated and mechanically tested using standard laboratory procedures (Hansen et al. 1997).

Degraded waste strength was recognized as a key parameter in a WIPP spallings model (Wilson et al. 1996a, 1996b). Lacking, however, were compelling data to validate the value of tensile strength $T_o = 1$ lb/in^2 used in the CCA erosional model. In an attempt to build an understanding of the mechanical properties of degraded WIPP wastes, Hansen et al. (1997) developed a test methodology to construct and examine surrogate wastes. They scanned the inventory of WIPP wastes and prepared recipes for various surrogate wastes. A wide variety of materials were cut, shred, compressed, and aged in the laboratory to create specimens appropriate for standard laboratory measurements such as tensile and compression tests. Overall, results from 38 specimens were reported in Hansen et al. (1997) quantifying properties including tensile strength, cohesion, friction angle, Poisson's ratio, and Biot's constant. These data helped to make the case that the $T_o = 1$ lb/in^2 value used in the CCA was indeed conservative.

Subsurface processes leading to extensive degradation are based on several contributing conditions including ample brine availability, extensive microbial activity, corrosion, and the absence of cementation and salt encapsulation effects. Property values from these surrogate materials are selected to represent the worst-case response to the process being investigated (Hansen et al. 2003b). In terms of the degraded waste properties, the model is highly conservative.

MASS-16.1.3 New Mechanistic Model for Spall

In addition to the work on waste degradation, Hansen's team also laid the groundwork for a new approach to modeling the WIPP spallings process. Instead of focusing on the end state after penetration, as is done in the erosional model, the new effort sought to capture the system behavior from just before penetration through to the end state. In doing so, many more phenomena were included in the model. Considered in this new conceptual model was unsteady, convergent gas flow from the repository toward the wellbore that caused mechanical stress and potential failure of solids near the face of the wellbore. Pressure in the cavity at the point of penetration was balanced by the mud column in the wellbore and the repository pressure. This represented a more complex modeling approach, and was developed sufficiently to satisfy the peer review panel that convened in April, 1997 that the spallings release values used in the CCA were conservative (Wilson et al. 1997).

The new spall model, DRSPALL (WIPP PA 2003a) is based on a predecessor code called GASOUT (Hansen et al. 1997, Appendix C). DRSPALL builds upon GASOUT by:

1. Adding a wellbore flow model that transports mud, repository gas, and waste solids from repository level to the land surface; and

2. Adding a fluidized bed model that evaluates the potential for failed particulate waste to fluidize and become entrained in the wellbore flow.

The wellbore flow model in DRSPALL utilizes one-dimensional geometry with a compressible, viscous, isothermal, homogeneous mixture of mud, gas, and solids. Standard mass and momentum balance, friction loss, and slurry viscosity equations are used. Wellbore flow model results were successfully verified against those from an independent commercial code for several test problems (WIPP PA 2003b).

DRSPALL applies the fluidized bed theory to determine the mobilization of failed material to the flow stream in the wellbore. If the escaping gas velocity exceeds the minimum fluidization velocity, failed material is fluidized and entrained for transport at the land surface. If gas velocity is too low to fluidize the bedded material, however, the cavity size is allowed to stabilize The spall volumes predicted by DRSPALL are based on conservative assumptions for material properties and for the flow geometry within the repository.

- The particle size distribution for spallings is based on a detailed analysis (Wang 1997) of data from an expert elicitation (DOE 1997). This analysis considered several limiting cases in developing a conservative distribution for mean particle size ranging from 1 mm to 10 cm (Hansen et al. 2003b).

- The shape factor for fluidization of particles has a potential range from 0 to 1.0. Smaller values of the shape factor denote particles that are less spherical, and therefore more easily fluidized and transported in the flow. The shape factor is conservatively set to a value of 0.1 for CRA-2004 (Lord 2003).

- The tensile strength of the waste assigned for the spalling process is uncertain, ranging from 0.12 MPa to 0.17 MPa (Hansen et al. 2003b). Tensile strength data was measured in laboratory experiments on surrogate materials that were chosen to conservatively represent highly degraded residuals from typical wastes. The given range is felt to represent extreme, low-end tensile strengths because it does not account for several strengthening mechanisms, such as MgO hydration and halite precipitation/cementation (Hansen et al. 1997).

- DRSPALL uses a hemispherical geometry (one-dimensional spherical symmetry) for the flow field and cavity in the waste. This conceptual model is appropriate when the drill bit first penetrates the repository. But as the drill bit passes completely through the compacted waste, the flow field will transition toward a cylindrically symmetric geometry. This transition is important because the largest spall release volumes are predicted to occur at late times, well after the drillbit has penetrated through the waste, and because the spall volumes predicted for a cylindrical geometry are less than for the hemispherical geometry (Lord et al. 2003).

In spite of this transition, the hemispherical geometry is used for the CRA-2004 spallings release calculations because it produces conservative results. Fifty calculations performed with DRSPALL in both the hemispherical and cylindrical flow geometries demonstrated that the spall volumes predicted with the hemispherical geometry are always larger than those for the cylindrical geometry (Lord and Rudeen 2003, Section 3.3 Sensitivity Analysis Report Part 2). In fact, the spall volumes are zero for all 50 realizations with a cylindrical geometry, which indicates that the likelihood of spalling is quite small in this geometry. It follows that the hemispherical geometry results in spall volumes that are conservative relative to the cylindrical geometry.

There is no consensus about how the driller will act as the drill approaches the waste horizon; that is, whether he or she will be able anticipate the presence of the gas-filled repository, or if he or she can or will control the drilling process once penetration occurs. For the WIPP intrusion scenarios, the conceptual model assumes the worst possible limiting situation, in which the borehole is driven through the waste by a driller without any knowledge of the existence of the repository, and the driller is unable or unwilling to control the subsequent gas release.

In summary, the conservative assumptions for waste properties, the waste flow geometry and the driller's actions provide very conservative spalling release volumes for CRA-2004 (see also Appendix PA, Section PA-4.6 for a description of the spallings model and Section 9.3.1.3.5.5 for the results of the new spallings model peer review).

MASS-16.1.4 Calculation of Cuttings, Cavings, and Spall Releases

As detailed in Appendix PA, Section PA-6.7, cuttings and cavings releases for intrusions into contact handled (CH)-TRU waste are computed by multiplying the volume released (calculated by the code CUTTINGS_S) with the radioactivity in three independently-selected waste streams, consistent with the conceptual assumption that waste is randomly placed within the repository. The effect of this assumption on PA results was examined in a separate PA (Hansen et al. 2003a) in which cuttings and cavings releases were computed by assuming that each intrusion encounters only a single waste stream. The differences in repository performance (determined by comparing the mean CCDFs for releases) were determined to be minor. For more details on the analysis, see Section MASS-21.0.

Because spallings may releases a relatively large volume of material (exceeding 4 m^3), spallings releases for intrusions into CH-TRU waste are computed by multiplying the volume of spalled material with the average concentration of radioactivity in the waste at the time of the intrusion. A separate PA (Hansen et al. 2003a) compared spallings releases computed using the average concentration of radioactivity in the waste to spallings releases computed by using the radioactivity of a single, randomly selected single waste stream. The analysis determined that the assumption had only a minor effect on the mean CCDF for releases. For more details on the analysis, see Section MASS-21.0.

MASS-16.2 Direct Brine Releases during Drilling

This model provides a series of calculations to estimate the quantity of brine released directly to the surface during drilling. Direct brine releases (DBRs) may occur when a driller penetrates the WIPP and unknowingly brings contaminated brine to the surface during drilling (these releases are not accounted for in the cuttings, cavings and spallings calculations, which model only the solids removed during drilling). Appendix PA, Section PA-4.7 described the DBR model used for the 2004 PA. CCA Appendix MASS, Attachment 16-2 describes the direct brine release model used for the 1996 PA. The conceptual model for DBRs is discussed in Section 6.4.7.1.1.

Uncertainty in the BRAGFLO direct-brine-release calculations is captured in the 10,000-year BRAGFLO calculations from which the initial and boundary conditions are derived. The model parameters that have the most influence on the direct brine releases are repository pressure and brine saturation at time of intrusion. Brine saturation is influenced by many factors, including

Salado and marker bed permeability and gas-generation rates (for undisturbed calculations). For E1 and E2 intrusions, Castile brine-reservoir pressure and volume and abandoned borehole permeabilities influence conditions for the second and subsequent intrusions. Dip in the repository (hence the location of intrusions), two-phase flow parameters (residual brine and gas saturation), time of intrusion, and duration of flow have lesser impacts on brine releases.

To account for changes in the BRAGFLO model (see Section MASS-2.0), the implementation of the DBR model has been adjusted for the CRA 2004-PA. Figure MASS-9 shows the DBR

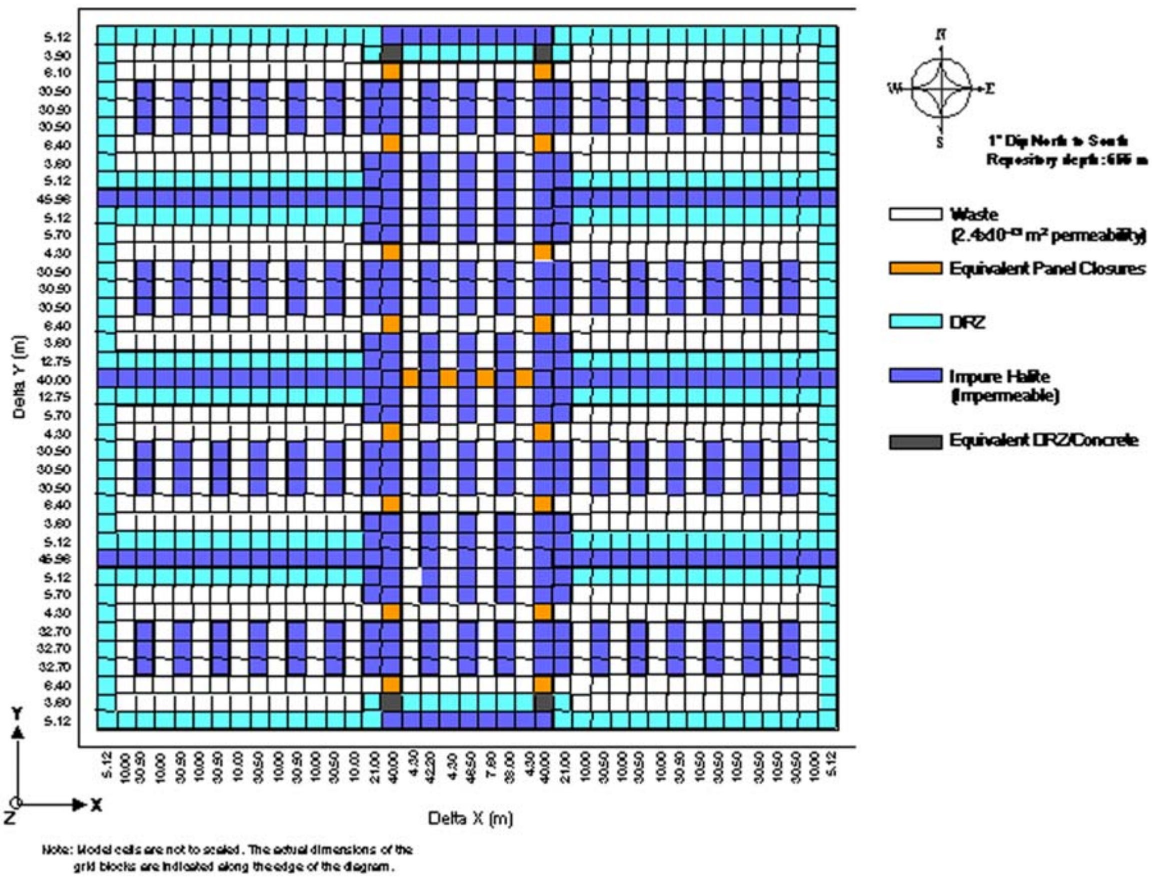

Figure MASS-9. Repository-Scale Horizontal BRAGFLO Mesh Used for Direct Brine Release Calculations

grid used in the 2004 PA. The grid dimensions and resolution are the same as in the CCA PA, but the material parameters assigned to the panel closures have been changed to be more consistent with the conceptual model for the Option D panel closures. In addition, the material parameters assigned to the DRZ have been changed to more consistently represent the DRZ. In the CCA PA, the pillars between rooms and the halite separating panels were assigned properties consistent with the DRZ material in the BRAGFLO grid. The DRZ permeability used in the CCA (10^{-15} m^2) was low enough that brine did not flow between panels during the 11-day DBR calculations. When the permeability of the DRZ was changed in the PAVT (from a constant value of 10^{-15} m^2 to a sampled value between $10^{-19.4}$ m^2 and $10^{-12.5}$ m^2), realizations with high

DRZ permeability allowed brine flow between panels during the 11-day period for DBR calculations. It is not reasonable to model the halite between panels as DRZ, since the DRZ would extend only a few meters into the 60-m thick ribs. Consequently, the material parameters assigned to cells separating panels were changed to be representative of undisturbed halite, rather than DRZ. Stein (2003b) provides details on the material parameters used in the DBR calculation and the rationale for the parameter values.

MASS-16.3 Long-Term Properties of the Abandoned Intrusion Borehole

The purpose of the model for the long-term properties of the intrusion borehole is to provide in BRAGFLO the physical properties relevant to fluid flow through a plugged and abandoned borehole that intersects the repository. The model includes several possible plugging and configuration patterns based on current practice in the Delaware Basin (CCA Appendix MASS, Attachment 16-1). Because plugging practice is closely controlled by state regulations, only the New Mexico portion of the Delaware Basin is considered. Section 6.4.7.2 of this application describes the properties assigned to the boreholes and the types of plug configurations considered in performance assessment.

The conceptual model for long-term flow up a plugged and abandoned borehole addresses the principal parameters in the intrusion borehole model for long-term flow: permeability, porosity, compressibility, and two-phase properties. Because these properties may change with time as the borehole plugs degrade, some types of boreholes have several defined stages for the evolution of borehole properties. No retardation of actinides or other transport-limiting effects in the borehole are assumed. This is considered a conservative assumption (see Table MASS-1).

Permeability, the most important borehole property, changes according to the stage of borehole degradation. The values assigned to other parameters are held constant for all stages and are set consistent with a borehole fill referred to as silty sand, consisting of the material that would naturally slough off the walls of the borehole or the remains of degraded plugs. The porosity of the plugged and abandoned borehole is set at a low value within the porosities expected of materials that will be in the borehole; the low value was chosen because smaller void volume in the borehole reduces storage in the borehole and slightly increases the total flux of fluids that may pass through it.

Predictions of the time-dependent permeability of plugged boreholes are based on three configurations for borehole plugs and two concepts of how the plug materials will be altered by fluids. The concepts include steel corrosion and concrete degradation. From the outside inward, the conceptual model for borehole plugs envisions concentric circles of ordinary portland cement as grout attaching the casing to the rock, low carbon steel (the casing), and a central disc of ordinary portland cement (the concrete plug). The bulk of the data used to predict the service lives of borehole plugs comes from the open literature on corrosion of low carbon steel and ordinary portland cement and from tabulated thermodynamic data bases.

Predictions of plug performance derived from the conceptual models are sensitive to both chemical and physical parameters. Key areas of uncertainty include the following:

- opened or closed nature of the physical and chemical systems,

- degree to which performance data from generic materials apply to WIPP-specific materials and conditions,
- conditions at the precise locations where WIPP plugs are emplaced, and
- physical dimensions of the plugs.

The conceptual models for predicting the time-dependent permeability of plugged boreholes recognize two types of systems: open and closed. Open systems are ones in which chemical components can be added or subtracted freely, whereas closed systems are ones in which the identity and amount of chemical components available for reaction are constant. In physical models, a closed system maintains a constant volume, while in open systems volume is unconstrained. The principal area of uncertainty in the conceptual models is the definition of the boundary between open and closed space. This boundary is significant because real systems are somewhere between totally open or closed, and open and closed systems result in very different expected performance lives for plugged boreholes.

In chemical systems, a very small addition or release of reacting components is insignificant, but a substantial change can have large effects: in open systems reactions proceed until the supply of reactants is exhausted. In open systems, equilibrium considerations may have little or no significance; hence treatment by equilibrium thermodynamics may be unenlightening. Similarly, in physical systems, a small amount of system expansion will have little effect on internal stresses, but unlimited expansion may cause the system to fail in tension.

MASS-16.3.1 Corrosion

There are many low-carbon-steel alloys, and not all corrode at the same rate in a given environment. However, because of the aggressive corrosion rate selected for the model, steel composition is not thought to introduce significant uncertainty about the rate. Corrosion of the casing steel has been modeled thermodynamically for plugged boreholes. Hydrogen is a common byproduct of corrosion. An equilibrium hydrogen pressure has been calculated for a number of potential reactions, using metallic iron to represent steel and pure water to represent brines. Attainment of equilibrium hydrogen pressure is taken to indicate cessation of corrosion. To reach equilibrium, the system must contain the hydrogen that is generated. The hydrostatic pressure of the brine column has been assumed to confine hydrogen when the pressure exceeds the equilibrium hydrogen pressure calculated for the corrosion reaction of interest.

Reactions most representative of corrosion of steel casing produce iron hydroxide corrosion products. Equilibrium hydrogen pressures for these reactions are exceeded by hydrostatic pressures at depths greater than about 1,100 ft (335 m). Corrosion of casing above this depth is treated as open; the casing corrodes until the supply of metallic iron is exhausted and the casing disintegrates. Without axial support supplied by the casing, the concrete plug also fails. In contrast, corrosion is assumed to take place in a closed system at depths greater than 1,100 ft (335 m). Hydrogen is not free to nucleate as a gas and leave the system. Although local perforations in the casing are expected, the casing does not disintegrate. It supports the concrete plugs, and permeability changes in the plugs are attributed to alteration of cement phases by the brine that flows through them.

The greatest uncertainty associated with composition is likely to arise from the thermodynamic calculations used in the model. Pure phases (Fe for steel and H_2O for brine) have been assumed so that hand calculations may be more readily performed. Various reactions and environments have been modeled without directly considering complexities in the chemical system (other than volatiles). Qualitatively, the added complexities are likely to have no substantial consequence on the ability of the brines to dissolve a pathway through the casing. However, system complexities might decrease the equilibrium hydrogen pressures calculated for the corrosion reactions or lead to unexpected reaction products.

Data supporting low-carbon-steel corrosion models come primarily from the literature. The empirical data support the assumption that general corrosion is the dominant mechanism for corrosion under oxic conditions and that pitting will occur under low oxygen (and high pH) or elevated carbon dioxide and hydrogen disulfide conditions. Corrosion rates are a function of the conditions under which corrosion occurs. Published data include rates as rapid as 3 mm per year, which is the value assumed in the model. Such rapid rates are not inconsistent with reports in the Delaware Basin of casing failures occurring from corrosion within months to years (CCA Appendix MASS, Attachment 16-3, B-17). Data from corrosion of steel enshrouded in concrete come from the literature on marine construction and the data base on reinforcing steels. These data support the assumption that steel encased in concrete cannot be assumed to corrode more slowly than exposed steel. This subject area is discussed in detail in CCA Appendix MASS, Attachment 16-3 (Section 3.2 and Appendix B).

MASS-16.3.2 Portland Cement Concrete

The cementitious materials used in hydrocarbon exploration are variable. The degree to which oil-field materials might perform differently from the cement mixtures investigated and reported in the literature is unknown. There is no standard mix formulation that specifies plugging cements precisely; the use of generic data is reasonable, because the vagaries of cement composition are implicitly included. The published empirical studies of concrete degradation include a large body of data for reacting solutions ranging from pure water to marine brines. Waters with higher chloride and magnesium contents cause greater reaction. This level of detail has not been factored into the model directly; rather, alteration by brines has been the favored source when extracting information on degradation.

Chemical alteration of cement phases by brine produces new solids with greater molar volumes than the unaltered, hardened cement phase. In a closed physical system, the alteration will lead to decreased internal porosity and consequent decrease in permeability. In an open physical system, alteration will lead to increased internal pore pressures that will eventually exceed the tensile strength of the concrete plug. The result is often seen on concrete sidewalks or other unreinforced concrete structures: without something to restrain expansion, the concrete cracks, increasing its porosity and permeability.

Current plugging practices create configurations that favor each model. Plugs installed to respond to the New Mexico Oil Conservation Division regulation R-111-P approach 2,000 ft (610 m) in length (State of New Mexico 1988). These plugs are judged to be long enough that they are self-confining. As a result, alteration of R-111-P plugs produces a situation in which performance is indistinguishable from the undisturbed rock. In contrast, plugs emplaced in response to regulations of the U.S. Bureau of Land Management have a mean length near 40 m. This length is judged to be too short to provide self-confinement; alteration of the concrete results in fracturing and increased porosity and permeability in the plug. The plug length that changes the physical system from open to closed is undetermined. For both chemical and physical model elements, a closed system enhances performance.

Simulation of concrete plug degradation follows a model proposed by Berner (1990), in which the matrix degrades after dissolution and removal of soluble materials such as alkali salts. The model is grounded in empirical observations that concrete alteration sequentially removes excess alkalis, portlandite, and tobermorite or calcium-silicate-hydrate (CSH). Decreased strength attends removal of portlandite.

A critical amount of flow must occur before this degradation threshold is crossed. A volume equivalent to 100 pore volumes has been taken as the critical flow volume, based on values for common compositions of ordinary portland cement concrete (Berner 1990). Also following Berner, the model tracks the amount of flow as pore volumes, reasoning that flow occurs only through pores and that alteration is therefore limited to the solids that surround the pores. The model does not explicitly account for the strength of the concrete but instead makes the conservative assumption that physical failure occurs suddenly at the onset of chemical attack on CSH, that is, at approximately 100 pore volumes. As a result, initial porosity of the hardened concrete is a key parameter for timing plug degradation.

The initial permeability of hardened cement is directly related to the connected porosity that permits flow to occur. Initial permeability of ordinary portland cement is a strong function of the water:cement ratio of the mix. Higher water contents produce higher porosity and permeability. To simplify the analysis, the CCA used an initial plug permeability of 5×10^{-17} m^2. This value lies in the upper range of permeabilities reported for ordinary portland cement and is verified by field measurements made during a single field test of borehole plugging conducted for the DOE (CCA Appendix MASS, Attachment 16-3, C-4). In their review of the CCA, the EPA required the DOE to treat this parameter as uncertain (EPA 1998b, Section 5.17). DOE implemented log-uniform distribution of values ranging from 10^{-19} to 10^{-17} m^2. This distribution is used for the 2004 PA calculations.

The initial permeability of the concrete plug is an important parameter because water must penetrate and flow through the structure before it can alter the hardened plug. The lower the permeability, the longer it takes for 100 pore volumes to pass through the plug. Somewhat paradoxically, the lower the porosity, the smaller the volume of water needed before attack of the CSH begins, because the model decouples the relationship between porosity and permeability by holding permeability constant. In the real world, cement formulations with low water:cement ratios generally produce fewer alkalis and have both lower porosities and lower permeabilities. Less water must pass through the concrete body before onset of CSH degradation, but the lower permeabilities lead to a longer life. The simplified model is conservative: it holds the permeability constant at the upper end of the established range while allowing porosity to vary over the full range commonly encountered in ordinary portland cement. This accommodation reflects better knowledge of permeabilities than porosities in as-emplaced borehole plugs. The range in porosity modeled (5 to 40 percent) can create an order-of-magnitude spread in predicted performance life.

Data supporting the concrete degradation model come primarily from two sources: the international repository literature and journals on concrete construction (for example, dams or bridges). The international literature on repositories contains both models and empirical studies confirming that alteration of concrete will result in decreased porosities and permeabilities in closed systems. Experience for dams confirms this conclusion and confirms the diffusion-driven concrete alteration rates used in the model. The general concrete literature confirms the values of initial permeability and porosity of hardened concrete used in the model.

Observations made on cores recovered from potash mines near the WIPP confirm that alteration of concrete plugs is not extensive after decades of service. Qualitative data have been produced by recovery, microscopic inspection, and leach testing of concrete cores recovered from nearby potash mines. These data establish that plugs placed in boreholes will have low initial permeabilities and that plugs placed in the Salado will form tight interfaces at the borehole-rock interface and will not degrade substantially by contact with formation brines in the amounts and compositions that might reasonably be expected. See CCA Appendix MASS, Attachment 16-3 for the historical discussions of concrete plug alteration and creep closure of boreholes.

MASS-16.3.3 Borehole Configurations

The conceptual models for borehole plugs examine three basic possibilities: a continuous plug through the evaporite sequence, a plug below the brine reservoir horizon coupled with a plug between the repository and the Rustler, and three or more plugs with at least one intermediate plug between the brine reservoir and the repository and another between the repository and the Rustler. These possibilities represent simplifications of the plugging schemes documented in a 1996 survey during the 1996 CCA and verified by the Delaware Basin Drilling Surveillance Program (see Appendix DATA, Attachment A; and Sections 6.4.7.2.1 through 6.4.7.2.3). Since the CCA, plugging data show these three plug configurations continue to represent plugging patterns employed within the WIPP vicinity (WRES 2003, Attachment C).

As stated, the basis for these assumptions is a detailed survey of plugging practices in the Delaware Basin. The survey examined the lengths, locations, and intervals plugged, as well as the materials used for construction. The locations of plugs are determined partly by stratigraphic changes and partly by operational considerations during exploration and recovery. Variations in plug length and location affect pressure regimes and flow rates through plugs. The 120-ft (40-m) length of the plugs is the approximate mean value of approximately 188 plugs in the survey. Minimum lengths prescribed by regulations are 50 ft (15 m) above plus 50 ft (15 m) below casing transitions or recovery points. Additional plug lengths sometimes occur for unspecified reasons. When all else is equal, performance life is proportional to plug length. For conservatism, the model does not consider the longer plugs. In the conceptual model, all plugs are taken to be 120 ft (40 m) long. See CCA Appendix MASS, Attachment 16-3 (Section 5.0), for a more detailed discussion of plug performance.

The borehole permeability model was assembled beginning in February 1996. Initially, the model considered only the plug configuration stipulated by Oil Conservation Division regulations, but it was subsequently expanded to consider all regulations and practices documented in the New Mexico portion of the Delaware Basin, without specific consideration of their applicability to the WIPP in the future. The model was developed to be straightforward and easy to understand. Use of hand calculations was favored over the use of complex computer codes. As a result, no detailed evaluation of potentially applicable codes was undertaken, and no screening of codes was performed.

CCA Appendix MASS, Attachment 16-3 describes the model and its predictions contains about 40 references with data that support the model. In general, these references support the plug configurations, steel corrosion mechanisms and rates, and concrete alteration processes that underpin the model. Additionally, the Delaware Basin Drilling Surveillance Program continuously monitors plugging practices in the WIPP vicinity (WRES 2003).

MASS-17.0 CLIMATE CHANGE

The purpose of this model is to allow quantitative consideration of the extent to which uncertainty about future climate may contribute to uncertainty in estimates of cumulative radionuclide releases from the disposal system. Consideration is limited to conditions that could result from reasonably possible natural climatic changes. The model is not intended to provide a quantitative prediction of future climate, nor is it intended to address uncertainty in system properties other than estimated cumulative radionuclide releases that may be affected by climate change. This model is also discussed in Section 6.4.9.

As discussed in CCA Appendix CLI, paleoclimatic data from the literature form the basis for reconstructing the climatic variability in southeastern New Mexico since late Pleistocene time, spanning the transition from full glacial conditions in North America (ice sheets as far south as the Northern Great Plains) to the present interglacial period. The wettest and coolest climate at the WIPP corresponded to periods of continental glaciation. During Holocene time (the past 10,000 years), the climate has been predominantly dry, like that of the present, with several wetter episodes.

Future climate at the WIPP may differ in the next 10,000 years from that of the present, but it should be bounded by the extremes of the late Pleistocene glaciation. For the purposes of performance assessment, the DOE assumes that uncertainty about future climate is adequately captured by considering two possible patterns: one in which the Holocene pattern of predominantly dry conditions alternating with wetter conditions continues; and one in which the climate becomes continuously wetter.

Effects of climatic change on the WIPP are limited in the performance assessment model to effects on groundwater flow in the Culebra. Flow (that is, specific discharge in the MODFLOW-2000 model) is increased from its present calibrated value by a sampled factor that ranges from 1.0 to 2.25 to simulate effects of wetter climates. Possible decreases in flow during drier climates are not considered. Justification for limiting the effects of climate change to flow in the Culebra is based on regional three-dimensional modeling that estimates the extent to which changes in recharge will alter the altitude of the water table and in turn affect flow in the Culebra and other units. Maximum recharge rates considered in the analysis result in a simulated water-table altitude at or near the ground surface throughout the region. Other effects of climatic change, including changes in temperature, wind, evapotranspiration, and vegetation, are not modeled explicitly but are qualitatively included in this analysis through the consideration of the effects of varying recharge.

The climate change model is implemented through the use of a single parameter, the Climate Index. This parameter is a dimensionless factor by which the specific discharge in each grid block of the MODFLOW-2000domain is multiplied. It is a sampled parameter in the PA, with a bimodal distribution ranging from 1.00 to 1.25 and from 1.50 to 2.25. See Corbet (1995) and CCA Appendix MASS, Attachment 17-1 for a discussion of this distribution.

The climate change model used for performance assessment is predicated on the assumption that climate will change during the next 10,000 years. The extent of this change is uncertain, but it should be bounded by the changes that occurred in the past during the peaks of Pleistocene glaciation. Other conceptual models for climate change are not consistent with present scientific understanding of the Earth's climate or with the EPA's guidance to consider natural processes of climatic change (EPA 1996, pp. 5227-5228). For example, climate could be assumed to remain constant for 10,000 years, but this would be inconsistent with scientific understanding of climate. Alternatively, climate could be assumed to change to conditions unlike any known from the Pleistocene; however, no natural processes are known that could result in such change within 10,000 years.

As discussed in Corbet (1995) and CCA Appendix MASS, Attachment 17-1, the implementation of climate change in the performance assessment incorporates uncertainty about future climates within the range known from the Pleistocene. Alternative approaches to treating climate change in the performance assessment (that is, varying boundary conditions rather than specific discharge) are discussed in the following section. Past analyses performed using a different approach as part of the 1991 and 1992 preliminary performance assessments suggest that disposal system performance is not sensitive to climate change (Swift et al. 1994, p. 12).

MASS-17.1 Historical Context of the Climate Change Model

See CCA Appendix MASS, Section MASS.17.1 for historical information on the Climate Change model. This Climate Change model is unchanged for the 2004 PA.

MASS-18.0 CASTILE BRINE RESERVOIR

The conceptual model for the hypothetical brine reservoir is included in the performance assessment to estimate the extent to which uncertainty about the existence of a brine reservoir under the waste disposal region may contribute to uncertainty in the estimate of cumulative radionuclide releases from the disposal system. The conceptual model is not intended to provide a realistic approximation of an actual brine reservoir under the waste disposal region: data are insufficient to determine whether such a brine reservoir exists.

The Castile is treated as an impermeable unit in PA and plays no role in the analysis except to separate the Salado from the modeled brine reservoir in the BRAGFLO grid. In human-intrusion scenarios, the hypothetical brine reservoir can be penetrated by an intrusion borehole connecting it to the repository. The amount of brine that can enter the repository from the brine reservoir is important to PA because brine is required for gas generation reactions to proceed and can transport radionuclides in solution, contributing to potential releases.

The properties of the hypothetical brine reservoir defined for PA include: permeability, porosity, pore volume, initial pressure, and various two-phase flow parameters. Values assigned for these properties were chosen to either be consistent with the available data from and analyses of borehole penetrations of brine reservoirs in the region, or to provide a reasonable response in the BRAGFLO model.

The treatment of the brine reservoir for the 2004 PA is different than that used in the 1996 CCA PA. The major changes to the brine reservoir representation were made by the EPA in their 1997 PAVT (EPA 1998b, V-B-14). In the 1997 PAVT, EPA defined new parameter ranges for bulk compressibility and total pore volume. The range of bulk compressibility was based on a reevaluation of field test data from the WIPP-12 borehole following the CCA (Beauheim 1997). Since the total volume of the grid cells used to represent the brine reservoir in BRAGFLO is fixed, the range of total pore volume was set by defining a range of "effective" porosity (pore volume = grid volume × effective porosity). This range of porosity values is not representative of the actual host rock rather it was chosen to produce a reasonable response in the BRAGFLO model by providing a predefined range of total pore volumes based on the field tests at WIPP-12.

For the 2003 WIPP PA, DOE has implemented this approach by assuming that the productivity ratio (PR) remains constant (2.0051×10^{-3} m^3/Pa). The productivity ratio is defined as:

$$PR = V\frac{C_r}{\phi},$$

where V is the grid volume of the brine reservoir (18,462,514 m^3), C_r is the bulk compressibility (2×10^{-11} to 1×10^{-10} Pa^{-1}), and φ is the effective porosity (0.1842 to 0.9208). The porosity range used in the CRA-2003 PA is slightly modified from that used by the EPA because the fixed-grid volume increased slightly from the volume assumed in the CCA BRAGFLO grid. In this approach, bulk compressibility and effective porosity are directly proportional (Stein 2003a). See Appendix PA, Section PA-4.2, for the details on the implementation in PA.

Basic geologic information about the Castile is given in Section 2.1.3.3. The hydrology of the known brine reservoirs is discussed in Section 2.2.1.2.2. The treatment of the hypothetical brine reservoir in the PA is discussed in Section 6.4.8, which also points to supplementary information included in this recertification application.

MASS-18.1 Historical Context of the Castile Brine Reservoir Model

See CCA Appendix MASS, Section MASS.18.1 for historical information on the Castile Brine Reservoir model.

MASS-19.0 OPTION D PANEL CLOSURES

The certification decision by the EPA (1998a) included several conditions that the DOE was required to meet. In the first of these conditions, the EPA required the DOE to implement a specific design for the panel closure system referred to as Option D and required the concrete monolith to be constructed using SMC. The DOE had included in the CCA four Options (A-D) for the panel closure design. The Option D design consisted of two components; a large monolith constructed of SMC and keyed into the surrounding DRZ, and an explosion wall constructed of concrete blocks, which is not keyed into the DRZ.

The PA calculations that supported the CCA and the subsequent 1997 PAVT calculations included generic panel closures in the BRAGFLO grid. These generic closures were not representative of the Option D design. Specifically, the Option D panel closures are designed to impede fluid flow (brine and gas) between panels over long-time scales. The generic panel closures included in the 1996 CCA and 1997 PAVT calculations were relatively permeable and allowed gas to flow freely between panels. In the 1996 CCA and 1997 PAVT PA calculations, a drilling intrusion into a single panel generally caused pressures in the entire repository to decrease.

Following the certification of the repository, the DOE updated the modeling of the panel closures in PA so that the mandated Option D design was adequately represented. A new panel closure representation was developed and presented to the Salado Flow Peer Review Panel in May 2002 and again in February 2003. The peer review panel approved the new conceptual models, which included the implementation of the Option D panel closures in the grid (Caporuscio et al. 2003).

In the CCA/PAVT BRAGFLO grid, only two panel closures were represented. For the 2004 PA, however, DOE included an additional set of panel closures. Preliminary tests of the Option D panel closure representation (Hansen et al. 2002) concluded that Option D panel closures were effective at impeding fluid flow between panels on the order of thousands of years, but that given enough time, pressures slowly equilibrated. These results suggest that the effect of a single intrusion event on pressures in other panels depends on the number of panel closures that lie between the intruded panel and the other panels. Therefore, DOE decided to divide the RoR region into two regions separated by a panel closure. This panel closure represents a set of four panel closures to be located between the northern and southern internal extended panels. The south RoR represents panels directly adjacent to an intruded panel and the north RoR represents panels that are farther away from the intruded panel (two sets of panel closures lie in between).

The DOE assumes that the effect of the Option D panel closures will be to impede fluid flow through and around the closures. Only the concrete monolith portion of the closure system is assumed to remain effective over the 10,000-year regulatory period. The explosion wall is assumed to effective only for a brief period during the operational period. The explosion wall and the open drift adjacent to the monolith are represented in the BRAGFLO grid by a column of grid cells with the properties of the waste area (e.g., high permeability) and include creep closure effects. The monolith is represented in the BRAGFLO grid by an adjacent column of grid cells with a length equal to the length of the monolith (7.9 m) multiplied by the number of panel closures in series and a width equal to the width of the monolith (10 m) multiplied by the number of panel closures in parallel. For instance, in Figure MASS-6, the southern panel closure in the

BRAGFLO grid represents a single set of two panel closures (in parallel) that separate a single external panel from the one of the two internal extended panels (9 and 10). The middle panel closure in the BRAGFLO grid represents a single set of four panel closures (in parallel) that separate the internal extended panels from one another. The northern panel closure in the BRAGFLO grid represents two sets (in series) of four panel closures (in parallel) that lie between the northern edge of the waste region and the shafts.

It is assumed in the modeling that the DRZ above the concrete monolith will heal and quickly attain a state of relatively low permeability. However, it is also assumed that if pressures exceed the fracture initiation pressure (~12.5 MPa), DRZ and anhydrite marker bed materials that intersect the waste room can fracture and allow gas or brine to circumvent the panel closures by flowing around the concrete monolith. This possibility is included in the implementation of the panel closures in the BRAGFLO by replacing the concrete monolith material with marker bed material everywhere the monolith intersects and cuts through the marker beds. This implementation is appropriate even at low pressures because the permeability range of the concrete and the marker beds is nearly equivalent. And at high pressures, fracturing is considered in these grid elements allowing fluids to flow, thus simulating the consequence of fractures extending around the monolith.

Additional information on panel closure effects on repository performances can be seen in the BRAGFLO Analysis package (SNL 2003c).

MASS-20.0 SUMMARY OF CLAY SEAM G MODELING ASSUMPTIONS

One of the changes to the repository design since the CCA is the raising of the repository horizon in the southern half of the waste panels. Specifically, Panels 3, 4, 5, 6, and 9 will be excavated at an elevation approximately 2.4 m above the level of Panels 1, 2, 7, 8, and 10, and the operations and experimental areas. This change in horizon will bring the roof of the raised rooms to the level of the Clay Seam G. The change is expected to improve roof conditions and enhance operations and mine safety. The DOE submitted a planned change request to EPA that described the change and presented an argument that the change would have minimal impact on long-term repository performance (DOE 2000). The EPA responded to the change request in a letter (EPA 2000) in which they agreed with the DOE that the effects to long-term performance would be minimal.

As part of the Salado Flow Peer Review in February 2003, the DOE did an impact assessment on the possible effects of the horizon change to PA to better demonstrate the minimal impact of this change on long-term performance. Two possible effects of this change on the results of PA were considered in this assessment.

First, it was considered that the horizon change might influence the creep-closure porosity surface calculated by the code SANTOS and used by BRAGFLO to determine the porosity of the waste rooms. This possibility was considered by simulating creep closure around a WIPP disposal room raised to Clay Seam G (Park 2002). The resulting Clay G porosity surface was then compared with the original porosity surface, which was used in the CCA. The differences were shown to be so minor that long-term PA would not be significantly altered (Park and Holland 2003).

The second effect that was considered was the possibility that the thickness of the upper and lower DRZ, as represented in the BRAGFLO grid, might change due to the horizon change. Specifically, in the raised part of the repository, the lower DRZ might become thicker since the distance from the floor of the rooms to MB 139 will be greater than in the unraised part of the repository. A similar decrease in the thickness of the upper DRZ might occur as the roof of the rooms would be nearer to MB 138. Since the DRZ is assumed to be an important source of brine in BRAGFLO, these potential changes to the thickness of the DRZ might affect the amount of brine available to the waste in the raised panels. To assess whether such a change would affect long-term performance, DOE ran a single replicate of 100 undisturbed BRAGFLO vectors in which the total pore volume in the DRZ was adjusted to account for the thickness changes (Stein and Zelinski 2003a). Pressure and saturation results within the waste regions were compared to results assuming the original DRZ thicknesses. It was concluded from these comparisons that the effects of the DRZ thickness changes were very minor and not at all significant for long-term repository performance (Stein and Zelinski 2003b).

The results of the impact assessment were presented to the Salado Flow Peer Review panel in February 2003. The panel accepted the position that the repository horizon change was adequately represented by the impact assessment and need not be implemented explicitly in the BRAGFLO grid for PA calculations (Yew et al. 2003). Based on the results of this impact assessment and the acceptance of the Salado Flow Peer Review, the DOE has determined that it is not warranted to include the change in the repository horizon to Clay Seam G explicitly in the BRAGFLO grid.

MASS-21.0 EVALUATION OF WASTE STRUCTURAL IMPACTS, EMPLACEMENT AND HOMOGENEITY

During the development of the CCA PA, the DOE choose to assume random placement of TRU waste in the WIPP, and developed conceptual and numerical models accordingly. The EPA reviewed these models and their results, and determined that DOE had modeled accurately random placement of waste in the disposal system. Since the time of the CCA, additional information about the waste and its emplacement has emerged, and requires the assumption of random placement to be reevaluated. The waste inventory estimates have been updated since the CCA PA (see Appendix TRU WASTE), resulting in different estimates of important waste components, such as CPR materials. Additionally, the CCA PA assumed that all waste could be modeled as if the waste was emplaced in 55-gallon drums. However, the DOE is emplacing waste using several different types of waste containers, including standard waste boxes (SWBs) and pipe overpacks (Section 4.1). Waste has been shipped to WIPP in campaigns from the generator sites, resulting in waste emplacement that appears inconsistent with the representation of the waste as a homogeneous material. Finally, DOE plans to emplace waste types, such as supercompacted waste, that were not considered in the CCA inventory (DOE 2002). As a result of this new information and these proposed changes, DOE performed a separate analysis (Hansen et al. 2003a) to determine if the modeling assumptions used in PA continue to adequately represent the waste.

Many important waste characteristics, such as the radionuclide content and the mass of CPR materials, are directly incorporated in PA by means of waste material parameters. These parameters have been updated consistent with the inventory update (see Appendix TRU WASTE) and thus are represented in the 2004 PA. However, PA does not account for heterogeneity in waste materials or in waste containers. At the Idaho National Engineering and Environmental Laboratory, for instance, debris waste will be volume-reduced by supercompaction, resulting in a very dense waste form containing a high concentration of CPR material. In addition, the Pu residues from the Rocky Flats Environmental Technology Site have been packaged in pipe overpacks, which are more rigid than the typical 55-gallon drum assumed in the CCA. Additionally, PA assumes that waste is emplaced in a random or homogeneous manner. Actual waste emplacement is determined by the availability of waste at generator sites and the shipping schedules. Pipe overpacks occupy about 43 percent of the containers emplaced in Panel 1, suggesting that actual emplacement will not be statistically random.

The analysis reported in Hansen et al. (2003a) focused on potential effects of supercompacted waste and of waste in pipe overpacks on repository performance. Both waste types are structurally stiffer than the generic waste model used in the CCA PA, and the supercompacted waste in particular has high concentrations of CPR materials. The analysis began with a systematic reevaluation the baseline FEPs to identify specific components of PA that could be affected by supercompacted waste. The reassessment concluded that the FEPs “screened in” were adequate to represent the variety of waste types and containers, and that none of the “screened out” FEPs should be reconsidered for implementation. The FEPs assessment concluded that creep closure of the repository, chemical conditions of the waste, gas generation models, and waste mechanical properties could be affected by heterogeneities in the waste materials and waste containers. In addition, DOE determined that the assumption of random waste emplacement should be reevaluated.

Analysis of creep closure of waste-filled rooms, accounting for several types of waste materials and packaging, indicated that a wider range of long-term porosities could occur relative to that established in the CCA, given the uncertainties about the structural integrity of waste packages and their spatial arrangement in the repository (Park and Hansen 2003). For this reason, the analysis in Hansen et al. (2003a) treated creep closure as an uncertain variable. Sensitivity analysis showed that this additional uncertainty did not affect the results of PA in a significant way.

Chemical conditions also were reexamined under a range of possible waste arrangements. The assessment found that regardless of actual waste emplacement, the MgO would still be sufficient to maintain desired chemical conditions. Moreover, the constituents of supercompacted waste would not alter the reactions that determine chemical equilibrium and, consequently, no changes to actinide solubilities or to the gas generation models were warranted.

Supercompacted waste contains elevated amounts of CPR materials relative to other waste streams, and the future arrangement of this waste in the WIPP repository is uncertain. Thus, the analysis treated the spatial distribution of CPR materials as uncertain. However, sensitivity analysis demonstrated that uncertainty in the spatial distribution of CPR materials had little effect on PA results.

The representation of the waste properties also was considered; however, it was determined that no changes to permeability, shear strength, or tensile strength were warranted. Based on this evaluation, no changes to the models for direct releases were necessary.

Direct releases as a consequence of a drilling intrusion are calculated with the assumption of random waste emplacement in the repository. In addition, releases by spallings, DBR, and long-term radionuclide transport assume that radionuclides are homogeneously distributed throughout the waste. A sensitivity analysis determined that PA results are not greatly affected by the assumption of random waste emplacement or by the assumption that radionuclides are homogeneously distributed.

Based on the analysis reported in Hansen et al. (2003a), DOE concluded that:

1. Explicit representation of the specific features of supercompacted waste and of waste in pipe overpacks, such as structural rigidity, was not warranted in modeling, since PA results were relatively insensitive to the effects of such features.

2. PA results were not affected significantly by the assumption of nonrandom waste emplacement and the representation of these waste types as a homogeneous material.

REFERENCES

Amyx, J.W., Bass, D.M. Jr., and Whiting, R.L. 1960. *Petroleum Reservoir Engineering, Physical Properties.* ISBN 07-001600-3, McGraw-Hill Book Company, New York, NY. (derived from equation 2-33) pp. 78.

Anderson, M.P., and Woessner, W.W. 1992. *Applied Groundwater Modeling: Simulation of Flow and Advective Transport,* Academic Press, Inc.

Avogadro, A., and de Marsily, G. 1984. "The Role of Colloids in Nuclear Waste Disposal," *Scientific Basis for Nuclear Waste Management VII, Materials Research Society Symposia Proceedings, Boston, MA, November 14-17, 1983.* Ed. G.L. McVay. Vol. 26, 495-505. North-Holland, New York, NY. Vol. 26, 495-505.

Bear, J. 1972. *Dynamics of Fluid in Porous Media*. ISBN 0-486-65675-6, Dover Publications, New York, NY.

Beauheim, R.L. 1987a. *Analysis of Pumping Tests of the Culebra Dolomite Conducted at the H-3 Hydropad at the Waste Isolation Pilot Plant (WIPP) Site.* SAND86-2311, Sandia National Laboratories, Albuquerque, NM. WPO 28468.

Beauheim, R.L. 1987b. *Interpretations of Single-Well Hydraulic Tests Conducted At and Near the Waste Isolation Pilot Plant (WIPP) Site, 1983-1987.* Sandia National Laboratories, Albuquerque, NM. WPO 27679.

Beauheim, R.L. 1997. "Revisions to Castile Brine Reservoir Parameter Packages," Memorandum to Palmer Vaughn, January 16, 1997. Sandia National Laboratories, Albuquerque, NM. ERMS # 244699.

Bennett, D.G., Liew, S.K., Nanu, L., Read, D., and Thomas, J.B. 1993. "Modelling Colloidal Transport of Radionuclides Through Porous Media," *High Level Radioactive Waste Management, Proceedings of the Fourth Annual International Meeting, Las Vegas, NV, April 26-30, 1993.* American Nuclear Society, La Grange Park, IL; American Society of Civil Engineers, New York, NY. Vol. 4, 638-645.

Berglund, J.W. 1992. *Mechanisms Governing the Direct Removal of Wastes from the Waste Isolation Pilot Plant Repository Caused by Exploratory Drilling.* SAND92-7295, Sandia National Laboratories, Albuquerque, NM. WPO 23946.

Berner, U. 1990. "A Thermodynamic Description of the Evolution of Pore Water Chemistry and Uranium Speciation During the Degradation of Cement," Technical Report 90-12, Paul Scherrer, Villigen, Switzerland.

Bertram, S.G. 1995. "NS-11: Subsidence Associated with Mining Inside or Outside of the Controlled Area." Summary Memo of Record to D.R. Anderson, December 8, 1995. SWCF-1:1.1.6.3. Sandia National Laboratories, Albuquerque, NM. WPO 30761.

Bertram-Howery, S.G., Marietta, M.G., Rechard, R.P., Swift, P.N., Anderson, D.R., Baker, B.L., Bean, Jr., J.E., Beyeler, W., Brinster, K.F., Guzowski, R.V., Helton, J.C., McCurley, R.D., Rudeen, D.K., Schreiber, J.D., and Vaughn, P. 1990. *Preliminary Comparison with 40 CFR Part 191, Subpart B for the Waste Isolation Pilot Plant, December 1990*. SAND90-2347, Sandia National Laboratories, Albuquerque, NM.

Brush, L.H. 1990. *Test Plan for Laboratory and Modeling Studies of Repository and Radionuclide Chemistry for the Waste Isolation Pilot Plant*. SAND90-0266, Sandia National Laboratories, Albuquerque, NM. WPO 26015.

Butcher, B.M., and Mendenhall, F.T. 1993. *A Summary of the Models Used for the Mechanical Response of Disposal Rooms in the Waste Isolation Pilot Plant with Regard to Compliance with 40 CFR Part 191, Subpart B*. SAND92-0427, Sandia National Laboratories, Albuquerque, NM. WPO 23356.

Callahan, G.D. 1994. *SPECTROM-32: A Finite Element Thermomechanical Stress Analysis Program Version 4.06*, RSI-0531, RE/SPEC Inc., Rapid City, SD. WPO 36814.

Caporuscio, F., Gibbons, J., and Oswald, E. 2003. *Waste Isolation Pilot Plant: Salado Flow Conceptual Models Final Peer Review Report*. Report prepared for the U.S. Department of Energy, Carlsbad Area Office, Office of Regulatory Compliance. ERMS # 526879.

Chapman, J.B. 1986. *Stable Isotopes in Southeastern New Mexico Groundwater: Implications for Dating Recharge in the WIPP Area*. EEG-35, DOE/AL/10752-35, Environmental Evaluation Group, Santa Fe, NM.

Chapman, J.B. 1988. *Chemical and Radiochemical Characteristics of Groundwater in the Culebra Dolomite, Southeastern New Mexico*. EEG-39, Environmental Evaluation Group, Santa Fe, NM.

Christian-Frear, T.L., and Webb, S.W. 1996. *The Effect of Explicit Representation of the Stratigraphy on Brine and Gas Flow at the Waste Isolation Pilot Plant*. SAND94-3173, Sandia National Laboratories, Albuquerque, NM. WPO 37240.

Corapcioglu, M.Y., and Jiang, S. 1993. "Colloid-Facilitated Groundwater Contaminant Transport," *Water Resources Research*. Vol. 29, no. 7, pp. 2216 – 2226.

Corbet, T. 1995. "NS-9: Justification of SECO2D Approximation for PA Transport Calculations." Summary Memo of Record to D.R. Anderson, September 21, 1995. SWCF-A:1.1.6.3. Sandia National Laboratories, Albuquerque, NM. Contained in WPO 30802.

Corbet, T.F., and Knupp, P.M. 1996. *The Role of Regional Groundwater Flow in the Hydrogeology of the Culebra Member of the Rustler Formation at the Waste Isolation Pilot Plant (WIPP), Southeastern New Mexico*. SAND96-2133, Sandia National Laboratories, Albuquerque, NM.

Davies, P.B. 1991. *Evaluation of the Role of Threshold Pressure in Controlling Flow of Waste-Generated Gas into Bedded Salt at the Waste Isolation Pilot Plant*. SAND90-3246, Sandia National Laboratories, Albuquerque, NM. WPO 26169

Davies, P.B., Webb, S.W., and Gorham, E.D. 1993. "Feedback on PA Modeling Using BRAGFLO -- 1992" memo by J. Schreiber, July 14, 1992, pp. A-23 through A-37 in Sandia WIPP Project, 1992. *Preliminary Performance Assessment for the Waste Isolation Pilot Plant, December 1993. Volume 3, Model Parameters*. SAND92-0700/3, Sandia National Laboratories, Albuquerque, NM.

Deal, D.E., Abitz, R.J., Belski, D.S., Case, J.B., Crawley, M.E., Deshler, R.M., Drez, P.E., Givens, C.A., King, R.B., Lauctes, B.A., Myers, J., Niou, S., Pietz, J.M., Roggenthen, W.M., Tyburski, J.R., and Wallace, M.G. 1989. *Brine Sampling and Evaluation Program, 1988 Report*. DOE-WIPP-89-015, Westinghouse Electric Corporation, Carlsbad, NM.

Deal, D.E., Abitz, R.J., Belski, D.S., Clark, J.B., Crawley, M.R., and Martin, M.L. 1991a. *Brine Sampling and Evaluation Program, 1989 Report*. DOE-WIPP-91-009. Prepared for U.S. Department of Energy by IT Corporation and Westinghouse Electric Corporation. Westinghouse Electric Corporation, Waste Isolation Division, Carlsbad, NM.

Deal, D.E., Abitz, R.J., Myers, J., Case, J.B., Martin, M.L., Roggenthen, W.M., and Belski, D.S. 1991b. *Brine Sampling and Evaluation Program, 1990 Report*. DOE-WIPP-91-036. Prepared for U.S. Department of Energy by IT Corporation and Westinghouse Electric Corporation. Westinghouse Electric Corporation, Waste Isolation Division, Carlsbad, NM.

Deal, D.E., Abitz, R.J., Myers, J., Martin, M.L., Milligan, D.J., Sobocinski, R.W., Lipponer, P.P.J., and Belski, D.S. 1993. *Brine Sampling and Evaluation Program, 1991 Report*. DOE-WIPP-93-026. Prepared for U.S. Department of Energy by IT Corporation and Westinghouse Electric Corporation. Westinghouse Electric Corporation, Waste Isolation Division, Carlsbad, NM.

Deal, D.E., and Case, J.B. 1987. *Brine Sampling and Evaluation Program, Phase I Report*. DOE-WIPP 87-008, Westinghouse Electric Corporation, Carlsbad, NM.

Deal, D.E., and Roggenthen, W.M. 1989. "The Brine Sampling and Evaluation Program (BSEP) at WIPP: Results of Four Years of Brine Seepage Data," *Waste Management '89, Waste Processing, Transportation, Storage and Disposal, Technical Programs and Public Education, Tucson, AZ, February* 26-March *2, 1989*. Ed. R.G. Post. University of Arizona, Tucson, AZ. Vol. 1, 405 B 406.

Deal, D.E., Case, J.B., Deshler, R.M., Drez, P.E., Myers, J., and Tyburski, J.R. 1987. *Brine Sampling and Evaluation Program Phase II Report*. DOE-WIPP-87-010, Westinghouse Electric Corporation, Carlsbad, NM.

Department of Energy (DOE). 1980. *Final Environmental Impact Statement, Waste Isolation Pilot Plant*. DOE/EIS-0026, U.S. Department of Energy, Washington, DC. Vols. 1 – 2. WPO 38835, WPO 38839.

Department of Energy (DOE). 1995. Conceptual Design for Operational Phase Panel Closure Systems. DOE-WIPP-95-2057, U.S. Department of Energy, Carlsbad Area Office, Carlsbad, NM.

Department of Energy (DOE). 1997. *Expert Elicitation on WIPP Waste Particle Size Distribution(s) During the 10,000-Year Regulatory Post-closure Period, Final Report*. June 3, 1997. (EPA Docket A-93-02, Item II-G-24) DOE transmittal letter to EPA dated June 4, 1997.

Department of Energy (DOE). 2000. Letter from Dr. I. Triay, Manager, Carlsbad Field Office, to Mr. F. Marcinowski, Director, Radiation Protection Division, dated June 26, 2000.

Department of Energy (DOE). 2002. *Assessment Of Impacts On Long-Term Performance From Supercompacted Wastes Produced By The Advanced Mixed Waste Treatment Project.* US Department of Energy Carlsbad Area Office. Carlsbad, NM. December 6, 2002.

Doherty, J. 2002. *Manual for PEST;* Fifth Edition. Watermark Numerical Computing, Australia.

Doherty, J. 2003. "Ground Water Model Calibration Using Pilot Points and Regularization," *Ground Water*. Vol. 41, No. 2, 170 – 177.

Environmental Protection Agency (EPA). 1996. "40 CFR Part 194. Criteria for the Certification and Re-Certification of the Waste Isolation Pilot Plant's Compliance with the 40 CFR Part 191 Disposal Regulations; Final Rule," *Federal Register*. Vol. 61, no. 28, 5224 – 5245.

Environmental Protection Agency (EPA). 1998a. 40 CFR Part 194: Criteria for the Certification and Recertification of the Waste Isolation Pilot Plant's Compliance With the 40 CFR Part 191 Disposal Regulations: Certification Decision; Final Rule, May 18 1998. *Federal Register.* Vol. 63, no. 95, 27354-27406. Office of Radiation and Indoor Air, Washington, D.C.

Environmental Protection Agency (EPA). 1998b. Technical Support Document for 194.23: Parameter Justification Report, *EPA Air Docket A93-02*, V-B-14, Washington D.C.

Environmental Protection Agency (EPA). 2000. Letter from F. Marcinowski, Director, Radiation Protection Division, to Dr. I. Triay, Manager, Carlsbad Field Office, August 11, 2000. Carlsbad, NM.

Environmental Protection Agency (EPA). 2002. August 6, 2002. Letter from F. Marcinowski, Director, Radiation Division, to Dr. I. Triay, Manager, Carlsbad Field Office.

Francis A.J., J.B. Gillow, and M.R. Giles. 1997. *Microbial Gas Generation under Expected Waste Isolation Pilot Plant Repository Conditions.* SAND96-2582. Sandia National Laboratories, Albuquerque, NM.

Francis, A.J., and J.B. Gillow. 2000. "Progress Report: Microbial Gas Generation Program." Memorandum to Y. Wang, January 6, 2000. Brookhaven National Laboratory, Upton, NY. ERMS # 509352.

Francis, A.J., and Gillow, J.B. 1994. *Effects of Microbial Processes on Gas Generation Under Expected Waste Isolation Pilot Plant Repository Conditions, Progress Report Through 1992*. SAND93-7036, Sandia National Laboratories, Albuquerque, NM. WPO 10673.

Freeze, G.A., Larson, K.W., and Davies, P.B. 1995. *Coupled Multiphase Flow and Closure Analysis of Repository Response to Waste-Generated Gas at the Waste Isolation Pilot Plant (WIPP).* SAND93-1986, Sandia National Laboratories, Albuquerque, NM. WPO 29557.

Friend, D.G., and Huber, M.L. 1994. Thermophysical Property Standard Reference Data from NIST, *International Journal of Thermophysics*. Vol. 15, no. 6, 1279 – 1288.

Gillow J.B., and A.J. Francis. 2001a. "Re-evaluation of Microbial Gas Generation under Expected Waste Isolation Pilot Plant Conditions: Data Summary Report, January 24, 2001," *Sandia National Laboratories Technical Baseline Reports*, WBS 1.3.5.4, Repository Investigations Milestone RI010, January 31, 2001. Sandia National Laboratories, ERMS # 516749. 19-46.

Gillow J.B., and A.J. Francis. 2001b. "Re-evaluation of Microbial Gas Generation under Expected Waste Isolation Pilot Plant Conditions: Data Summary and Progress Report (February 1 – July 13, 2001), July 16, 2001, Rev. 0," *Sandia National Laboratories Technical Baseline Reports,* WBS 1.3.5.4, Repository Investigations Milestone R1020, July 31, 2001. Sandia National Laboratories, Carlsbad, NM. ERMS # 518970. 3-1 to 3-21.

Gillow J.B., and A.J. Francis. 2002a. "Re-evaluation of Microbial Gas Generation under Expected Waste Isolation Pilot Plant Conditions: Data Summary and Progress Report (July 14, 2001 – January 31, 2002), January 22, 2002" *Sandia National Laboratories Technical Baseline Reports,* WBS 1.3.5.3, Compliance Monitoring; WBS 1.3.5.4, Repository Investigations, Milestone RI110, January 31, 2002. Sandia National Laboratories, Carlsbad, NM. ERMS # 520467. 2.1 - 1 to 2.1 – 26.

Gillow J.B., and A.J. Francis. 2002b. "Re-evaluation of Microbial Gas Generation under Expected Waste Isolation Pilot Plant Conditions: Data Summary and Progress Report (February 1 – July 15, 2002), July 18, 2002" *Sandia National Laboratories Technical Baseline Reports,* WBS 1.3.5.3, Compliance Monitoring; WBS 1.3.5.4, Repository Investigations, Milestone RI130, July 31, 2002. Sandia National Laboratories, Carlsbad, NM. ERMS # 523189. 3.1 - 1 to 3.1 - A10.

Gorham, E., Beauheim, R., Davies, P., Howarth, S., and Webb, S. 1992. "Recommendation to PA on Salado Formation Intrinsic Permeability and Pore Pressure for 40 Subpart B Calculations, June 15, 1992," pages A-49 through A-65 in Sandia WIPP Project, 1992. *Preliminary Performance Assessment for the Waste Isolation Pilot Plant, December 1993. Volume 3, Model Parameters*. SAND92-0700/3, Sandia National Laboratories, Albuquerque, NM.

Grindrod, P. 1993. "The Impact of Colloids on the Migration and Dispersal of Radionuclides Within Fractured Rock," *Journal of Contaminant Hydrology*. Vol. 13, no. 1 – 4, 167-181.

Grindrod, P., and Worth, D.J. 1990. *Radionuclide and Colloid Migration in Fractured Rock: Model Calculations*. SKI Technical Report 91:11, Swedish Nuclear Power Inspectorate, Stockholm, Sweden.

Guzowski, R.V. 1990. *Preliminary Identification of Scenarios for the Waste Isolation Pilot Plant, Southeastern New Mexico.* SAND90-7090, Sandia National Laboratories, Albuquerque, NM. WPO 25771.

Hansen, C.W., Leigh, C., Lord, D., and Stein, J. 2002. *BRAGFLO Results for the Technical Baseline Migration.* Sandia National Laboratories; Carlsbad, NM. ERMS # 523209.

Hansen, C.W., Brush, L. H., Gross, M. B., Hansen, F. D., Byoung Yoon, P., Stein, J. S., and Thompson, T. W. 2003a. *Effects of Supercompacted Waste and Heterogeneous Waste Emplacement on Repository Performance,* Revision 1, Sandia National Laboratories. Carlsbad, NM. ERMS # 532475

Hansen, F.D., Pfeifle, T.W., and Lord, D.L. 2003b. *Parameter Justification Report for DRSPALL,* SAND2003-2930, Sandia National Laboratories: Carlsbad, NM.

Hansen, F.D., Knowles, M.K., Thompson, T.W., Gross, M., McLennan and Schatz, J.F. 1997. *Description and Evaluation of a Mechanically Based Conceptual Model for Spall,* SAND97-1369. Sandia National Laboratories: Albuquerque, NM.

Harbaugh, A.W., Banta, E.R., Hill, M.C., and McDonald, M.G. 2000. *MODFLOW-2000 and U.S. Geological Survey Modular Ground-Water Model: Users Guide to Modularization Concepts and the Ground-Water Flow Process.* U.S. Geological Survey Open-File Report 00-92.

Harmand, B., and Sardin, M. 1994. "Modelling the Coupled Transport of Colloids and Radionuclides in a Fractured Natural Medium," *Chemistry and Migration Behaviour of Actinides and Fission Products in the Geosphere, Proceedings of the Fourth International Conference, Charleston, SC, December 12-17, 1993*. R. Oldenbourg Verlag, Munich. Vol. 66/67, 691-699.

Haug, A., Kelley, V.A., LaVenue, A.M., and Pickens, J.F. 1987. *Modeling of Ground-Water Flow in the Culebra Dolomite at the Waste Isolation Pilot Plant (WIPP) Site: Interim Report.* SAND86-7167, Sandia National Laboratories, Albuquerque, NM. WPO 28486.

Holt, R.M., and Powers, D.W. 1984. *Geotechnical Activities in the Waste Handling Shaft.* WTSD-TME-038, U.S. Department of Energy, Carlsbad, NM.

Holt, R.M., and Powers, D.W. 1986. *Geotechnical Activities in the Exhaust Shaft.* DOE-WIPP 86-008, U.S. Department of Energy, Carlsbad, NM.

Holt, R.M., and Powers, D.W. 1988. *Facies Variability and Post-Depositional Alteration Within the Rustler Formation in the Vicinity of the Waste Isolation Pilot Plant, Southeastern New Mexico.* DOE-WIPP 88-004, U.S. Department of Energy, Carlsbad, NM.

Holt, R.M., and Powers, D.W. 1990. *Geologic Mapping of the Air Intake Shaft at the Waste Isolation Pilot Plant.* DOE-WIPP 90-051, U.S. Department of Energy, Carlsbad, NM.

Hunter, R.L. 1989. *Events and Processes for Constructing Scenarios for the Release of Transuranic Waste from the Waste Isolation Pilot Plant, Southeastern New Mexico.* SAND89-2546, Sandia National Laboratories, Albuquerque, NM. WPO 27731.

Hwang, Y., Pigford, T.H., Lee, W.W.-L., and Chambre, P.L. 1989. "Analytic Solution of Pseudocolloid Migration in Fractured Rock," *Transactions of the American Nuclear Society*. Vol. 60, 107 – 109.

Ibaraki, M., and Sudicky, E.A. 1995. "Colloid-Facilitated Contaminant Transport in Discretely Fractured Porous Media. 1. Numerical Formulation and Sensitivity Analysis," *Water Resources Research*. Vol. 31, No. 12, 2945 – 2960.

Jacquier, P. 1991. "Geochemical Modelling: What Phenomena are Missing?" *Radiochimica Acta*. Vol. 52/53, pt. 1, 493 – 499.

James, S.J., and Stein, J. 2002. *Analysis Plan for the Development of a Simplified Shaft Seal Model for the WIPP Performance Assessment*. #AP-094. Sandia National Laboratories. Carlsbad, NM. ERMS # 524958.

James, S.J. and Stein, J.S. 2003. *Analysis Report for the Development of a Simplified Shaft Seal Model for the WIPP Performance Assessment* Rev 1. Sandia National Laboratories, Carlsbad, NM ERMS # 525203.

Jones, T.L., Kelley, V.A., Pickens, J.F., Upton, D.T., Beauheim, R.L., and Davies, P.B. 1992. *Integration of Interpretation Results of Tracer Tests Performed in the Culebra Dolomite at the Waste Isolation Pilot Plant Site.* SAND92-1579, Sandia National Laboratories, Albuquerque, NM. WPO 23504.

Kanney, J.F. 2003. *"Hydrogen Gas as a Surrogate for Waste-Generated Gas Physical Properties in BRAGFLO."* Sandia National Laboratories, Carlsbad, NM, Technical Memorandum, ERMS # 532900.

Lappin, A.R., Hunter, R.L., Gabber, D.P., and Davies, P.B., eds. 1989. *Systems Analysis, Long-Term Radionuclide Transport, and Dose Assessments, Waste Isolation Pilot Plant (WIPP), Southeastern New Mexico; March 1989.* SAND89-0462, Sandia National Laboratories, Albuquerque, NM. WPO 24125.

LaVenue, A.M., and RamaRao, B.S. 1992. *A Modeling Approach to Address Spatial Variability Within the Culebra Dolomite Transmissivity Field.* SAND92-7306, Sandia National Laboratories, Albuquerque, NM. WPO 23889.

LaVenue, A.M., Cauffman, T.L., and Pickens, J.F. 1990. *Ground-Water Flow Modeling of the Culebra Dolomite: Volume 1 - Model Calibration*. SAND89-7068/1, Sandia National Laboratories, Albuquerque, NM.

Leigh, C. 2003. *"Radionuclides Expected to Dominate Potential Releases in the Compliance Recertification Application, Supercedes ERMS 529245,"* Revision 1. Sandia National Laboratories. Carlsbad, NM. ERMS # 531086.

Light, W.B., Lee, W.W.-L., Chambre, P.L., and Pigford, T.H. 1990. "Radioactive Colloid Advection in a Sorbing Porous Medium: Analytical Solution," *Transactions of the American Nuclear Society*. V*ol. 61, 81 – 83.*

Lord, DL., 2002. Analysis Plan for Completion of Spalling Model for WIPP, Revision 0, AP-096, Sandia National Laboratories: Carlsbad, NM. ERMS # 524993.

Lord, D.L., 2003. *Justification for Particle Diameter and Shape Factor used in DRSPALL,* Sandia National Laboratories: Carlsbad, NM. ERMS # 531477.

Lord, D.L., Rudeen D.K., and Hansen, C.W. 2003. *Analysis Package for DRSPALL: Compliance Recertification Application.* Sandia National Laboratories: Carlsbad, NM. ERMS # 532766.

Lord, D.L., and Rudeen D.K. 2003. Sensitivity Analysis Report – Parts 1 and 2, DRSPALL version 1.00. Report for Conceptual Model Peer Review Panel Convening July 7-11, 2003. Sandia National Laboratories: Carlsbad, NM. ERMS # 524400.

Marietta, M.G., Bertram-Howery, S.G., Anderson, D.R. (Rip), Brinster, K.F., Guzowski, R.V., Iuzzolino, H., and Rechard, R.P. 1989. *Performance Assessment Methodology Demonstration: Methodology Development for Evaluating Compliance with EPA 40 CFR 191, Subpart B, for the Waste Isolation Pilot Plant.* SAND89-2027, Sandia National Laboratories, Albuquerque, NM. WPO 25952.

McCarthy, J.F., and Zachara, J.M. 1989. "Subsurface Transport of Contaminants," *Environmental Science and Technolology*. Vol. 23, no. 5, 496 – 502.

McTigue, D.F. 1993. *Permeability and Hydraulic Diffusivity of Waste Isolation Pilot Plant Repository Salt Inferred from Small-Scale Brine Inflow Experiments*. SAND92-1911, Sandia National Laboratories, Albuquerque, NM.

Mendenhall, F.T., and Gerstle, W. 1993. WIPP Anhydrite Fracture Modeling. Memorandum to Distribution, December 6, 1993. SWCF-A: W.B.S. 1.1.7.1 (WPO #39830). Sandia National Laboratories, Albuquerque, NM. WPO 39830.

Mercer, J.W., and Orr, B.R. 1979. *Interim Data Report on the Geohydrology of the Proposed Waste Isolation Pilot Plant Site, Southeast New Mexico.* Water-Resources Investigations 79-98, U.S. Geological Survey, Albuquerque, NM.

Molecke, M.A. 1979. *Gas Generation from Transuranic Waste Degradation: Data Summary and Interpretation.* SAND79-1245, Sandia National Laboratories, Albuquerque, NM. WPO 26715.

NIST (National Institute of Standards and Technology). 1992. *Thermophysical Properties of Hydrogen Mixtures Database (SUPERTRAPP): Version 1.0 User's Guide.* U.S. Department of Commerce, National Institute of Standards and Technology Standard Reference Data Program, Gaithersburg, MD.

Nowak, E.J., Tillerson, J.R., and Torres, R.M. 1990. *Initial Reference Seal System Design: Waste Isolation Pilot Plant*. SAND90-0355, Sandia National Laboratories, Albuquerque, NM.

Nyhan, J.W., Drennon, B.J., Abeele, W.V., Wheeler, M.L., Purtymun, W.D., Trujillo, G., Herrera, W.J., and Booth, J.W. 1985. "Distribution of Plutonium and Americium Beneath a 33-yr-old Liquid Waste Disposal Site," *Journal of Environmental Quality*. Vol. 14, no. 4, 501 – 509.

Papenguth, H.W., and Behl, Y.K. 1996a. "Test Plan for Evaluation of Colloid-Facilitated Actinide Transport at the Waste Isolation Pilot Plant." SNL Test Plan TP 96-01, Sandia National Laboratories, Albuquerque, NM. WPO 31337.

Papenguth, H.W., and Behl, Y.K. 1996b. "Test Plan for Evaluation of Dissolved Actinide Retardation at the Waste Isolation Pilot Plant." TP 96-02, Sandia National Laboratories, Albuquerque, NM. WPO 31336.

Park, B.Y. 2002. *Analysis Plan for Structural Evaluation of WIPP Disposal Room Raised to Clay Seam G,* Rev 1. AP-093. Sandia National Laboratories: Carlsbad, NM. ERMS # 524805.

Park, B.Y. and Hansen F.D. 2003. *Determination of the Porosity Surfaces of the Disposal Room Containing Various Waste Inventories for the WIPP PA.* Sandia National Laboratories: Albuquerque, NM.

Park, B.Y., and Holland, J.F. 2003. *"Analysis Report for Structural Evaluation of WIPP Disposal Room Raised to Clay Seam G."* SAND 2003-3409, Sandia National Laboratories, Carlsbad, NM.

Pruess, K. 1991. *TOUGH2: A General-Purpose Numerical Simulator for Multiphase Fluid and Heat Flow.* LBL-29400, Earth Science Division, Lawrence Berkeley Laboratories, Berkeley, CA.

Ramsey, J. 1996. "Culebra Dissolved Actinide Parameter Request." Unpublished memorandum to E. J. Nowak, March 18, 1996. Sandia National Laboratories, Albuquerque, NM. WPO 35269.

Rechard, R.P., Beyeler, W., McCurley, R.D., Rudeen, D.K., Bean, J.E., and Schreiber, J.D. 1990. *Parameter Sensitivity Studies of Selected Components of the Waste Isolation Pilot Plant Repository/Shaft System.* SAND89-2030, Sandia National Laboratories, Albuquerque, NM. Chapter 5, Summary and Conclusions, pp. 153 - 160. WPO 25946.

Reed, D.T., Okajima, S., Brush, L.H., and Molecke, M.A. 1993. "Radiolytically-Induced Gas Production in Plutonium-Spiked WIPP Brine," *Scientific Basis for Nuclear Waste Management XVI, Materials Research Society Symposium Proceedings, Boston, MA, November 30-*

December 4, 1992. Eds. C.G. Interrante and R.T. Pabalan. SAND92-7283C, Materials Research Society, Pittsburgh, PA. Vol. 294, 431-438. WPO 28639.

Reeves, M., Ward, D.S., Johns, N.D., and Cranwell, R.M. 1986. *Theory and Implementation for SWIFT II, The Sandia Waste-Isolation Flow and Transport Model for Fractured Media, Release 484.* SAND83-1159, NUREG/CR-3328, Sandia National Laboratories, Albuquerque, NM.

Sandia National Laboratories (SNL). 1992 – 1993. *Preliminary Performance Assessment for the Waste Isolation Pilot Plant, December 1992*. SAND92-0700, Vols. 1-5, Sandia National Laboratories, Albuquerque, NM. Vol. 1 – WPO 20762, Vol. 2 – WPO 20805, Vol. 3 – WPO 23529, Vol. 4 – WPO 20958, Vol. 5 – WPO 20929.

Sandia National Laboratories (SNL). 1997. *Supplemental Summary of EPA-Mandated Performance Assessment Verification Test (All Replicates) and Comparison with the Compliance Certification Application Calculations.* ERMS # 414879.

Sandia National Laboratories (SNL). 2001a. *Sandia National Laboratories Technical Baseline Reports, WBS 1.3.5.4, Repository Investigations,* Milestone RI010, January 31, 2001. Sandia National Laboratories: Carlsbad, NM. ERMS # 516749.

Sandia National Laboratories (SNL). 2001b. Sandia *National Laboratories Technical Baseline Reports, WBS 1.3.5.4, Repository Investigations*, Milestone RI020, July 31, 2001. Sandia National Laboratories: Carlsbad, NM. ERMS # 518970.

Sandia National Laboratories (SNL). 2002a. *Sandia National Laboratories Technical Baseline Reports, WBS 1.3.5.3, Compliance Monitoring; WBS 1.3.5.4, Repository Investigations,* Milestone RI110, January 31, 2002. Sandia National Laboratories: Carlsbad, NM. ERMS # 520467.

Sandia National Laboratories (SNL). 2002b. *Sandia National Laboratories Technical Baseline Reports, WBS 1.3.5.3, Compliance Monitoring; WBS 1.3.5.4, Repository Investigations*, Milestone RI130, July 31, 2002. Sandia National Laboratories. Carlsbad, NM. ERMS # 523189.

Sandia National Laboratories (SNL). 2002c. *Sandia National Laboratories Annual Compliance Monitoring Parameter Assessment for 2002,* WBS 1.3.5.3.1, Pkg. No. 510062, November 2002. Sandia National Laboratories: Carlsbad, NM. ERMS # 524449

Sandia National Laboratories (SNL). 2003a. *Features Events and Processes Reassessment for Recertification Report.* June 30, 2003. Sandia National Laboratories: Carlsbad, NM. ERMS # 530184.

Sandia National Laboratories (SNL). 2003b. *Sandia National Laboratories Technical Baseline Report, WBS 1.3.5.3, Compliance Monitoring; WBS 1.3.5.4, Repository Investigations,* Milestone RI 03-210, January 31, 2003. Sandia National Laboratories: Carlsbad, NM. ERMS # 526049.

Sandia National Laboratories (SNL). 2003c. *Program Plan, WIPP Integrated Groundwater Hydrology Program,* FY03-FY09, Revision 0, March 14, 2003. Sandia National Laboratories: Carlsbad, NM. ERMS # 526671

Schreiber, J.D. 1997. *WIPP PA User's Manual for BRAGFLO,* Version 4.10. May 1997. Sandia National Laboratories: Carlsbad, NM. ERMS # 245238.

Sewards, T. 1991. *Characterization of Fracture Surfaces in Dolomite Rock, Culebra Dolomite Member, Rustler Formation*. SAND90-7019, Sandia National Laboratories, Albuquerque, NM. WPO 23872.

Sewards, T., Brearly, A., Glenn, R., MacKinnon, I.D.R., and Siegel, M.D. 1992. *Nature and Genesis of Clay Minerals of the Rustler Formation in the Vicinity of the Waste Isolation Pilot Plant in Southeastern New Mexico*. SAND90-2569, Sandia National Laboratories, Albuquerque, NM. WPO 26157.

Sewards, T., Williams, M.L., and Keil, K. 1991. "Mineralogy of the Culebra Dolomite," *Hydrogeochemical Studies of the Rustler Formation and Related Rocks in the Waste Isolation Pilot Plant Area, Southeastern New Mexico*. SAND88-0196. Eds. M.D. Siegel, S.J. Lambert, and K.L. Robinson. Sandia National Laboratories, Albuquerque, NM. 3 – 1 to 3 – 43. Chapter 3 of WPO 25624.

Siegel, M.D., Lambert, S.J., and Robinson, K.L., eds. 1991. *Hydrogeochemical Studies of the Rustler Formation and Related Rocks in the Waste Isolation Pilot Plant Area, Southeastern New Mexico.* SAND88-0196, Sandia National Laboratories, Albuquerque, NM. WPO 25624.

Smith, P.A., and Degueldre, C. 1993. "Colloid-Facilitated Transport of Radionuclides Through Fractured Media," *Journal of Contaminant Hydrology*. Vol. 13, no. 1 – 4, 143 – 166.

State of New Mexico, Oil Conservation Division, Energy, Minerals, and Natural Resources Department. 1988. Application of the Oil Conservation Division Upon Its Own Motion to Revise Order R-111, As Amended, Pertaining to the Potash Areas of Eddy and Lea Counties, New Mexico. Case 9316, Revision to Order R-111-P, April 21, 1988. Santa Fe, NM.

Stein, J.S. 2002. "Errors Identified in Waste Storage Volume Parameters used to Construct BRAGFLO grid." Memorandum to M. K. Knowles, Sept. 17, 2002. Sandia National Laboratories: Carlsbad, NM. ERMS # 523760.

Stein, J.S. 2003a. "Correlation Between Bulk Compressibility and Porosity in the Castile Brine Pocket as Modeled in BRAGFLO." Memorandum to D. Kessel, April1, 2003. Sandia National Laboratories: Carlsbad, NM. ERMS # 526858.

Stein, J.S. 2003b. Analysis Plan for Calculations of Direct Brine Releases : Compliance Recertification Application. AP-104. Sandia National Laboratories: Carlsbad, NM. ERMS # 528743.

Stein, J.S., and Zelinski, W. 2003a. *"Analysis Plan for the Testing of a Proposed BRAGFLO Grid to be used for the Compliance Recertification Application Performance Assessment Calculations."* AP-106. Sandia National Laboratories: Carlsbad, NM. ERMS # 525236.

Stein, J.S., and Zelinski, W. 2003b. *"Analysis Report for: Testing of a Proposed BRAGFLO Grid to be used for the Compliance Recertification Application Performance Assessment Calculations."* Sandia National Laboratories: Carlsbad, NM. ERMS # 526868.

Stein, J.S., and Zelinski, W. 2003c. *"Analysis Package for BRAGFLO: Compliance Recertification Application."* Sandia National Laboratories. Carlsbad, NM. ERMS 530142.

Stormont, J.D. 1988. *Preliminary Seal Design Evaluation for the Waste Isolation Pilot Plant.* SAND87-3083, Sandia National Laboratories, Albuquerque, NM.

Swift, P.N., Baker, B.L., Economy, K., Garner, J.W., Helton, J.C., and Rudeen, D.K. 1994. *Incorporating Long-Term Climate Change in Performance Assessment for the Waste Isolation Pilot Plant*. SAND93-2266, Sandia National Laboratories, Albuquerque, NM. WPO 27827.

Telander, M.R., and R.E. Westerman. 1997. *Hydrogen Generation by Metal Corrosion in Simulated Waste Isolation Pilot Plant Environments.* SAND96-2538. Sandia National Laboratories: Albuquerque, NM.

Telander, M.R., and Westerman, R.E. 1993. *Hydrogen Generation by Metal Corrosion in Simulated Waste Isolation Pilot Plant Environments, Progress Report for the Period November 1989 Through December 1992*. SAND92-7347, Sandia National Laboratories, Albuquerque, NM. WPO 23456.

Tierney, M.S. 1991. *Combining Scenarios in a Calculation of the Overall Probability Distribution of Cumulative Releases of Radioactivity From the Waste Isolation Pilot Plant, Southeastern New Mexico.* SAND90-0838, Sandia National Laboratories, Albuquerque, NM. WPO 26030.

Trauth, K.M., Hora, S.C., Rechard, R.P., and Anderson, D.R. 1992. The Use of Expert Judgment to Quantify Uncertainty in Solubility and Sorption Parameters for Waste Isolation Pilot Plant Performance Assessment. SAND92-0479, Sandia National Laboratories, Albuquerque, NM. WPO 23526.

Travis, B.J., and Nuttall, H.E. 1985. "A Transport Code for Radiocolloid Migration: With an Assessment of an Actual Low-Level Waste Site," *Scientific Basis for Nuclear Waste Management VIII, Materials Research Society Symposia Proceedings, Boston, MA, November 26-29, 1984*. Eds. C.M. Jantzen, J.A. Stone, and R.C. Ewing. Materials Research Society, Pittsburgh, PA. Vol. 44, 969-976.

van der Lee, J., de Marsily, G., and Ledoux, E. 1993. "Are Colloids Important for Transport Rate Assessment of Radionuclides? A Microscopic Modeling Approach," *High Level Radioactive Waste Management, Proceedings of the 4th Annual International Conference, Las Vegas, NV, April 26-30, 1993*. American Society of Civil Engineers, New York, NY. 646-652.

van der Lee, J., Ledoux, E., and de Marsily, G. 1994. "Microscopic Description of Colloid Transport in Fractured or Porous Media," *Transport and Reactive Processes in Aquifers: Proceedings of the IAHR/AIRH Symposium, Zurich, Switzerland, April 11-15, 1994*. Eds. Th. Dracos and F. Stauffer. A.A. Balkema, Brookfield, VT. 349 – 355.

Vaughn, P., Lord, M., and MacKinnon, R. 1995. S-6: Dynamic Alteration of the DRZ/Transition Zone: Summary Memo of Record to D.R. Anderson, September 28, 1995. SWCF-A (WPO #30798). Sandia National Laboratories, Albuquerque, NM.

Vaughn, P., Lord, M., and MacKinnon, R. 1995a. "DR-6: Brine Puddling in the Repository due to Heterogeneities." Summary Memo of Record to D.R. Anderson, December 21, 1995, SWCF-A:1.1.6.3. Sandia National Laboratories, Albuquerque, NM. WPO 30795.

Vaughn, P., Lord, M., and MacKinnon, R. 1995b. "DR-7: Permeability Varying with Porosity in Closure Regions." Summary Memo of Record to D.R. Anderson, December 21, 1995, SWCF-A:1.1.6.3. Sandia National Laboratories, Albuquerque, NM. WPO 30796.

Vaughn, P., Lord, M., and MacKinnon, R. 1995c. "DR3: Dynamic Closure of the North End and Hallways." Summary Memorandum of Record to D. R. Anderson, September 28, 1995. SWCF-A:1.1.6.3. Sandia National Laboratories, Albuquerque, NM. WPO 30798.

Vaughn, P., Lord, M., and MacKinnon, R. 1995e. "DR-2: Capillary Action (Wicking) within the Waste Materials." Summary Memo of Record to D.R. Anderson, December 21, 1995, SWCF-A:1.1.6.3. Sandia National Laboratories, Albuquerque, NM. WPO 30793.

Vaughn, P., Lord, M., Garner, J., and MacKinnon, R. 1995d. "GG-1: Radiolysis of Brine." Summary Memo of Record to D.R. Anderson, October 10, 1995, SWCF-A:1.1.6.3. Sandia National Laboratories, Albuquerque, NM. Contained in WPO 30791.

Wang, H.F, Anderson, M.P. 1982. *Introduction to Groundwater Modeling: Finite Difference and Finite Element Methods,* Academic Press, Inc.

Wang, Y. 1997. Memorandum from Yifeng Wang to Margaret Chu *"Estimate WIPP Waste Particle Sizes on Expert Elicitation Results: Revision 1"* 5 August, 1997. ERMS #246936.

Washington Regulatory and Environmental Services (WRES), 2003. "Delaware Basin Supplemental Information, August 2003," memorandum from S. Kouba to T. Pfeifle, Sandia National Laboratories, ERMS # 525157.

Webb, S. 1995. "DR-1:3D Room Flow Model with Dip." Planning Memo of Record to D.R. Anderson, May 30, 1995. SWCF-A:1.1.6.3. Sandia National Laboratories, Albuquerque, NM. WPO 22494.

Wilson, C., Porter, D., Gibbons, J., Oswald, E., Sjoblom, G., and F. Caporuscio. 1996a. *Conceptual Models Supplementary Peer Review Repor*t, U.S. Department of Energy, Carlsbad Area Office, Office of Regulatory Compliance, July, 1996.

Wilson, C., Porter, D., Gibbons, J., Oswald, E., Sjoblom, G., and F. Caporuscio. 1996b. *Conceptual Models Supplementary Peer Review Report*, U.S. Department of Energy, Carlsbad Area Office, Office of Regulatory Compliance, December, 1996.

Wilson, C., Porter, D., Gibbons, J., Oswald, E., Sjoblom, G., and F. Caporuscio. 1997. *Conceptual Models Third Supplementary Peer Review Report*, U.S. Department of Energy, Carlsbad Area Office, Office of Regulatory Compliance, April, 1997.

WIPP PA, 2003a. *Design Document for DRSPALL* Version 1.00, document version 1.10. Sandia National Laboratories. Carlsbad, NM. ERMS # 529878.

WIPP PA, 2003b. *Verification and Validation Plan/Validation Document for DRSPAL*L Version 1.00, document version 1.00. Carlsbad, NM. Sandia National Laboratories. ERMS # 524782.

WIPP Performance Assessment Department. 1991. *Preliminary Comparison with 40 CFR Part 191, Subpart B for the Waste Isolation Pilot Plant,* December 1991, Volumes 1-4. SAND91-0893/1-4, Sandia National Laboratories: Albuquerque, NM.

WIPP Performance Assessment Department. 1993. *Preliminary Performance Assessment for the Waste Isolation Pilot Plant, December 1992,* Volumes 1-4. SAND92-0700/4, Sandia National Laboratories, Albuquerque, NM. WPO 23528.

Yew, C., Hanson, J., and Teufel. 2003. *Spallings Conceptual Model Peer Review Report,* Time Solutions Corp. Albuquerque, NM. ERMS # 532520